

Doctoral thesis

Doctoral theses at NTNU, 2022:121

Oskar W Angenete

Imaging of the temporomandibular joint in children with juvenile idiopathic arthritis; references and novel scoring systems for active and permanent disease

NTNU
Norwegian University of Science and Technology
Thesis for the Degree of
Philosophiae Doctor
Faculty of Medicine and Health Sciences
Department of Circulation and Medical Imaging



Norwegian University of
Science and Technology

Oskar W Angenete

Imaging of the temporomandibular joint in children with juvenile idiopathic arthritis; references and novel scoring systems for active and permanent disease

Thesis for the Degree of Philosophiae Doctor

Trondheim, May 2022

Norwegian University of Science and Technology
Faculty of Medicine and Health Sciences
Department of Circulation and Medical Imaging



Norwegian University of
Science and Technology

NTNU

Norwegian University of Science and Technology

Thesis for the Degree of Philosophiae Doctor

Faculty of Medicine and Health Sciences

Department of Circulation and Medical Imaging

© Oskar W Angenete

ISBN 978-82-326-6430-6 (printed ver.)

ISBN 978-82-326-6820-5 (electronic ver.)

ISSN 1503-8181 (printed ver.)

ISSN 2703-8084 (online ver.)

Doctoral theses at NTNU, 2022:121

Printed by NTNU Grafisk senter

Sammendrag / Summary in Norwegian

Bilddiagnostikk av kjeveleddet hos barn med barneleddgikt; referansemateriale og skåringssystemer for å vurdere aktiv sykdom og permanent skade

Barneleddgikt (juvenil idiopatisk artritt, JIA) er den vanligste, kroniske revmatiske sykdommen hos barn og rammer årlig ca. 15 barn per 100 000 i Norge. Sykdommen er en betydelig belastning for barnet i form av smerte og stivhet i ledd, langvarig behandling og hyppige kontroller i helsevesenet. Kjeveleddet er involvert hos en stor andel av pasientene, med smerter og ubehag, og mulig dårligere munnhelse. Bilddiagnostikk er et viktig hjelpemiddel for å vurdere om kjeveleddene er affiserte, om der er pågående inflammasjon og om det er tilkommet permanent skade.

Moderne bilddiagnostikk som magnetkamera (MR) og cone-beam datortomografi (CBCT) er utfordrende å tolke. Det finnes også lite kunnskap om kjeveleddenes utseende hos friske barn. Derfor er det vanskelig å skille friske kjeveledd fra syke.

For å lære mer om friske barns kjeveledd fikk vi lov å se på allerede utførte MR-undersøkelser av 101 barn som ikke har JIA for å finne pålitelige bildefunn og målinger. Vi fikk også lov å gjennomføre MR og CBCT på barn med JIA. På 86 av barna med JIA testet vi et stort antall målinger og bildefunn for å se hvilke som var pålitelige.

Vi fant ut at mange bildefunn og målinger av kjeveledd hos barn både med og uten JIA er upålitelige. Hos barn uten JIA er det vanlig å se kontrastvæske i kjeveleddet. Det er noe som man tidligere trodde bare forekom hos syke barn. På MR er syv bildefunn pålitelige nok til å brukes for å beskrive permanent skade og fire bildefunn kan brukes til å beskrive aktiv sykdom. Hos barn med JIA er ni bildefunn på CBCT pålitelige nok til å brukes for å beskrive permanent skade. Vi har sett at mange typer målinger av anatomiske strukturer i kjeveleddet er forbundne med stor usikkerhet.

Basert på erfaringene fra pålitelighetstestene, anbefaler vi et eget skåringssystem for MR og et for CBCT. Systemene kan brukes til å vurdere kjeveleddet hos barn med JIA.

Kandidat: Oskar W Angenete
Institutt: Institutt for sirkulasjon og bildediagnostikk (ISB)
Hovedveileder: Karen Rosendahl
Biveiledere: Marite Rygg, Knut Haakon Stensæth
Finansieringskilder: Klinikk for bildediagnostikk, St. Olavs hospital HF
Samarbeidsorganet, Helse Midt-Norge
Felles Forskningsutvalg, St. Olavs hospital HF og MH-fakultetet

Summary in English

Imaging of the temporomandibular joint in children with juvenile idiopathic arthritis; references and novel scoring systems for active and permanent disease

Juvenile idiopathic arthritis (JIA) is the most common, chronic rheumatic disease in children. Globally, there are large variations in incidence, ranging from 1.6-23 per 100 000 children/year and prevalence from 3.8-400 per 100 000 children. The annual incidence in Norway is estimated at 15 per 100 000 children. Disease course and prognosis varies between different categories of JIA, and recent publications indicate that the temporomandibular joint (TMJ) is affected in a large proportion of children with JIA. Children diagnosed with JIA are more prone than their peers to develop orofacial pain, growth disturbances of the TMJ, and reduced quality of life.

A large multicenter, prospective, observational, case-control study on JIA (The Norwegian JIA Study – Imaging, oral health, and quality of life in children with juvenile idiopathic arthritis, NorJIA) www.norjia.com was conducted from 2015 to 2020, including a large cohort of children with JIA in three regions of Norway. One of the focus areas for the NorJIA study is the evaluation of medical imaging of the temporomandibular joint (TMJ). Herein lies the aim to document normal variation of imaging findings and to develop robust image-based classification systems. Moreover, these aims are in line with the research strategy of the European Society of Paediatric Radiology (ESPR).

Several publications during the last 10-15 years have shed light on the normal and pathological image features of the paediatric TMJ. The publications address findings using radiographic techniques, cone-beam computed tomography (CBCT), and magnetic resonance imaging (MRI), but thorough testing of the precision of these image features is lacking. Without proof of acceptable precision, the results from imaging studies will be associated with uncertainty.

In this thesis we first aimed to establish normal standards for the development of the TMJ, based on the most robust MRI-based image features and continuous measurements. We then aimed to identify and test the precision of a wide set of MRI-

based and CBCT-based image features of the TMJ in children with JIA. Subsequently, the aim was to propose a CBCT-based and MRI-based scoring system, based on the most precise imaging findings.

In the first paper we used a retrospectively collected dataset including 101 head MRI examinations, of which 36 included images before and after intravenous contrast, performed for other reasons than JIA. Following thorough calibration three experienced radiologists performed consensus reading twice to determine agreement between each reading. In this cohort of children without JIA we found that continuous measurements showed wide limits of agreement, which is a statistical indication of low agreement between readers. Several of the categorical image features were also hampered with inaccuracy. We found that the anterior inclination increases by age, that condylar flattening in the coronal plane is a common finding, and that mild contrast enhancement of the joint tissue is very common in children without JIA.

In paper two, we used a balanced dataset consisting of the MRI examinations of 86 of the participants in the NorJIA study. Two consultant radiologists scored the MRI dataset according to 25 different image features (twice by one of the radiologists). We found seven image features in the osteochondral domain and four in the inflammatory domain to be of acceptable precision. Several image features previously used to characterize disease of the TMJ in JIA turned out to be imprecise.

In paper three, we used a balanced dataset consisting of 84 CBCT examinations, also drawn from the NorJIA study. Three consultant radiologists scored the dataset after thorough discussion, calibration and testing. One of the radiologists scored the dataset twice. As in paper one and two, essentially all continuous measurements of the TMJ turned out to be imprecise. From the categorical image features nine were deemed precise enough to be used further.

Conclusion: For an MRI-based scoring system of the TMJ in JIA, we propose seven image features of the osteochondral domain and four in the inflammatory domain. For a CBCT-based scoring system in JIA, we propose a scoring system consisting of nine image features suitable for evaluation of TMJ deformity.

Acknowledgements

I would like to show my gratitude to the people supporting me and this work. Without the support of the Department of Radiology and Nuclear Imaging this would not have been possible. I could not have devoted so much time and energy into this thesis without my hardworking colleagues at the section for orthopedic radiology, led by dr Grove. Further, the support from the Institute of Circulation and Medical Imaging at NTNU has been paramount in the fulfilling of this thesis.

I would like to thank my main supervisor Karen Rosendahl for letting me be a part of the NorJIA team, for inspiring me with her curiosity, her vast knowledge and her way of showing how fruitful it is to include old and new friends in the work for paediatric radiology.

I would also like to show my great gratitude to co-supervisor Marite Rygg for being the one to invite me to the world of science, and for showing me what it means to be a researcher and a caring clinician at the same time. Her way of seeing the big picture and yet never lose the sense for details represents a role model for me.

My thanks also go to co-supervisor Knut Haakon Stensæth who contributed with resources, logistic support and who is a facilitator of research at the Department of Radiology.

My friend and research partner Thomas Angell Augdal deserves a special note for always being there with an alternative perspective and constructive criticism, and for being a thorough and caring clinical radiologist and researcher. Many in our research group are grateful for the work you do!

I want to thank Stein Atle Lie for helping me with statistical calculations of hierarchical multiple regression, one of many methods beyond my competence.

Thomas B. Johnsen contributed with a beautiful drawing of the temporomandibular joint, I thank you for that.

Many were involved and invaluable in the vast collection of data of the NorJIA study and I would like to thank the patient coordinators and the radiographers at St Olavs for their tireless efforts.

The Liaison Committee between the Central Norway Regional Health Authority, the Trond Mohn foundation, the Norwegian Rheumatism Association and the Joint Research Committee between St. Olavs Hospital and the Faculty of Medicine and Health Sciences NTNU-FFU have all contributed with financial support of different parts of the Nor JIA study.

Last but certainly not least, my gratitude and love go to my family, to Guro, my wife and partner for life who always supported me even when the days were long and the goal line seemed too far away.

Table of Contents

Title page	1
Sammendrag / Summary in Norwegian.....	3
Summary in English	5
Acknowledgements	7
List of papers	11
Other publications	12
Abbreviations	13
1. General introduction.....	15
1.1 Normal references in paediatric radiology.....	15
1.2 Juvenile idiopathic arthritis.....	16
1.2.1 Historical overview	16
1.2.2 Pathology and diagnosis.....	17
1.2.3 Epidemiology	21
1.2.4 Disease course and outcome	22
1.2.5 Treatment	23
1.3 The temporomandibular joint in JIA	25
1.3.1 Normal development of the TMJ	25
1.3.2 Pathology of the TMJ.....	28
1.4 Imaging of the TMJ	29
1.4.1 Radiographic techniques	29
1.4.2 Ultrasound	29
1.4.3 Magnetic Resonance Imaging (MRI).....	30
1.4.4 Computed tomography (CT) and Cone-Beam (CB) CT of the TMJ	34
1.5 Assessing agreement in radiology	35
1.5.1 Measuring precision	37
2. Objectives	45
Paper 1	45
Paper 2	45
Paper 3	45
3. Materials and methods.....	47
3.1 Patients.....	48

3.2 Collection of imaging data.....	49
3.3 Image reading	50
3.4 Statistical methods	55
3.5 Ethics	55
4. Summary of results.....	57
Paper 1	57
Paper 2	59
Paper 3	61
5. Discussion.....	63
5.1 Methodological considerations	63
5.1.1 Study design.....	63
5.1.2 Technical aspects of MRI.....	67
5.1.3 Technical aspects of CBCT.....	69
5.1.4. The image readers	70
5.1.5 Statistical considerations	71
5.2 Ethical considerations	74
5.3 Results.....	76
5.3.1 Image features of the TMJ in children without JIA	76
5.3.2 Image features in the osteochondral domain.....	76
5.3.3 Image features in the inflammatory domain	78
5.3.4 Recommendations on a future scoring system.....	81
5.4 Clinical implications	82
5.5 Strengths and limitations	83
6. Conclusions	85
7. Future perspectives	87
8. Errata	89
9. References	93
10. Appendices	103
11. Papers	123

List of papers

The thesis is based on the following three papers.

Paper 1: **Angenete O**, Augdal TA, Jellestad S, Rygg M, Rosendahl K. Normal magnetic resonance appearance of the temporomandibular joints in children and young adults aged 2-18 years. *Pediatric Radiology*. 2018 Mar;48(3):341-349

Paper 2: **Angenete O**, Augdal TA, Rygg M, Rosendahl K. MRI in the assessment of TMJ-arthritis in children with JIA; Repeatability of a newly devised scoring system. *Academic Radiology*. 2021 November 19 (in press)

Paper 3: Augdal TA, **Angenete O**, Shi XQ, Nordal E, Rosendahl K. Cone beam computed tomography in the assessment of TMJ deformity in children with JIA; repeatability of a newly devised scoring system, manuscript, not peer-reviewed

Other publications

El Assar de la Fuente S, **Angenete O**, Jellestad S, Tzaribachev N, Koos B, Rosendahl K. Juvenile idiopathic arthritis and the temporomandibular joint: A comprehensive review. *J Craniomaxillofac Surg*. 2016 May;44(5):597-607

Rosendahl K, Lundestad A, Bjørlykke JA, Lein RK, **Angenete O**, Augdal TA, Müller LO, Jaramillo D. Revisiting the radiographic assessment of osteoporosis-Osteopenia in children 0-2 years of age. A systematic review. *PLoS One*. 2020 Nov 2;15(11):e0241635.

Starck L, Andersen E, Macicek O, **Angenete O**, Augdal TA, Rosendahl K, Jirik R, Grüner R. Effects of motion correction, sampling rate and parametric modelling in dynamic contrast enhanced MRI of the temporomandibular joint in children affected with juvenile idiopathic arthritis. *Magnetic resonance imaging*. 2021 Apr;77:204-212

Fischer J, Augdal TA, **Angenete O**, Gil EG, Skeie MS, Åstrøm AN, Tylleskär K, Rosendahl K, Shi XQ, Rosén A; NorJIA (Norwegian JIA Study — Imaging, oral health, and quality of life in children with juvenile idiopathic arthritis). In children and adolescents with temporomandibular disorder assembled with juvenile idiopathic arthritis - no association were found between pain and TMJ deformities using CBCT. *BMC Oral Health*. 2021 Oct 12;21(1):518.

Abbreviations

CBCT	Cone-beam computed tomography
CT	Computed tomography
DXA	Dual energy x-ray absorptiometry
ETL	Echo train length
FOV	Field of view
Hg (mm)	Unit of blood pressure
HLA	Human leukocyte antigen
IACI	Intraarticular corticosteroid injection
ICC	Intraclass correlation coefficient
IL	Interleukin
ILAR	International League of Associations for Rheumatology
JIA	Juvenile idiopathic arthritis
LOA	Limit of agreement
MAS	Macrophage activation syndrome
MHC	Major histocompatibility complex
MPRAGE	Magnetization-prepared rapid gradient-echo
MRI	Magnetic resonance imaging
NorJIA	Norwegian JIA Study – Imaging, oral health, and quality of life in children with juvenile idiopathic arthritis
NSA	Number of single averages
NSAID	Non-steroid anti-inflammatory drug
PACS	Picture archive and communication system
PD-fs	Proton-weighted images with fat-saturation
RA	Rheumatoid arthritis
RCT	Randomised controlled trial
RF	Rheumatoid factor
SD	Standard deviation

Sv	Sievert (SI unit of radiation absorption)
T	Tesla (field strength)
T1	T1-weighted images
T2-fs	T2-weighted images with fat-saturation
TMD	Temporomandibular dysfunction
TE	Echo time
TMJ	Temporomandibular joint
TNF- α	Tumor necrosis factor alpha
TR	Repetition time
TSE	Turbo spin echo

1. General introduction

Temporomandibular joint (TMJ) disorders in children include congenital deformities and acquired diseases such as inflammatory juvenile idiopathic arthritis (JIA), neoplasms and growth disturbances following trauma, infection, and the rare condition idiopathic condylar resorption.

Recent technical advances have made it possible to visualize the TMJ in detail, both the bony parts, the cartilage, and the soft tissues, using different imaging modalities and techniques. However, to recognize pathology, knowledge of the normal appearances is crucial, particularly in children where the imaging appearances change significantly during maturation and growth. Documenting normal variation in imaging findings to be able to confidently differentiate disease from normal, constitutes one of four key aims of the European Society of Paediatric Radiology (ESPR) research strategy, the others being facilitation of multicentre studies and data sharing, development of robust, image-based classification systems and last, but not least, the development of evidence-based clinical guidelines (1).

The work in this thesis addresses two of the issues above, namely reference standards and development of robust classification systems for TMJ imaging in children with JIA, based on two different data sets. First, retrospectively collected MRIs of the TMJs in children and adolescents without TMJ disease, upon which reference values for MRI are based. Next, a cohort of children with JIA for the establishment and testing of novel MRI and CBCT scoring systems for TMJ disease in this condition.

1.1 Normal references in paediatric radiology

References are essential to the pursuit of high academic standards in radiology. Atlases demonstrating the normal skeletal maturation process have been published (2), however, references from population-based studies are sparse. This may lead to both over- and underdiagnosis for a variety of diseases, such as growth abnormalities,

fractures and arthritic sequelae, as normal variations may mimic disease (3). The almost constantly changing size and form of the paediatric skeleton, the evolution of the joint surfaces, and, especially on MRI, the varying appearance of the bone marrow makes imaging interpretation prone to misdiagnosis. Further, altering growth rates and imaging appearance of the physis before and after puberty has been subject for debate in the radiologic community for years. In sum, there is a need for age-related normal imaging standards of the paediatric skeleton and joints for all imaging modalities.

1.2 Juvenile idiopathic arthritis

Juvenile idiopathic arthritis is a condition affecting a wide range of joints, but also extraarticular manifestations like soft tissue around the joints, bone marrow, eyes, and, in rare occasions, also the liver and spleen. Medical imaging, such as radiography, computed tomography, ultrasound, and magnetic resonance imaging (MRI) play a significant, and increasing, role in the diagnostic process and in follow-up of the patients.

1.2.1 Historical overview

In 1897 the British paediatrician George Frederick Still (1868-1941) described what he called “a form of chronic joint disease in children”. Despite dr. Stills accomplishments on several other fields of paediatric medicine, the eponym is still regarded as the beginning of the exploration of juvenile idiopathic arthritis. In 1946 the Canadian Red Cross Memorial Hospital in Taplow, Berkshire was created as the first hospital dedicated to diagnosis and treatment of paediatric rheumatic disease. Five years later dr. Barbara Ansell (1923-2001) started working at the hospital where she began not only a research career that would last for more than 50 years, but also defined a new, holistic approach to treatment of children with rheumatic disease. She and her colleagues discovered that treating chronic disease in children not only is a matter of using the right medicine, but success also is dependent on co-working with other experts such as orthopaedic surgeons, radiologists, ophthalmologists, physiotherapist, podiatrists,

dentists, and social workers. The recognition of the importance of interdisciplinary work has since then inspired treatment of rheumatic disease all over the world and has, in a way, also been the inspiration to the backbone of this thesis, the NorJIA study.

The nomenclature defining JIA has evolved since Dr. Still's first attempt to define the disease. In the United States, the term juvenile rheumatoid arthritis (JRA) was commonly used. In Europe, the medical community over many years preferred the term juvenile chronic arthritis (JCA). Today however, paediatric rheumatologists all over the world have agreed on replacing these terms with the term juvenile idiopathic arthritis (JIA). As there is rapidly expanding knowledge on genetic predispositions, further understanding of cellular and molecular pathogenesis and greater appreciation of epidemiology, the nomenclature will probably continue to evolve.

1.2.2 Pathology and diagnosis

Although the aetiology of JIA is still not understood, genetic predisposition, environmental factors, and processes in the immune system seem to be important contributors to the disease.

1.2.2.1 Genetics

There are assumed to be genetic factors associated with increased risk for development of JIA, and the risk for family members to a patient with JIA to develop the disease is increased (4). The major histocompatibility complex (MHC) contains several loci that increase the risk for developing JIA, many of those in the human leukocyte antigen alleles (HLA). Further, many of these loci differ significantly from the loci associated to increased risk for adult rheumatic disease. On the other hand, risk genes found in early-onset adult rheumatoid arthritis (RA) are similar to the genes associated to polyarticular JIA, positive for rheumatoid factor (RF positive) indicating that this category of JIA might be more closely related to adult disease than the other JIA categories. Although the HLA genes so far have shown the strongest association to JIA, there are also other genes, not associated to HLA that increase the risk for JIA (5, 6). Further, there is evidence that some genes associated to increased risk for JIA have an age-dependent

effect. This is expressed as an increased risk of developing JIA during a certain time window, but also as a decreased risk in a later time window (7). In total, as knowledge on genetics expand and the techniques to study genetics rapidly develop, one can hope to find even more robust and clinically relevant associations in the future (8).

1.2.2.2 Environmental factors

The pathogenesis of JIA is likely related to disturbances in the immune system. Therefore, the relation between infection and increased risk for JIA has been the focus of multiple studies. Exposure to parvovirus B19 and Epstein-Barr virus have been linked to JIA, albeit the causality and direct correlation has not been clearly stated (9-11). Several studies have explored the possible correlation between breast feeding rate and risk for developing JIA. Some studies imply there could be a correlation, yet other studies did not find proof for the same (12). Similar, conflicting results have been shown between risk for JIA and maternal smoking during pregnancy. A recent, comprehensive, systematic review of studies on environmental factors influencing the risk for JIA found evidence for a small increased risk associated with delivery by caesarean section. A small risk reduction was associated with having siblings and with maternal prenatal smoking. However, an equally important message of the publication is probably the demonstration of the challenges of performing comparable, epidemiological studies in a clearly defined study population (13).

1.2.2.3 Pathogenesis of arthritis

Activation of inflammatory cells and aggregation of them in and around the joint synovium is a cornerstone of the pathogenesis in JIA. Lymphocytes, plasma cells, macrophages, fibroblast-like synoviocytes, osteoclasts and other inflammatory cells are recruited from the peripheral blood circulation. The cells migrate over the endothelial blood vessel wall into the synovium and into the joint fluid. At the same time, local inflammation in the synovium induces increased vascularity and blood flow, probably mediated by vascular endothelial growth factor (VEGF). Aggregation and migration of inflammatory cells over the endothelial wall is facilitated by several factors e.g. tumour

necrosis factor alpha (TNF- α) and interleukins (e. g. IL-1, IL-6, IL-12 and IL-15). Inflammatory factors also influence local blood perfusion factors such as flow, mean transit time of the blood and exchange rate of substances over the synovial membrane. These features are thought to represent the hallmark of arthritis, namely synovitis. The amount of synovial fluid in joints affected by arthritis is often increased, a process that probably also is regulated by inflammatory cells and inflammatory factors. Further the inflammatory process induces aggregation of a tumour-like tissue component called pannus in and around the joint and synovium. Pannus is thought to be composed of an ongoing recruitment of inflammatory cells from the peripheral circulation, not a neoplastic process per se. Pannus and hypertrophy of the synovium further are important components in production and release of enzymes that affect the integrity and stability of bone and chondral tissue of the joint (14). Release of these enzymes affect and destabilize the extracellular matrix of both chondrocytes and the different kinds of collagen that constitute much of the joint tissue. In time, focal aggregation of inflammatory cells and the following degradation of joint tissue leads to defects in chondral tissue and bone (erosions).

1.2.2.4 Diagnosis

As stated, juvenile idiopathic arthritis (JIA) is mostly described to be an autoimmune condition. The disease affects children with onset of symptoms before the 16th birthday. Arthritis in one or more joints must persist for at least 6 weeks and other causes of arthritis must be excluded (15). The presentation of the disease is variable with symptoms ranging from joint pain, joint stiffness, reduced range of motion, fatigue, fever, rash, and visual impairment. Some patients are affected in one or a few joints, while others display many affected joints. JIA is probably not one disease, but a diagnostic term covering many different conditions with some common features. The diversity of symptoms and differing prognosis has led to a classification system suggested by The International League of Associations for Rheumatology (ILAR) dividing JIA into seven categories (Table 1). One of these categories, systemic JIA, is clearly distinguished from all the other forms, and is probably an autoinflammatory, not

an autoimmune disease. This category was probably what dr. Still described in 1897 and was for nearly a century named Still's disease.

Table 1. Typical features of the International League of Associations for Rheumatology (ILAR) categories of juvenile idiopathic arthritis. Adapted from reference 16

Classification category	Onset age	Typical features	Sex ratio
Systemic arthritis	Throughout childhood	Fever, rash, systemic symptoms	F=M
Oligoarthritis	Early childhood	Arthritis in <5 joints the first 6 months	F>>>M
RF-positive polyarthritis	Late childhood or adolescence	Arthritis in >4 joints the first 6 months and RF positive at least twice 3 months apart	F>>M
RF-negative polyarthritis	Peak at 2-4 years and at 6-12 years	Arthritis in >4 joints the first 6 months and RF negative	F>>M
Enthesitis-related arthritis	Late childhood or adolescence	Enthesitis and lower extremity arthritis and mostly HLA-B27 positive	M>>F
Psoriatic arthritis	Peak at 2-4 years and at 9-11 years	Arthritis and psoriatic rash (or family history of psoriasis)	F>M
Undifferentiated arthritis	Not relevant	Arthritis that fulfils criteria of none or >1 of the other categories	...

1.2.3 Epidemiology

JIA is the most common chronic rheumatic disease in childhood, and girls are generally more often affected than boys (16). The reported incidence and prevalence rate of JIA vary considerably. In 2014, Thierry (17) published a review of 43 epidemiological studies from Europe. A striking variation in both annual incidence (1.6-23 per 100 000 children) and prevalence (3.8-400 per 100 000 children) was found. The cause of these differences is thought to be found in varying genetic predisposition in different ethnic

groups, somewhat differing interpretation of the disease classification system and differing design and inclusion criteria for the studies. In the Nordic countries the annual incidence is approximately 15 per 100 000 children, with the highest incidence found in Northern and Central Norway (23/100 000) (18).

1.2.4 Disease course and outcome

The development of the disease, the probability of achieving remission, and the risk of complications vary considerable between the different categories of JIA. Numerous papers have been published on predictors of remission, and risk factors for ongoing or destructive joint disease. Severity of disease at onset, presence of symmetrical disease, presence of rheumatoid factor, and persisting active disease are predictors that have been associated with worse prognosis. The systemic JIA category displays a variable course ranging from unremitting arthritis accompanied by the rare, but life-threatening macrophage activation syndrome, to a more benign disease course resulting in drug-free remission (16). Oligoarthritis, especially the persistent category, is generally regarded as the JIA category with the least aggressive disease course. In total, despite modern and probably adequate treatment, a large proportion of the JIA patients do not achieve remission (19, 20).

As shown, JIA is a disease characterized by inflammation affecting joints and periarticular tissue. Naturally, much of the treatment generally therefore focuses on preventing deteriorating bone health e.g., joint deformity, growth impairment and osteoporosis. The disease however can also affect other types of tissue, such as inflammation of the iris (iridocyclitis), and for systemic JIA, also affect inner organs and result in hepatomegaly, splenomegaly, serositis and lymph node engagement. Some of these complications, especially iridocyclitis, can present in asymptomatic patients. Detection and treatment of these, potentially devastating complications to arthritis demands follow-up by highly specialized paediatricians (21).

1.2.5 Treatment

The prognosis and risk of complications of all categories of JIA is highly dependent on early detection and treatment of active disease (22). Today, treatment of JIA is not only depending on pharmacological intervention, but physical and occupational therapy and psychosocial support / education also significantly affects the quality of life of the patients. As the implementation of these non-pharmacological interventions usually do not depend on the results of medical imaging, further explanation of these interventions will not be pursued here.

In the middle of the 20th century corticosteroids, gold salts, penicillamine and hydroxychloroquine represented the known medical treatment options for children with rheumatic disease. In the 1980s and 1990s placebo-controlled studies proved their ineffectiveness and these drugs, except corticosteroids, were abandoned. In the same era, a series of studies were performed studying several nonsteroidal anti-inflammatory drugs (NSAIDs) proving their effectiveness and relatively low risk of adverse events (23). Under the Cold War, a Soviet-American prospective, double-blinded, randomized, placebo-controlled multi-centre study was performed on the effectiveness of methotrexate, a slow-acting antirheumatic drug. The study confirmed low-dose treatment of the drug as effective and safe, under certain requirements (24). Methotrexate soon become one of the most extensively used disease-modifying antirheumatic drugs (DMARDs) to treat children with JIA.

The intraarticular injection of corticosteroids (IAC) is used to reduce joint inflammation and to achieve fast, local relief of symptoms of arthritis. The technique has been practiced at least since 1986 and is mainly used in the oligoarticular and polyarticular JIA categories (25). The IAC procedure is not considered controversial, and its use is widespread, although there is a paucity of randomized controlled studies (26).

Further, the long-term outcomes of IAC procedures are not thoroughly studied, partly due to the ethical difficulties in randomizing patients in a study with a “treatment arm” and a “non-treatment arm”. Not until 2017, Ravelli and co-authors tested the efficacy of combining methotrexate with IAC vs. a group with IAC but no methotrexate in a

prospective, randomised study on children with oligoarticular JIA. The study did not find convincing evidence supporting the combination of IAC and methotrexate (27).

As mentioned earlier, the inflammatory process in JIA is mediated and maintained by disturbances in the regulatory mechanisms of the immune system. Aiming at modulation of these mechanisms, a new class of therapeutic agents, the biologic drugs, was implemented in clinical use in the late 1990s. Biologic treatment is divided in different categories, influencing different types of mediators of inflammation such as interleukins, tumour necrosis factor alpha, B-cells, and interferons. The advent of the biologic DMARDs (bDMARDs) in contrast to the class of synthetic DMARDs (sDMARDs) such as methotrexate, has proven to be a milestone regarding effectiveness of pharmacologic treatment of JIA (28). In general, the safety profile of biologic treatment is acceptable, given the good anti-inflammatory effect (29, 30). Biologic drugs, sometimes in combination with NSAIDs or methotrexate, is therefore often used to achieve remission or at least suppress inflammation as extensively as possible in an increasing population of children with JIA not reaching inactive disease on methotrexate alone.

The goal of treatment of arthritis in the temporomandibular joint (TMJ) in JIA is the same as in other joints, full remission. There are few, if any, prospective, randomised studies on the effect of systemic treatment focusing specifically on TMJ arthritis. Still, systemic treatment of TMJ arthritis is common and not controversial (22). In their upcoming publication, Schmidt and co-workers found evidence resulting in similar recommendations for diagnosis and treatment of the TMJ in JIA (31).

As in other joints, intraarticular injection of corticosteroids (IAC) has been tried to achieve remission, albeit studies on their efficacy and safety have shown diverging results (32). In 2018, a joint American-Danish statement addressed that IAC is associated with significant adverse events and that robust evidence for the continuation of IAC procedures in the TMJs is lacking (33).

1.3 The temporomandibular joint in JIA

In JIA, the temporomandibular joint is commonly affected (39-78%) although the exact prevalence of TMJ arthritis in JIA is not known (34-37). It is usually hypothesized that arthritis in the TMJ affects the joint in similar ways as in other joints e.g. hip, knee, ankle and wrist. However, robust evidence for this is lacking and differences in anatomical and physiological features between the TMJ and other joints may hamper comparisons. The consequences of arthritis in the TMJs are discussed below.

1.3.1 Normal development of the TMJ

In utero, usually at the end of the first trimester, the TMJ begins to differentiate from three separate mesenchymal condensations which differs from the development of other synovial joints. The most cranial condensation develops into the glenoid fossa of the temporal bone, while the most caudal condensation develops into the mandibular condyle. In between, the third condensation develops into the articular disc (38). Being composed of fibroblasts (approximately 70%) and chondrocytes (approx. 30%), the articular disc closely resembles the menisci of the human knee joint. However, the exact composition of the articular surfaces of the glenoid fossa and the mandibular condyle during early childhood is not entirely known.

The mandibular condyle is defined as a secondary cartilage which differs from the primary cartilages in the limbs and cranium. A significant feature of the secondary cartilage is the presence of cells with periosteal origin. These cells, the periosteal cambium, and the adjoining cells is probably where most growth occurs and constitute the most superficial part of the joint surface, overlying a zone of fibrocartilaginous cells. This feature is essential to the understanding of growth of the mandibular condyle as there is no mandibular equivalent to the physis of the long tubular bones of the extremities. The joint surface of the mandible and the glenoid fossa is thus histologically different from surfaces of joints with primary cartilage (39).

The chondrocytes of the TMJ surfaces produce fibrocartilage, not hyaline cartilage, containing collagen type 1, collagen type II and collagen type X (40, 41). Genetic studies on mice with knock-out-genes and studies focusing on altered mechanics of the TMJ have shown intricate relationships between genes and physical strain on the joint surfaces. The normal development of the glenoid fossa therefore seems dependent on the appropriate load exerted by the mandibular condyle. Following the development of the three mesenchymal condensations into the glenoid fossa, the articular disc, and the mandibular condyle, the TMJ is divided into two joint cavities lined by a thin synovium; the lower cavity below the disc and the superior cavity above the disc (Figure 1).

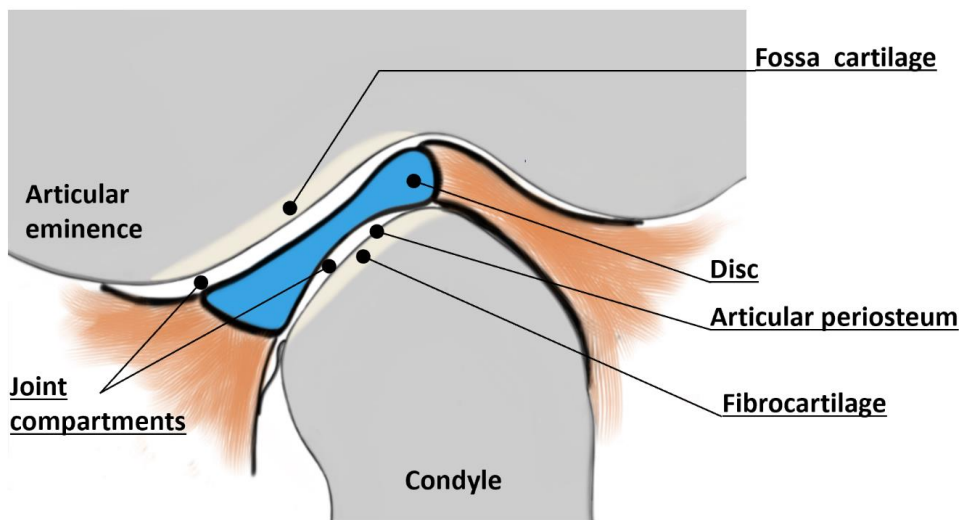


Figure 1. Schematic presentation of the temporomandibular joint shown in the sagittal plane. With permission from Thomas Johnsen

In the postnatal period, during childhood and into early adulthood, the morphology of the TMJ undergoes almost constant change. The articular eminence of the temporal bone, in front of the glenoid fossa, grows rapidly during the child's first three years and then, more slowly until completion in late adolescence. During the same period, substantial

growth and remodeling occurs in the mandibular condyle and ramus. This process of lateralization of the condyles and vertical growth of the ramus is essential in the development of the growing skull, and to make place for the erupting teeth (38, 42, 43). More specifically, the mandibular condyle grows significantly in the mesiolateral dimension, and to a lesser extent, in the anteroposterior dimension. In late adolescence, when visualized in the transverse plane of cross-sectional imaging, the condyle reaches an elliptical or sickle-like form with a slight tilt in the anteromedial direction (Figure 2).



Figure 2. Cone-beam computed tomography in the transverse plane of an adolescent, showing the sickle-like form of the centre of the mandibular condyles with a tilt in the anteromedial direction.

In the growing child and teenager there is an increasing anterior tilting of the mandibular condyle relative to the ramus known as anterior inclination. The grade of inclination increases by age and is usually determined by medical imaging. However, robust data on the normal growth rate and appearance of the condyle and its inclination in healthy individuals is sparse. The paucity of data is probably mainly due to inclusion and measuring challenges resulting in only a few, debatable publications on this topic (44, 45).

1.3.2 Pathology of the TMJ

Pathological change of the TMJ in JIA is characterized by a series of findings, many of which, but not all, are similar to pathological changes in other arthritic joints. As mentioned earlier these findings include joint effusion, increased synovial and bone perfusion leading to synovitis and edema-like changes, synovial thickening, aggregation of pannus, degradation of joint surfaces, and growth disturbances. In severe cases, growth disturbances in the TMJ can lead to facial asymmetry and malocclusion. Recently, a series of publications have acknowledged the difficulties in diagnosing arthritis in the TMJs. Clinical examination is hampered with low sensitivity, and it is hard to differentiate arthritis from other oral health issues. Sometimes clinical findings in TMJ arthritis can overlap with clinical findings with non-arthritic individuals, with so-called temporomandibular dysfunction (TMD) (46-48). A consensus-based statement from the TMJaw group (49) proposed the term “TMJ arthritis” to be signs indicating active inflammation. The same group acknowledge the low sensitivity and specificity of clinical examination of the TMJ, promoting medical imaging with MRI as a necessary means for evaluation of active TMJ inflammation (50). The term “TMJ deformity” has been suggested for JIA-related structural change such as joint surface irregularities, altered shape of the joint surfaces, volumetric change of the bones and growth disturbances.

In terms of clinical symptoms, a JIA diagnosis is associated with increased risk of orofacial pain, increased frequency of periodontal conditions, reduced orofacial function and general quality of life in the early phases of the disease (51, 52). Orofacial symptoms include several findings, but often include muscle pain on palpation, reduced ability to open the mouth compared to age-related healthy peers, and asymmetric mouth opening. During a three-year follow-up, Stoustrup and colleagues found an increasing cumulative incidence of orofacial symptoms and dysfunction, regardless of JIA category (53). Similarly, significant signs of disease and symptoms were found in a controlled follow-up study of JIA patients 17 years after diagnosis. The adult JIA patients showed increased TMJ pain, morning stiffness, and problems with chewing compared to a healthy population (36).

Pathologic change such as joint effusion, synovitis, joint surface degradation and deformity are presumed to correlate with clinical symptoms, but the exact mechanism and correlation between them is not clear.

1.4 Imaging of the TMJ

As mentioned in the section on pathology, the diagnostic work-up, management and follow-up of arthritis in the TMJ in patients with JIA is more influenced by medical imaging than other joints affected by the disease (46-48). The purpose of medical imaging of the TMJ in children with JIA is to detect and monitor signs of inflammation, to detect and monitor signs of structural joint deformity and lastly, to detect and monitor growth disturbances. To achieve these goals, the imaging modality must satisfy certain technical conditions regarding spatial resolution, tissue contrast, feasibility, and radiation dose.

1.4.1 Radiographic techniques

In the 20th century, imaging of the TMJ was dominated by radiographic methods such as plain radiographs, orthopantomogram (OPG), and cephalometric radiographs. Despite their advantage of low radiation dose and high feasibility, the drawbacks of these modalities such as geometric distortion, superimposition of multiple structures, limited ability to detect early, bony change and inability to detect soft tissue pathology have reduced their impact in the diagnostic process (54-56).

1.4.2 Ultrasound

Ultrasound is a relatively cheap, accessible, easy-to-use imaging modality without ionizing radiation. In general, ultrasound is well suited for imaging of soft tissues and is mostly well tolerated by children. However, the anatomic configuration of the TMJ severely limits the possibility to examine the whole joint, leaving only the lateral aspect available. There are no known, standardized scoring systems for ultrasound-guided

evaluation of the TMJ in JIA and there is a lack of anatomic, age-related standards of the normal paediatric TMJ. Further, the problematic interobserver variability and relatively low sensitivity and specificity for arthritis-related pathology precludes ultrasound from being the primary imaging modality of the TMJ in patients with JIA (54, 57, 58).

1.4.3 Magnetic Resonance Imaging (MRI)

MRI is an imaging modality able to depict both bony structures and soft tissue with imaging appearance basically depending on the inherent molecular structure of the tissue. By placing the tissue in a large, static magnetic field and manipulating the tissue with radiofrequency pulses, one can spatially localize the different structures in the tissue. Depending on the density and mobility of the protons in the tissue, a specific signal is sent out from the tissue. To detect this magnetic signal sent out from the tissue, a coil is applied around the patient; in TMJ imaging, more specifically around the patient's head. By adjusting the timing and the way the system detects signal from the tissue, images with different weighting of the inherent tissue contrast are produced. Depending on the timing properties of the acquisition, the produced image is categorized in contrast groups called T1-weighted, T2-weighted, or proton-density-weighted (PD) images. To collect sufficient signal data, an ordinary MRI sequence focussing on a certain tissue contrast, is acquired in 1-6 minutes. A conventional, clinical MRI examination usually is composed of 3-6 sequences with some pauses in between. In total, an MRI examination of the TMJ requires the patient to stay in the scanner for approximately 25-50 minutes, depending on the specific MRI protocol. Due to the strong magnetic field, the usefulness of MRI is restricted in patients with metallic devices. The narrow conditions in the MRI camera, combined with the narrow-fitting coil around the head not seldomly gives the patient a feeling of being constrained which can lead to considerable claustrophobia. The abovementioned properties of the MRI examination obviously make the procedure demanding and sometimes unpleasant for the paediatric patient. Thus, sedation is needed for patients under the age of four to six years of age.

1.4.3.1 Osteochondral tissue on MRI

MRI uses the alternating polarity of hydrogen protons to produce an image. In human cortical bone there is a paucity of mobile hydrogen protons which renders a relative lack of signal from that area. This lack of signal is depicted as black areas on all MRI sequences. Mostly, imaging focussing on cortical structures is based on T1-weighted images either presented as thin slices in a 2-dimensional acquisition or as a volume in a 3-dimensional acquisition. Due to the small size of the TMJ and the relatively low spatial resolution of conventional MRI sequences as compared to other modalities, much effort has been spent in establishing MRI sequences with higher spatial resolution. For that purpose, Karlo and co-workers (59) used a high-resolution computed tomography (micro-CT) examination as reference on 8 cadaveric heads to evaluate a series of MRI sequences. They found the 3D-fast spoiled gradient recalled echo sequence to outperform the other sequences in terms of visualizing cortical, bony abnormalities.

On the joint surfaces of the TMJ, overlying the cortical bone, there is a thin rim of articular cartilage. As described earlier, the joint surfaces of the TMJ differ from other joints being profoundly involved in the mandibular growth and composed by fibrocartilage in contrast to hyaline cartilage in other joints. In the TMJ, as in other joints, image interpretation of the joint cartilage is dependent on PD-weighted images, with important support by the T1- and T2-weighted images. The small size of the TMJ, the even smaller size of the TMJ cartilage, and the complex anatomy of the joint makes MR-imaging of its cartilage particularly challenging, given the relatively low resolution of the technique. However, no other imaging modality has shown its superiority over MRI in imaging cartilage of the TMJ (60). The presence of pathological aberrations in the cortex and fibrocartilage as presented by MRI in a patient with arthritis is thought to represent structural change due to the disease although there is increasing knowledge of the overlap between normal and pathological findings (50).

The medullary space lies deep to the cartilage and cortical bone, consisting of trabecular bone and bone marrow. In the growing child, this tissue is in almost constant change. In the younger child the bone marrow is dominated by hematopoietic, cell-rich tissue, but in the adolescent and young adult the marrow is converted into fat-rich, yellow marrow, with more sparse distribution of cells (61). This has implications on the MRI-based imaging of the TMJ as bone marrow edema, or “edema-like marrow signal intensity (ELMSI)” (62) is thought to represent an important sign of inflammation in the arthritic patient. In theory, the inflammatory process in the bone is characterized by aggregation of inflammatory cells, mediated by cytokines, replacing the adipocytic cells, although studies confirming the histopathologic correlation of this statement are sparse. In MRI this process is expressed as reduced signal intensity on T1-weighted images as the fraction of fat is reduced. Respectively, the signal in water-sensitive sequences as T2 and proton-weighted images is increased (63, 64). The conspicuity of this finding in water-sensitive sequences is increased by applying fat-suppressing (fs) techniques in the MRI acquisition (65).

The clinical implications of the presence of bone marrow alterations in MRI examinations are complex and highly dependent on the clinical setting (66, 67). Nevertheless, in adults with rheumatoid arthritis bone marrow edema has been shown to precede structural change in the joint surfaces, subsequently leading to joint destruction (68, 69). In the paediatric patient however, interpreting imaging changes in the bone marrow signal strictly as signs of pathology is disputed (70).

The exact background for the sometimes heterogenous depiction of the paediatric bone marrow as presented on MRI is not clear. The general concept of the age-related conversion of red marrow to yellow marrow from the periphery towards central regions is accepted (61). This concept gives some guidance to the radiological interpretation of bone marrow changes in children, although robust, age-related normal standards of the paediatric bone marrow is lacking. Some publications can be found (71-73) but the selection of patients, the age-categories under study, and sample sizes make the

transferability to the JIA population questionable. Further, moderately heterogeneous bone marrow on MRI in close proximity to the growth zones of tubular bones in the asymptomatic, adolescent and adult patient is thought to be caused by residual red bone marrow and as such represents a normal finding.

The TMJ is considered part of the axial skeleton and as such is included in the later phases of red marrow conversion. The mandibular, medullar cavity is close to the growth centre in the joint surface of the condyle. These issues most likely hamper the specificity of the radiologic interpretation of bone marrow change. An attempt to define the MRI-based appearance of the normal TMJ bone marrow was made by Junhasavasdikul (44). However, patients with imaging findings believed to represent pathology were excluded and the study also included patients with JIA. Thus, the usefulness of the publication as a population-based reference for the TMJ of healthy children is questioned.

1.4.3.2 Soft tissue on MRI

MRI is the only modality which can depict the soft tissues of the whole TMJ. Using separate sequences or combinations of sequences the radiologist can evaluate anatomical structures thought to be essential in the diagnostic work-up of the JIA-patient.

The synovium, and the changes affecting it, is thought to be the structure showing the earliest signs of pathology in the arthritic joint. As described earlier, the synovium is composed of a thin, intimal layer of cells and a subintima consistent of an intricate network of arterial, venous and lymphatic structures (74). In the early phase of inflammation various cytokines influence the synovial tissue by increasing local blood perfusion, increasing permeability of the capillary walls and later, locally aggregating inflammatory cells. In terms of MRI findings in the TMJ, the increased perfusion and vascular permeability can be visualised on gadolinium enhanced, mainly T1-weighted images with fat-suppression (75, 76). Numerous researchers have tried to define MRI-markers of pathological synovial distribution of intravenous contrast, demonstrating a

significant overlap between children with and without JIA, probably depending on imaging plane, timing of contrast injection and image acquisition and heterogeneity of the studied patient cohort (77-81).

Further, the aggregation of inflammatory cells in the synovium, leading to synovial thickening, a finding usually seen in long-standing arthritis, is represented by areas of intermediate signal intensity on water-sensitive sequences with fat-suppression (T2-fs) (82). Synovial thickening is thought to be a definite sign of pathology, although to the best of our knowledge, no true population-based reference standards have been published.

As in other parts of the body, pathologic effusion of joint fluid in the TMJ is an important marker of arthritis (34). The detection and the assessment of the amount of joint fluid on MRI is dependent on water-sensitive sequences such as T2-fs and PD-fs. There are publications defining what amount of joint fluid is within normal, mostly setting a cut-off at 1 mm thickness of a joint compartment (83). A parallel definition also exists, defining a normal MRI-based amount of joint fluid in the TMJ as “small dots or lines” on T2-weighted images (84).

Despite its shortcomings in many areas of TMJ imaging in JIA, MRI has emerged to one of the mostly used imaging modalities to diagnose and monitor TMJ arthritis in JIA and further research efforts will probably develop the technique even more (85).

1.4.4 Computed tomography (CT) and Cone-Beam (CB) CT of the TMJ

Computed tomography (CT) and cone-beam computed tomography (CBCT) are imaging modalities utilizing ionizing radiation to depict anatomic structures. The different types of tissues in the visualised object attenuate the radiation in different ways and by analysing the attenuation patterns, detailed anatomic images can be produced. Both techniques produce a 3-dimensional image dataset by acquiring image data from multiple angles of the object, a method known as tomography. Twenty to thirty years ago, CBCT emerged as the preferred imaging modality in many areas of maxillofacial radiology showing comparable accuracy, lower cost, higher availability and lower radiation dose than conventional CT (86-88). Compared to radiographic techniques,

CBCT gives significantly higher radiation dose, ranging from 0.02-0.500 mSv, depending on equipment, field of view and exposure parameters. Nevertheless, the typical dose, being around 0.1 mSv, is relatively low compared to CT (0.12-1.2 mSv) (89, 90) as well as compared to the annual background radiation dose of 4.5 mSv (91). The CBCT-technique has the advantage of providing exquisite visualisation of complex anatomic structures, avoiding problems with distortion and superimposition of structures (92). However, as CBCT-imaging is dependent on relatively large differences in tissue density to produce image contrast, the technique is not able to separate different types of soft tissue, leaving osseous structures as its primary focus (54, 93, 94).

The spatial resolution of CBCT supersedes MRI by far with possibilities to achieve isotropic voxel sizes down to 80 μm (95). The high resolution gives unmatched opportunities to depict small, osseous changes in the TMJ, usually focusing on abnormalities in the joint surface (96, 97).

By producing high-resolution, reproducible, relatively cheap image datasets at the expense of an acceptable radiation dose, CBCT has been defined as the optimal means of mapping the osseous details of the TMJ in JIA (49). Nevertheless, the lack of a population based, age-related reference standard of healthy children underscores the need for further research, as stated by Caruso et al in their review from 2017 (93).

1.5 Assessing agreement in radiology

A radiology report consists of a series of conscious and unconscious decisions made by the radiologist interpreting the images, ideally leading to a clear conclusion. In an ideal setting, another radiologist presented with the same image dataset and clinical information would reach the same conclusion, the definition of perfect inter-observer agreement. This is seldom the case. Many factors, both connected to the image acquisition, the way the images are presented to the radiologist and the radiologist him/herself, will affect the agreement of the two radiologic conclusions. To further understand the concept of agreement, the terms precision and accuracy need to be addressed. The precision of a diagnostic method is defined by how close two separate

measurements are to each other, e.g. if two separate measurements of blood pressure with a cuff around the patient's arm both show exactly 120 / 80 mm Hg, the precision is high. The accuracy of the method, on the other hand, is defined by how close the measurement is to a "true value" or golden standard, e.g. the blood pressure as defined by an intra-arterial measurement technique. Ideally, a diagnostic method is both precise and accurate, but this is not always the case.

In their much-cited work from 1991 Fryback and Thornbury (98) presented a hierarchical 6-level model of efficacy for diagnostic methods in medical decisions, which can help the radiologic community to higher levels of agreement (Figure 3). In short, the paradigm states that a high level of efficacy in the upper part of the hierarchical model necessitates a high level of efficacy of the underlying levels. Opposite, a high level of efficacy in a low level does not automatically translate into high efficacy at a higher level.

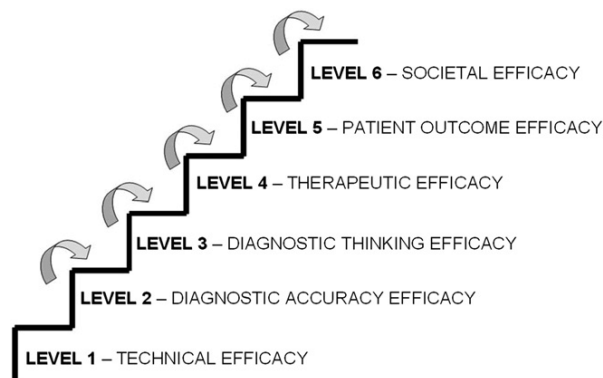


Figure 3. Fryback and Thornburys hierarchal model for efficacy, Adapted from reference 98

At the first level of the model, the importance of consistency and precision in technical parameters such as resolution, contrast, sharpness etc of the diagnostic method is evaluated. The importance of robust, thorough studies at this level must not be underestimated, although the absence of complex human interaction on these parameters often makes the studies less prone to bias.

At level 2, more complex variables of the diagnostic method are evaluated, such as precision, sensitivity, specificity, predictive value of a positive and negative test, receiver operating characteristics (ROC) etc. The major difference between levels 1 and 2 is the introduction of the operator (radiologist). This explicitly includes the operator in the medical decision and by that also includes the complex, human, cognitive processes that lead up to this decision. The decision is no longer a function of the image alone, but a function of the image and operator together. Another complicating factor at level 2 is the fact that measures of accuracy of a diagnostic method often are dependent on the prevalence of the disease (99). By selecting which patient or group of patients are referred to medical imaging, the referring clinician thereby influences the test accuracy.

At level 3 the impact of the result of the diagnostic test is measured. If the clinician changes the treatment regime, if the range of differential diagnoses is changed, if a diagnostic hypothesis is strengthened, or just if the referring clinician is reassured the patients is well, they are all impacts of the result of the diagnostic test. If no impact can be shown, the diagnostic test is probably not justified.

To justify spending of economic and human resources on a new diagnostic method, and not to mention justify exposing patients to the method, it needs to be tested at least according to the three basic levels of Fryback and Thornburys model.

In the light of the presented model, the terms precision and accuracy now can be seen as necessary elements of a robust, clinically, and societally justified diagnostic method.

1.5.1 Measuring precision

Precision of diagnostic methods can be measured in many ways and along different scales. Precision measured along a scale of intra-observer agreement is used when testing the repeatability of a test method used at least twice by the same observer. Further, inter-observer agreement is used when testing the reproducibility of a test method used by at least two observers. Thus, measurement of agreement is not dependent on a ground truth or golden standard, but a means to compare results for the same observer (intra-), between observers (inter-) or between methods (inter-method).

Different statistical methods should be used for measurement of agreement of continuous and categorical variables, respectively (100-102). For example, the clinical difference of a tumour measuring 1 or 2 cm cannot be directly compared to the difference between a grade 1 or grade 2 osteosarcoma.

1.5.1.1 Categorical variables

Data which can be categorised in discrete groups, such as pregnant/non-pregnant, smoker/non-smoker is called categorical data. Categorical data can also consist of more than two groups (or grades) e.g. non-smoker/present smoker/smoked earlier. There is no clear, linear relationship between the grades, even if the data can be assigned numerical labels.

Assessing the absolute agreement in a setting of binary, categorical variables can be expressed as $P_o = (A+D)/n$, where P_o denotes the proportion of observed agreement and n the total number of examinations (Table 2).

Table 2. Contingency table for calculation of Cohen’s Kappa

	Observer 1		
		Positive	Negative
Observer 2	Positive	A	B
	Negative	C	D
	$A * C$	$B * D$	n
			$A * B$
			$C * D$

This gives an easily understood measurement of the proportion of cases where the two observers agree. However, this equation does not take into consideration the number of cases where the observers would have agreed simply by chance. To assess agreement beyond chance Jacob Cohen demonstrated a method to adjust the proportion of absolute agreement (103). By considering the products of the marginals in the contingency table in table 2 one can calculate the expected agreement by chance (P_e) (Equation 1)

Equation 1:

$$\text{Expected agreement by chance} = \frac{\left(AC * \frac{AB}{n}\right) + \left(BD * \frac{CD}{n}\right)}{n}$$

By subtracting the chance agreement (P_e) from the observed agreement (P_o) and divide the sum by the proportion of agreement that did not occur by chance ($1 - P_e$) one can estimate the agreement that occurs beyond chance, Cohen's kappa (κ) (Equation 2).

Equation 2:

$$\kappa = \frac{\text{Observed agreement} - \text{Chance agreement}}{1 - \text{Chance agreement}}$$

This gives a result scaled from -1 to +1, where 1 indicates perfect agreement, 0 indicates chance agreement and -1 indicates perfect disagreement. The method is not restricted to binary variables but can be used also on variables with more than 2 grades.

The presented method assumes that all disagreement is equally important, which is often not true. For example, the difference between no pathology and mild pathology can be clinically more important than the difference between mild and moderate pathology. To adjust for this assumption but still correcting for agreement by chance, Cohen proposed weighting of the disagreement, a method called weighted kappa (104).

The standard error of the κ value can be calculated and thus one can estimate the confidence interval of the κ value, usually defined as $\kappa \pm 1.96 * SE(\kappa)$. The kappa value and its confidence interval does not represent an absolute measurement that uncritically can be used as a comparator when assessing different methods. The value must be seen in a clinical context, considering prevalence of the disease, number of categories, the abilities and experience of the readers and, most importantly, the clinical importance of diagnostic disagreement. Further, there is no evidence-based scale to guide the

interpretation of the kappa value. In 1977, Landis and Koch proposed values ranging from < 0 as poor agreement, 0-0.2 as slight, 0.21-0.4 as fair, 0.41-0.6 as moderate, 0.61-0.8 as substantial and 0.81-1 as almost perfect (105). The authors explicitly noted that the divisions are arbitrary, and others therefore have implemented the guide with minor modifications.

In many situations, a diagnostic method is used by more than two operators, e.g. three radiologists separately interpreting images of the same patient. Since Cohen's kappa does not allow for calculation of agreement of more than two readers, Fleiss proposed a kappa-like model allowing for 3 or more readers of the same patient (106). Like its predecessor, Fleiss kappa also produces values ranging from -1 to 1, where 1 denotes perfect agreement between all readers.

In a setting with skewed distribution of the number of observations in each box in Table 2, a situation with high observed agreement (P_o) but low κ can occur, sometimes called "the kappa paradox". This is often the case in a study with low prevalence of the studied disease, giving an unbalanced distribution in the contingency table. This phenomenon occurs despite unaltered sensitivity of the readers. If the distribution of the marginal totals (A*C, B*D etc) is closely analysed one can see that symmetrically, unbalanced marginal totals leads to a low κ . Opposite, asymmetrically unbalanced marginal totals lead to a high κ (107). This problem was addressed by Gwet (108), who constructed a model for assessing agreement which produces reliable results also when the prevalence of the finding is low or extremely high. The method probably has some strengths compared to Cohen's and Fleiss' kappa, but it is not as thoroughly tested and known as its predecessors and will not be used in this thesis.

1.5.1.2 Continuous variables

Data which can be presented along a scale of continuous values, such as weight, angles or blood pressure is called continuous data. There is usually a clear, mathematic relation in the distribution of the data.

When measuring agreement of two sets of continuous data, e.g. angles measured by two different radiologists, one can use different statistical methods. Bland and Altman

propose a graphical way of presenting the data in a plot (109). Amongst other factors, the transparency of the data distribution and the ease with which agreement can be evaluated has rendered the publication great impact.

The method plots the difference of the two measurements against the average of the two measurements. By calculating the standard deviation of the differences between the measurements (SD), one can define the 95 % limit of agreement as the mean difference ± 1.96 SD. This way of plotting the agreement (or lack thereof) gives the reader an opportunity to determine if the difference is important in a clinical setting relevant to him or her. Plotting the measured differences against the average of the two measurements further presents any skewing of the agreement. For example, two methods may show high degree of agreement in one range of averages, but low degree of agreement in another range of averages, Figure 4.

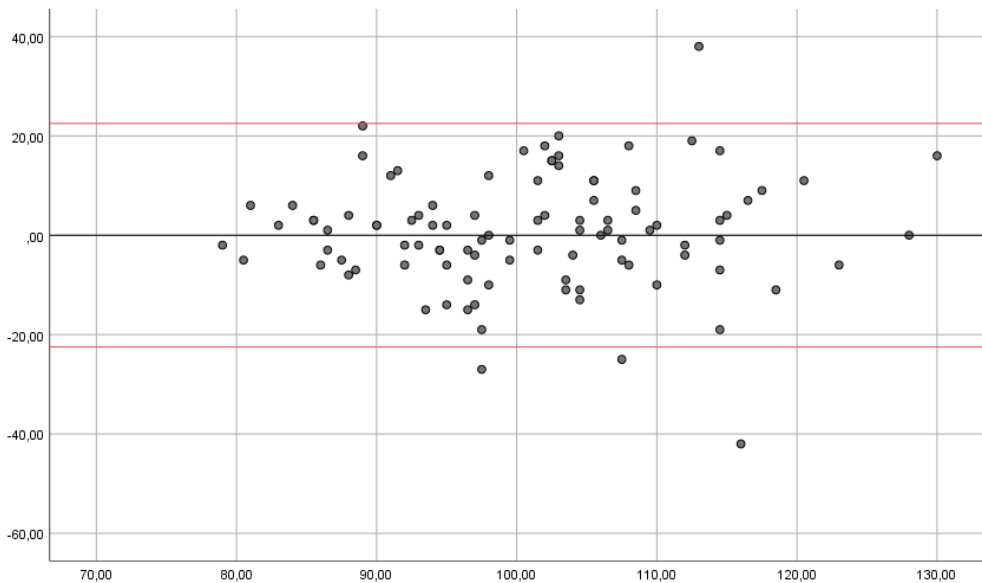


Figure 4. Example of a Bland-Altman plot showing 95 % limits of agreement (red lines) between two readers. (Y-axis denotes the difference between measurements and x-axis denotes the mean of the measurements). The plot illustrates a trend towards increasing disagreement moving from low to higher mean of the measurements.

Another commonly used method to evaluate the agreement of a diagnostic method is the intraclass correlation coefficient (ICC). Simply put, this method exploits the relation between two inherent properties of the dataset; the variability of measurements between the patients, and the measurement error (110)(Equation 3)

Equation 3:

$$\text{ICC} = \frac{\text{Variability between patients}}{\text{Variability between patients} + \text{Measurement error}}$$

As indicated in the formula, the ICC is highly dependent on the variation of measurements in the study sample. Thus, to be clinically relevant, the variation of the study sample must be somewhat similar to the population of the clinical situation the method is meant for. Further, many subtypes of ICC exist; addressing different sets of raters, whether the calculation is based on a single reader or an average of many readers, if the consistency or agreement is to be measured etc (111). The ICC-equation results in a single number ranging from 0-1, preferably with a 95 % confidence interval. This is by some seen as an advantage of the model as it gives the impression of being easy to compare to the ICC of other methods. However, the condensation of the result to a single number also reduces the amount of information brought to the reader. For example, the demonstration of the variation between the measurements is often lost, as is the possibility to relate the disagreement to a clinical setting. Neither does the method demonstrate if the amount of agreement varies as a function of the average of the measurements (112). Hence, the ICC method will not be used in this thesis, although it is commonly used in other publications.

2. Objectives

The overall aim of the work in this thesis is to establish normal standards for the development of the TMJ, next, to establish and validate scoring systems for MRI and CBCT of the TMJ in children with a known diagnosis of JIA.

Paper 1

The aim was to evaluate the reliability of established and new measurements for describing the normal MRI-based anatomy of the TMJ, and based on the most robust measures, to characterize the appearances of the normal TMJ in children and adolescents.

Paper 2

The aim was to identify and examine the precision of a set of MRI-based imaging markers for the assessment of inflammatory and destructive changes of the TMJ in children and adolescents with juvenile idiopathic arthritis. Next, to propose an MRI-based scoring system based on the most precise imaging markers.

Paper 3

The aim was to identify and examine the precision of a set of CBCT-based imaging markers for the assessment of destructive changes of the TMJ in children and adolescents with juvenile idiopathic arthritis. Next, to propose a CBCT-based scoring system based on the most precise imaging markers.

3. Materials and methods

Paper one is a retrospective, cross-sectional study, based on cerebral MR examinations of children examined for other reasons than TMJ issues.

Papers two and three are part of a large multicenter, prospective, observational, case-control study on JIA (Norwegian JIA Study – Imaging, oral health and quality of life in children with juvenile idiopathic arthritis, NorJIA) www.norjia.com. The study is registered on clinicaltrials.gov with identifier NCT03904459.

The NorJIA study is founded on the collaboration between multiple institutions in three Norwegian Regional Health Authorities, The Western Region, the Central Region, and the Northern Region. The participating centers invited patients aged 4-16 years, with a diagnosis of JIA according to the ILAR criteria from their catchment area to participate in the study. Data collection was performed from 2015 to 2020 and consisted of a baseline study visit and a follow-up visit 2 years after the first visit. A large amount of data was collected at each visit, ranging from disease characteristics and demographics, clinical examination with joint status, anthropometric and pubertal data by a paediatric rheumatologist, oral health examinations by experienced dentists, blood test results, biobank sampling (blood and saliva), patient-/parent-reported questionnaires, and extensive medical imaging including ultrasound, CBCT, bitewing, MRI, radiographs, and dual energy x-ray absorptiometry (DXA).

Sex- and age-matched controls, without JIA, were invited based on recruitment from the regular dental health control of children and adolescents in the same catchment area. Controls contributed with data in some of the aforementioned areas, although, due to constraints in ethics regulations and resources, imaging and blood test were not collected in controls in the baseline study. At the follow-up visit, we had ethical allowance to ask the controls if they would contribute with blood tests, DXA, radiographs of the hand and ultrasound. A small number of MRI examinations without intravenous contrast was also performed in this control cohort. No CBCTs were performed in controls.

3.1 Patients

In paper one, 101 patients who had undergone MRI of the head in the time interval 2005-2015 at Haukeland University hospital were identified in the hospital PACS. Inclusion criteria were age 2-18 years at the time of examination, and an examination performed on a 1.5 T or 3 T machine with a dedicated head coil. The MRI examination had to include at least a T2-weighted sequence with or without fat suppression, and a high-resolution 3D T1-weighted sequence (MPRAGE) with or without intravenous contrast. Exclusion criteria were a known diagnosis of systemic inflammatory disease, tumor affecting head or brain, hydrocephalus, cerebral malformations, skeletal dysplasia, suboptimal MRI examination and images showing known pathology in or close to the TMJ. Further, patients were stratified according to age and sex to ensure balance of the dataset.

In paper two, the MRI examinations of 86 participants of the NorJIA study were evaluated. The subset included participants from all three participating tertiary hospitals: Haukeland University Hospital, Bergen, St. Olavs University Hospital, Trondheim, and University Hospital of North Norway, Tromsø. Inclusion criteria were a diagnosis of JIA according to the ILAR criteria (15) and age between 4-16 years at inclusion. Exclusion criteria were suboptimal MRI examinations and the use of dental braces. The 86 participants represent a subset of the totally 228 children included in the first visit of the NorJIA study. The subset was selected to ensure a balanced dataset regarding age, gender, skeletal development, and TMJ pathology as defined by the radiology report. The rationale behind the selection of patients was to create a dataset which allowed testing of a wide range of imaging variables with a reasonable impact in terms of statistical significance. At the same time, inclusion of all 228 patients was not feasible due to time constraints and logistic challenges.

In paper three, the data was substantially based on the same, balanced population as described in paper two, namely 84 participants of the NorJIA study. Two participants from the population in paper two did not perform CBCT. The participants underwent CBCT examination in either the Oral Health Centre of Expertise in Western Norway

(TkV), Center of Oral Health Services and Research (TkMidt), or Public Dental Health Service Competence Centre of Northern Norway (TkNN). Exclusion criteria were suboptimal examinations due to artefacts.

3.2 Collection of imaging data

In paper one, 96 of the 101 patients were examined with a 64-channel head coil in a 1.5 T scanner (Siemens Symphony, Siemens Healthineers, Erlangen, Germany) with a T1-MPRAGE 3D sequence with slice thickness 1.1 mm, repetition time (TR) 2110 ms, echo time (TE) 3.93 ms, number of averages (NSA) 1, flip angle 15°, field of view (FOV) 260 x 280 mm, and image matrix 256 x 240. In 47 of the 96 patients examined in the 1.5 T scanner, the T1-weighted sequence was performed immediately after injection of intravenous contrast (0.2 ml/kg body weight of gadoterate meglumine (Dotarem, Guerbet, France). An axial or coronal T2-weighted sequence was performed in 87 patients with slice thickness 5 mm, TR 3240, TE 86, NSA 2, and matrix 256 x 190.

In five of the 101 patients the examination was performed with a 32-channel head coil in a 3 T MRI system (Signa HDxt, General Electric Medical Systems, Milwaukee, USA) with similar examination parameters as in the 1.5 T MRI system.

In paper two, the 86 patients were examined in a 3 T system at all three sites (Skyra, Siemens Healthineers, Erlangen, Germany) with a 64-channel head coil (32-channel at St Olav). An extensive MRI protocol was used in all patients, including coronal T1-weighted, sagittal T1-weighted MPRAGE, sagittal/oblique fat-saturated T2-weighted, sagittal/oblique fat-saturated T1-weighted, sagittal/oblique proton density-weighted with closed and open mouth and sagittal/oblique fat-saturated T1-weighted images after intravenous contrast. A more thorough description of the sequences is presented in appendix A. The main study protocol included intravenous contrast which was given in a standardised way in an antecubital vein with injection rate 2 ml/s (Dotarem 279.3 mg/ml, 0.2 ml/kg body weight) followed by 20 ml saline chaser. Demographic and clinical data was extracted from the NorJIA database, according to the NorJIA study research protocol.

In paper three, the 84 patients underwent a CBCT-examination of the TMJ on either a 3D Accuitomo 170, a Promax 3D or a Scanora 3D depending on study site (Table 3).

Table 3. Acquisition parameters of the three CBCT machines used in paper three

CBCT model (number of patients = n)	kVp	mAs	Field of view (mm)	Isotropic voxel dimension (mm)
3D Accuitomo 170 (n=30)	85	175	40 x 40 x 40	0.08
Promax 3D (n=29)	90	13.6	200 x 200 x 60	0.40
Scanora 3D (n=25)	90	45	60 x 60 x 60	0.13

3.3 Image reading

In paper one, before image reading, the three observers with special interest in paediatric musculoskeletal imaging (O. Angenete, T. Augdal and K. Rosendahl) studied available literature on normal development of the TMJ. Further, published scoring protocols for presumed, image-based, pathological change of the TMJ were reviewed. The literature and scoring protocols were thoroughly discussed and differing interpretations were resolved in consensus. The image reading was then performed on high-resolution diagnostic viewing screens in consensus between the three radiologists. To establish identical imaging planes, the high-resolution 3D-datasets were exported to a post-processing software (SyngoVia, Siemens Healthcare GmbH) and reconstructed in a standardized sagittal/oblique plane, along the mandible (Figure 5). In addition, conventional sagittal, transversal, and coronal acquisitions were used as appropriate.

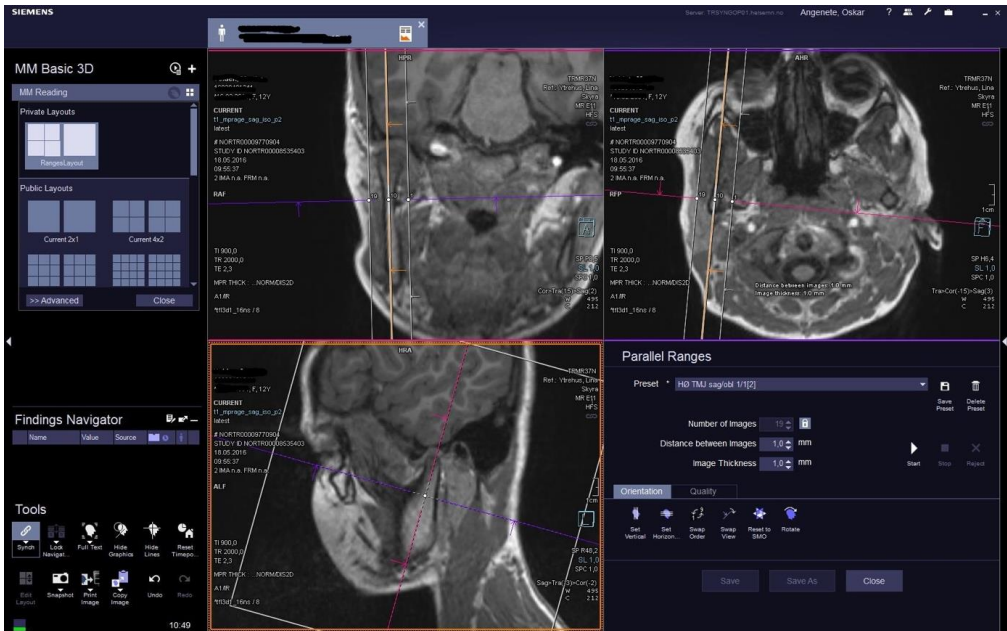


Figure 5. Post-processing software (SyngoVia) showing reconstruction procedure ensuring standardized sagittal/oblique presentation of the mandible.

A wide range of imaging features were scored in consensus, first by all three readers, and then, following a three-month interval, by two readers in consensus (OA and TA).

Morphological features which hopefully can help determine the difference between normal and pathological development were scored both in the standardized sagittal/oblique reconstruction, or in the standard presentations in the coronal or transverse plane. Condylar shape (0-3), anterior beak, condylar inclination (0-2), shape of the glenoid fossa (0-3), joint space width and disc position were all assessed in the sagittal/oblique plane. Condylar shape (0-2) was assessed in the coronal plane, while joint surface irregularities (0-1) was assessed in all available planes (Appendix B).

Image features previously thought to define signs of active arthritis, or lack thereof, were also scored. Bone marrow oedema was defined as an area of high signal on a fluid-sensitive sequence with corresponding areas on T1 returning low signal. Assessment of joint fluid was made in a semiquantitative way on a 0-2 scale, ranging from no fluid to

more than two mm of fluid in one or two joint compartments. Contrast enhancement was assessed on a 0-2 scale by judging the area in and around the TMJ as a) without enhancement, b) with mild enhancement seen directly around the condyle, or as c) moderate when enhancement was seen exceeding the joint tissue (78).

In paper two, the authors (O. Angenete and T. Augdal) first thoroughly studied published literature and scoring protocols aimed at defining TMJ pathology as assessed by MRI. Additional features, thought to represent future markers for JIA pathology, based on the initial work on paper one, were added to the test protocol. After the establishment of a final set of imaging features, the readers fine-tuned their understanding of the definitions of the imaging features. This form of inter-reader calibration was carried out on five MRI examinations of the paediatric TMJ, during two 1-day meetings and two video conferences.

T. Augdal read all 86 MRI examinations once and O. Angenete read all 86 MRI examinations twice, at an interval of at least 4 weeks. A total of 25 imaging features were scored, using high-resolution diagnostic screens in an appropriate environment (Figures 6 and 7) (Appendix C-F).

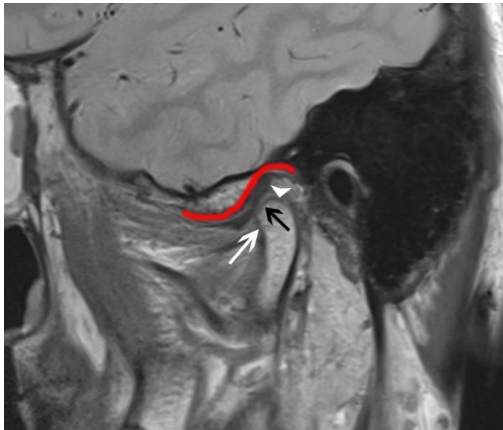


Figure 6

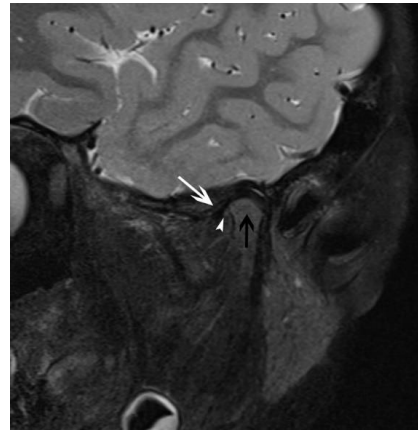


Figure 7

Figure 6. Sagittal/oblique proton-weighted image of the right TMJ of a 15-year-old boy with enthesitis-related juvenile idiopathic arthritis and disease duration 4 years, showing examples of imaging features in the osteochondral domain; condylar inclination (white arrow), condylar shape (black arrow), condylar irregularities (arrowhead), shape of the articular eminence and glenoid fossa (red line)

Figure 7. Sagittal/oblique T2-weighted fat-saturated image of the right TMJ of a 7-year-old girl with oligoarthritic juvenile idiopathic arthritis and disease duration 5 years, showing examples of imaging features in the inflammatory domain. The locations are typical, but not exclusive, for evaluation of bone marrow oedema (black arrow), synovial thickening (white arrow), and joint fluid (arrowhead)

In paper three, a similar approach as in paper two was used. Published literature on interpretation of CBCT-based findings in the paediatric TMJ was scrutinized, interpreted, and our understanding of the definitions was discussed. A wide set of imaging features was assembled, including both known, published morphologic definitions of the TMJ, published scoring systems, and experiences drawn from the results of papers one and two (Appendix G). The three participating study sites all used different CBCT machines and associated image viewing software. Hence, potential bias caused by small differences in the setup of image datasets could occur, which made us

address and correct these small differences. O. Angenete read all the CBCT datasets once, XQ. Shi read all the CBCT datasets once and T. Augdal read all the CBCT datasets twice, after an interval of at least three weeks. A total of 20 categorical features and five measurements were scored using high-resolution diagnostic screens in appropriate environment (Figures 8 and 9)

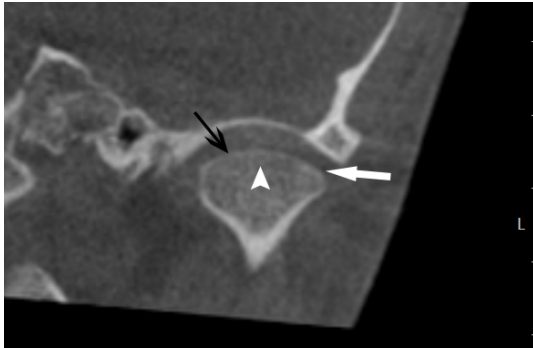


Figure 8

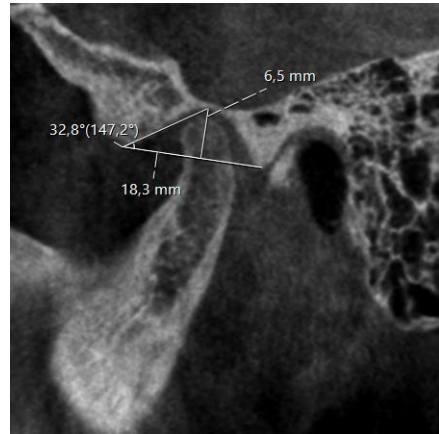


Figure 9

Figure 8. Coronal CBCT-based reconstruction of an 8-year-old girl with persistent oligoarthritic juvenile idiopathic arthritis and disease duration 6 years, showing examples of the imaging features surface irregularities (black arrow) scored as absent, condylar shape (white arrow) scored as convex, and subchondral sclerosis (arrowhead) scored as absent.

Figure 9. Sagittal CBCT-based reconstruction of an 8-year-old girl with persistent oligoarthritic juvenile idiopathic arthritis and disease duration 6 years, showing measurements of fossa depth (6.5 mm), fossa length (18.3 mm) and fossa-eminence inclination angle (32.8°)

In all three papers, measurements of continuous variables with digital measuring technique were standardized by defining the degree of magnification of the images and definitions of measuring points. Measures were registered with one decimal.

3.4 Statistical methods

In paper one the association between age, with patients categorized in age groups, and anterior inclination of the condyle was tested with Pearson chi-square test.

In paper one we used hierarchical multiple regression to explore the influence of gender and age group on the subjective grading of anterior inclination

In all three papers Cohen's kappa was used to determine intra-observer and inter-observer agreement. Cohen's simple kappa was used for binary variables and Cohen's linear, weighted kappa for variables with three categories or more.

In paper three Fleiss' kappa was used for assessment of inter-observer agreement between three readers. The results of Cohen's and Fleiss kappa must be seen in a clinical setting, but generally a kappa value of < 0 is regarded as poor agreement, 0-0.2 as slight, 0.21-0.4 as fair, 0.41-0.6 as moderate, 0.61-0.8 as substantial, and 0.81-1 as almost perfect agreement.

In all three papers the intra-observer and inter-observer agreement for continuous variables was analyzed according to Bland and Altman (109). Bland-Altman plots are generally interpreted informally and a maximal disagreement of 15% of the mean was considered clinically acceptable. For evaluation of bias in measurements of continuous variables two-tailed one-sample t-test was applied.

All statistical analyses were performed in the SPSS software (IBM SPSS Statistics version 23 or 26). A level of significance of 5% ($p \leq 0.05$) was considered significant and all reported p-values are two-tailed.

3.5 Ethics

Research on human beings in general, and children in particular, forces us to make specific ethical considerations. In "Helseforskningsloven" §18, it is stated that there must be an insignificant disadvantage or risk associated to participating in a research project. As no study has been able to prove long-time adverse effects of MRI

examinations in humans, the examination is considered safe (113). All participation was voluntarily, and informed consent was obtained. The researchers made sure the children did not feel obliged to undergo an investigation in order to satisfy parents, caretakers, or health workers. The child was allowed to stop the investigation at any time, before or during the uptake. In research on volunteering controls, there is always a risk of incidental findings, thus, we implemented a system for detecting and handling of such findings.

Paper one was approved by the Regional Ethics committee; REK nr 2016/257/REK vest.

Paper two and three were part of the approval from the Regional Ethics Committee for the NorJIA study; REK nr 2012/542. Written informed consent was given by the participant for children ≥ 16 years and by the parents if the participant was younger than 16 years. Data was collected and stored according to the General Data Protection Regulation (GDPR).

4. Summary of results

Paper 1

Normal MRI-based appearances of the temporomandibular joints in children aged 2-18 years

The purpose of the study was to evaluate the reliability of a set of imaging variables for assessment of the TMJ in children without JIA or known diseases in, or close to the TMJ. Based on the most precise features and measurements, we aimed to describe the normal appearance of the TMJ in children and adolescents aged 2-18 years.

A total of 101 head MRI examinations performed at Haukeland University Hospital, from 2005-2015 were retrospectively reviewed twice to determine intra-observer consensus agreement. The sample was stratified by age and gender to ensure a balanced data set.

The study included MRI examinations of 45 girls and 56 boys, mean age 10.7 years (SD 5.3). No significant differences were seen between right or left side, neither between sexes, hence the results for both sexes were merged, and the right side was presented.

The mean joint space height was 3.8 mm with a 0.2 mm difference between the first and second measurement. The 95% limit of agreement (LOA) ranged from -1.5 to 1.1 mm. Mean condylar angle was 20.4° with LOA from -17.4 to 23.2°. The mean fossa angle was 101.3° with LOA from -21.8 to 19.9°.

The main findings regarding the categorical variables were moderate to substantial intra-observer consensus levels of agreement for the features anterior condylar inclination in the sagittal/oblique plane and condylar shape in the coronal plane (Figure 10). The other imaging features showed lower intra-observer consensus agreement, deeming them unsuited for the MRI-based definition of the normal TMJ.

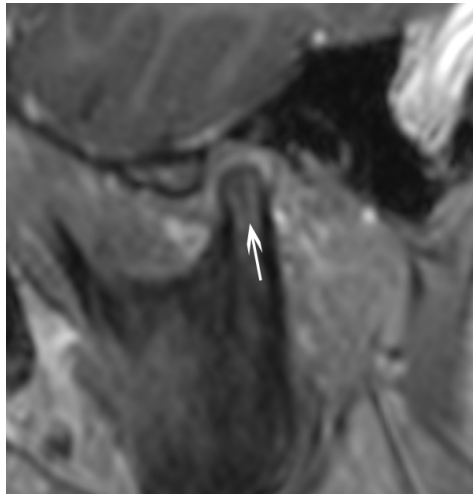


Figure 10

Figure 10. Sagittal/oblique reconstruction of high-resolution T1-weighted post-contrast MR images of an 8-year-old girl without juvenile idiopathic arthritis, undergoing examination because of headache. The image shows a straight mandibular condyle (arrow).

Some of the pre-defined imaging features such as bone marrow oedema, presence of an anterior beak and condylar surface irregularities showed very low prevalence, which was a relevant finding per se, but the low prevalence made kappa calculation unfeasible.

Further, the study showed significantly increasing anterior inclination by age, when the anterior inclination was subjectively graded from 0-2. Slight condylar flattening, as seen in the coronal plane was present in 20% of the subjects, but none of the cases were clearly flattened.

Contrast enhancement of varying degree in the TMJs was seen in 35 of the 36 patients that were possible to evaluate. Three of the 35 cases were classified with at least unilateral, moderate enhancement, but mild enhancement was the most common feature.

Paper 2

MRI in the assessment of TMJ arthritis in children with JIA; Repeatability of a newly devised scoring system

This study was performed to test the precision of a set of MRI-based image features of the TMJ in a balanced dataset of children with JIA. The most robust features can then be used as components in a future scoring system.

The MRIs of 86 children with JIA (51 girls) with median age 13 years (IQR 5) were read. Median duration of disease at the time of MRI was 4.5 years (IQR 6) and median age at diagnosis was 6 years (IQR 8).

Continuous measurements of joint fluid, in both the upper and lower joint compartments showed wide LOA. In the upper compartment the mean measurement was 0.2 mm (95% LOA -0.6 to 0.4 mm). In the lower compartment mean measurement was 0.3 mm (95% LOA -1.0 to 0.7 mm).

In the osteochondral domain a total of seven out of twelve imaging features showed acceptable kappa values. These features, i.e., loss of condylar volume, condylar shape in the coronal and sagittal plane, and condylar irregularities etc. are variables that are thought to be indicative of structural deformity and/or growth disturbances due to arthritis. The results render the imaging features a role in a future scoring system where their clinical importance can be determined.

In the inflammatory domain, the imaging features generally showed slightly lower kappa values than in the osteochondral domain. Features for single items such as joint fluid, synovial enhancement, and bone marrow oedema, but also the composite variable “overall impression of inflammation” showed acceptable kappa values (Figure 11). Other items, such as synovial thickening, which is interesting from a pathophysiologic point-of-view, showed low kappa values (Figure 12).

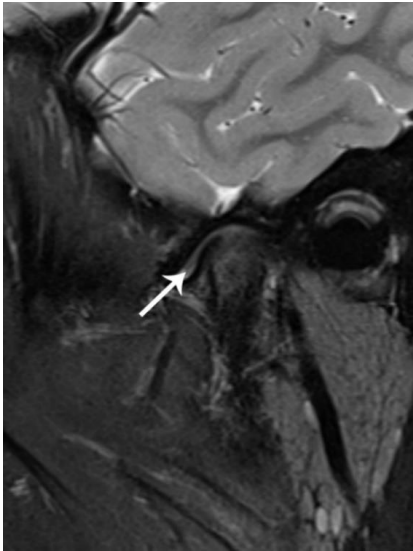


Figure 11

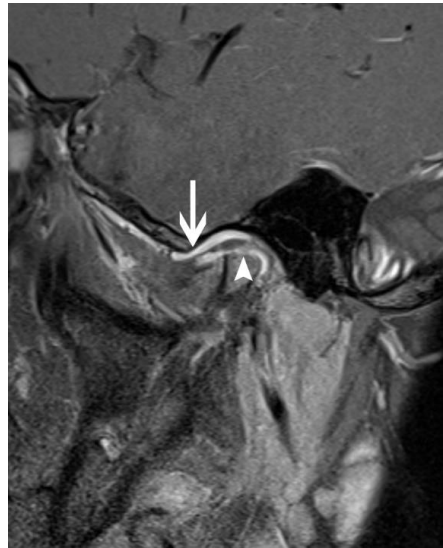


Figure 12

Figure 11. Sagittal/oblique T2-weighted fat-saturated image of a 14-year-old girl with undifferentiated juvenile idiopathic arthritis and disease duration 3 years, showing possible, synovial thickening, shown as an area of intermediate signal in the joint space (arrow). Synovial thickness was shown to be an image feature with low kappa value.

Figure 12. Sagittal/oblique T1-weighted fat-saturated image post intravenous contrast of the left TMJ of a 15-year-old boy with persistent oligoarthritic juvenile idiopathic arthritis and disease duration 14 years, showing loss of condylar volume (arrowhead). The image also demonstrates synovial enhancement, grade 2 (arrow). Both imaging features showed acceptable kappa values.

A set of seven image features in the osteochondral domain and four features in the inflammatory domain showed agreement levels within and between observers acceptable for inclusion in a future scoring system of the TMJ in JIA.

Paper 3

Cone beam computed tomography in the assessment of TMJ deformity in children with JIA; repeatability of a newly devised scoring system

This study was performed to test the precision of a set of CBCT-based image features of the TMJ in a balanced dataset of children with JIA. The most robust features can then be used as components in a future scoring system.

The CBCTs of 84 children with JIA (51 girls) with median age 14 years (IQR 4) were read. Median duration of disease at the time of CBCT was 6.3 years (IQR 6) and median age at diagnosis was 6 years (IQR 9).

Initially, assessment of image features was made with the mandibular condyle and the articular eminence divided in multiple regions and each region was then scored separately. The results of this regionalized assessment showed poor agreement both for categorical and continuous variables. Thus, the regionalized assessment was abandoned.

Subsequently, scoring of 19 categorical image features and five continuous measurements was carried out for each TMJ (Figure 13). Continuous measurements showed wide 95% LOA where essentially all variables exceeded the pre-defined, clinically acceptable limit of 15% of the sample mean.

Nine of the tested categorical variables showed acceptable agreement within and between observers. Based on these results the features overall impression of deformity, flattening of the condyle and articular eminence/glenoid fossa, reduced condylar volume, joint surface irregularities, joint surface continuity, and osteoarthritis can thus be studied further.



Figure 13

Figure 13. Sagittal CBCT-based reconstruction of a 13-year-old girl with polyarthritic, RF negative juvenile idiopathic arthritis and disease duration 11 years, showing mild flattening of the fossa/eminence (arrow), grade 2 condylar irregularity (arrowhead) and general loss of volume of the condyle (grade 1)

5. Discussion

Research on chronic diseases, such as JIA, is constantly developing, addressing aims in many areas such as diagnostic procedures, treatment options, follow-up regimes, and consequences of the disease. Before undertaking the work on the papers in this thesis, we performed a thorough review of published literature on imaging of the TMJ (54). The experiences drawn from this work, combined with extensive knowledge in study design in the NorJIA research group, led the way in the idea phase and design phase of the three papers in this thesis. Designing a diagnostic research study requires amongst many other things, a defined hypothesis, an adequate study design, correct selection of study population, the use of adequate techniques and statistical methods and, not least, the work should be original.

The overall aims of this thesis, as stated in the introduction, was firstly to explore the appearances of the presumed normal TMJ, in order to create robust tools to differentiate pathologic joints from normal joints. Secondly, we aimed to explore the usefulness of a wide range of image features in a population of children with known JIA. Features addressing morphologic changes were studied on both MRI and CBCT examinations, while features addressing active inflammation were studied on MRI.

5.1 Methodological considerations

5.1.1 Study design

According to the hypothesis of the study, an adequate study design must be chosen. An observational study design differs from an experimental study design, where the latter studies the effect of an intervention. In the observational study, at least in its ideal form, the subject is not in any way influenced by the observer or the observing procedure. Observational studies can be examinations of prevalence of disease, health-related issues such as risk factors for disease, or prevalence of image findings. The observational study is highly dependent on factors such as the period for data collection, which patients are included in the study, and which patients are excluded from the study.

Observational studies can in some regards be carriers of a lower level of evidence than the randomized, controlled trial (RCT). The RCT is often seen as gold standard for evidence-based medicine, being less prone to many forms of bias than other study designs. The RCT, however, is not suited for research on the precision and accuracy of diagnostic methods as the latter studies usually do not include any kind of intervention. Observational studies can be divided into three groups: Cohort studies, case-control studies, and cross-sectional studies. The cross-sectional study evaluates a defined population at a given time-point and does not consider change over time in the status of the study subject. The data in a cross-sectional study can be collected prospectively, beginning after the formal opening of the data collection. Opposite, the data can be extracted from previously collected data which would define a retrospective, cross-sectional study.

Two cohorts were used in this thesis. In paper one, the retrospective cross-sectional design was used, defining a group of children and adolescents without known disease in or around the TMJ. The cohort in paper one was balanced in terms of gender and age. The cohort had an overweight of children being under diagnostic work-up for epilepsy (49%) compared to other diagnoses (benign brain tumor 12%, and headache 11%). Applying a very strict way of defining bias, this skewing of the clinical indication for MRI could represent a selection bias and as such a source of misinterpretation of the results. However, the current clinical knowledge on the pathophysiology of epilepsy and the subtle morphologic changes it is associated with, makes the probability of bias less likely.

One could argue that a prospectively collected material of presumed healthy volunteers would constitute a more valid representation of the normal TMJ. Concerning the morphologic features of the TMJ, such as shape, flattening, appearance of the disc and even bone marrow oedema, the author agrees. Data collection not associated to hospitalization or other forms of visits in the health care system can reduce inclusion bias and has been successfully used by others (114). Other kinds of inclusion bias, such as socioeconomic factors and unintended motives for participating must be addressed in such a prospective study design as well as funding for the extensive apparatus which is

necessary to collect the data. Methodologically, such an approach would probably represent an even more reliable dataset of the normal appearance of the TMJ. However, the normal standards of synovial perfusion and bone marrow enhancement would be ethically challenging to study in a cohort of healthy volunteers. The degree of synovial perfusion and bone marrow enhancement represents two of the cornerstones of diagnostic imaging in arthritis, therefore the cut-off value between normal and pathologic perfusion is essential to define. As per today, the visualization of synovial perfusion and bone marrow enhancement requires injection of intravenous contrast which, in an MRI examination contains gadolinium. Intravenous contrast with gadolinium is very well tolerated in a large majority of patients where it is clinically indicated to use it. In patients with severe renal dysfunction, injection of earlier forms of gadolinium-containing contrast was associated with the severe adverse reaction of nephrogenic system fibrosis (115). Further, numerous publications have shown subtle, but measurable depositions of gadolinium in certain regions of the brain, following repeated injection of contrast material (116, 117). The clinical consequence of this deposition of gadolinium is not known, but further research will hopefully shed light on the important topic (118). From an ethical point-of-view, the potential risks associated with injection of intravenous gadolinium makes it not acceptable to use in a healthy cohort. As one of the aims of paper one was to define the synovial distribution of intravenous contrast material in presumed normal TMJs, a retrospective extraction of MRI examinations with intravenous contrast performed for other reasons was considered the most appropriate.

In paper one a sample size of 101 patients was selected. Ideally a power calculation would have given a somewhat clear indication on what number of patients to include. Calculation of power, however, assumes some knowledge of the prevalence and variance of the item under study. It also assumes some amount of *a priori* knowledge of a clinically relevant cut-off value (119). Again, one of the aims of the thesis was to study the unknown prevalence of imaging features in assumed normal TMJs and, if possible, also define the variance of the findings. These aims, together with the lacking evidence of a clinically relevant cut-off between normal and pathologic findings makes a power calculation hard or even impossible to perform. Instead, a pragmatic approach

was used by defining a time frame where homogeneous MRI acquisitions were available, including a number of examinations that would represent a balanced dataset regarding age and gender.

Methodologically, paper two and three are very similar. Both represent cross-sectional studies with prospective collection of data. In the NorJIA study, we prospectively invited patients with a JIA diagnosis during the period 2015 to 2020. Diagnosing a child or adolescent with JIA is a delicate matter, requiring expertise in clinical skills, vast knowledge on differential diagnoses of other kinds of joint pain, access to laboratory resources and opportunity to follow-up of patients with borderline symptoms. Thus, in a prospective study there is a possibility of inclusion bias where children erroneously are diagnosed with JIA. To reduce the risk for this type of bias the recruitment of patients was restricted to tertiary, paediatric hospitals staffed with consultant paediatric rheumatologists working in close collaboration with other, related medical specialties. Another form of inclusion bias, possibly affecting the study population, is the risk that patients with more active disease tend to participate in research studies more often than patients with milder forms of the disease. Preliminary results from the epidemiologic analysis of the NorJIA population indicate that 63% of the patients accepted the invitation to participate and a slight overweight of patients with more active disease cannot be excluded. In a population-based study the possibility of this kind of inclusion bias could represent a problem that must be addressed. The population under study in paper two and three is not intended to represent a population-based sample. Rather, the sample is selected to include a balanced range of pathology, ranging from none to severe, a balanced proportion of girls and boys, and a balanced range of age groups of the participants. By ensuring this form of balance, the image features under study can ideally be tested on all relevant age groups and the full range of pathologic phenotypes in a dataset that allows for adequate statistical evaluation.

As in paper one, a definition of an adequate sample size based on power calculation was not performed in paper two and three. The rationale behind this decision was similar to the one in paper one, based on lacking clinically relevant cut-off values, lacking gold

standards, and lacking knowledge of the prevalence of the relevant imaging features under examination.

A diagnostic imaging test has many purposes. One important purpose is to, if possible, distinguish between normal and pathologic findings. One might then argue that an image-based classification system based on a cohort of patients with a known disease does not consider the variability of findings in a population under diagnostic work-up, yet not diagnosed with the disease. This argument is not invalid, but the aim of this thesis was not to establish a diagnostic tool for JIA or arthritis in the TMJ, but to define image features with acceptable level of agreement. Further studies are warranted to define the clinical relevance of the image features, both in a population with and without JIA.

5.1.2 Technical aspects of MRI

Choosing MRI sequences for a protocol of clinical examinations on humans is a complicated task. The task of choosing an MRI protocol for a multicentre study on children is not less complicated. Not only must a suitable MRI scanner and a suitable MRI coil be available, thorough considerations such as defining the desired weighting of the sequences, method of administration of intravenous contrast and standardization of open-mouth acquisitions also had to be done. In addition, an adequate, child-friendly environment had to be established all the way from the child entering the imaging department, staying comfortable in the scanner and lastly, leaving the department with a feeling of being sound and taken care of. At all three sites a Siemens Skyra 3 Tesla scanner with a dedicated head coil was used.

MRI protocols is not only the set of parameters usually described in scientific publications, such as field strength (Tesla), TR, TE, fat-saturation, and slice thickness. The protocol also includes a breadth of parameters less often presented. Examples of such parameters are echo-train length, number of averages, phase-encoding direction, receiver bandwidth, acceleration techniques, interslice gap, and sampling percentage. These are all factors with a direct impact on the acquisition, affecting both the possibilities of post-processing and the quality of the images presented to the

radiologist. The complexity of the setup of an MRI protocol is a problem that must be addressed when implementing a new method in the MRI department. To reduce the risk of using slightly different MRI parameters in the different study sites, a final definition of all the parameters was made on an MRI scanner at Haukeland University Hospital. A USB-unit containing all MRI parameters was then distributed to the other two study sites and the information was directly copied on the scanners, respectively. Thus, we believe that harmonization of the three MRI systems in the study is carried out as far as reasonably possible.

MRI acquisitions can be obtained in either separate slices (2D) or as a whole volume (3D) which then can be presented in slices. The 2D acquisition requires the radiographer to manually define the direction of the slices and the size of the volume to obtain signal from. Further, the slice thickness, the interslice gap, and the matrix of the acquisition puts restrictions on the ability to detect small changes in the tissue. As the TMJ is an anatomically complex joint with numerous asymmetric curvatures in both soft tissue and joint surfaces the slice direction affects the visualization of small structures. Similar experiences have been drawn regarding the slice directions in the sacroiliac joints (120). To minimize the radiographer's potentially varying impact on the slice direction, an anatomically based instruction for placing of the sagittal/oblique slice direction was implemented. We did not aim to quantify the importance of the slice direction on the visualization of small structures. However, during the work with paper one, and during data collection of paper two, the importance of correct MRI image acquisitions became apparent. Newer, faster ways of performing truly isotropic 3D volume acquisitions could reduce the impact of the radiographer, as the reconstructions would be adjustable by the radiologist at the PACS station. The technique has been tested on larger joints such as the knee, with promising results regarding image quality (121). Whether the technique is useful as a substitution or adjunct to 2D imaging of small joints, such as the TMJ, remains unknown.

All three study sites used the same type of fat suppression in the MRI protocol. Both the sagittal/oblique T2-weighted sequence and the sagittal/oblique T1-weighted sequence after intravenous contrast used a fat-suppression technique dependent on a homogenous magnetic field. The TMJ is located peripherally in the receiver head coil and it is

situated close to an interface between tissue and surrounding air. These factors are known to impede the effectiveness of the fat saturation which can lead to reduced contrast to noise ratio in the TMJ (122). Using a head coil, it is not easy to overcome this drawback of the fat saturation technique and it is not unthinkable that this affects the visualization of bone marrow oedema. A potential way around this challenge could be quantification of water content by Dixon technique (123), which possibly would be less affected by local inhomogeneities in the magnetic field.

5.1.3 Technical aspects of CBCT

Being a modality dependent on ionizing radiation, the diagnostic impact of the CBCT examination has to be weighed against the risk associated with radiation. Children are more sensitive to radiation than adults, probably due to higher cellular turnover and longer life expectancy. Epidemiologic studies on radiation-induced risk of cancer in children are neither easy to conduct, nor to interpret. In a review from 2016, Kutanzi demonstrate the slightly diverging results of a series of studies ending up with a conclusion that head CT performed in children most likely is associated with a small increase in risk for brain cancer (124). As far as we know, epidemiologic studies on the association between CBCT and cancer risk in children are not published. However, estimations and projections of risk for cancer induced by dental CBCT are published (125, 126) based on phantoms and models for risk prediction. These models support the theory that even the relatively low doses associated with CBCT can be associated with increased risk for cancer. Thus, the ALARA statement (As Low As Reasonably Achievable) seems to hold true and before referring a child to CBCT thorough weighing of the benefits contra the radiation-associated risk must be made.

An unchallenged advantage of CBCT is the exceptional ability to visualize very small, bony structures, as explained in the introduction. Small irregularities in the joint surface, both on the condylar side, and on the side of the temporal bone can theoretically represent subtle, superficial, osseous degradation caused by inflammatory enzymes. If that finding really represents ongoing inflammation, the treat-to-target paradigm would recommend systemic, treatment with the goal of stopping, or hopefully reversing the process. However, as normal standards of age-related CBCT findings are sparse or

almost absent, and CBCT examinations of healthy volunteers is ethically challenging, the radiology report of the CBCT will be associated with some uncertainty, when it addresses very small irregularities. Hopefully, increasing technical development of MRI systems to detect very small cortical alterations can bring more knowledge to this topic (127).

Contrary to CT, the CBCT is relatively sensitive to motion artefacts. The rotation of the gantry requires the patient to remain still for 10 to 40 seconds, depending on machine and acquisition parameters. Although suboptimal examinations due to artefacts were excluded from paper three, we did notice small variations of image quality. As quantification of image quality in terms of signal-noise ratio or similar types of rating was not an aim of paper three, the impact of this small variation is not clear. It is not unlikely that patient motion during acquisition was the cause of the small variation.

Another useful ability of the CBCT is the isotropic dataset, giving the reader the opportunity to adjust the slice direction to his or her preference. In a setting with experienced readers, who are comfortable using standardized definitions of slice directions, the flexibility of the dataset most likely is a benefit. Opposite, we experienced that even small alterations of the reconstructed slice directions altered the conspicuity of small lesions such as surface irregularities.

5.1.4. The image readers

Image reading in consensus as done in paper one can be both advantageous and problematic. In paper one we aimed to define robust image features of the normal TMJ. As there is no pre-existing age-related image atlas, and data on the normal appearances of the paediatric TMJ is sparse, we first sought out to unconditionally review, discuss, calibrate, and harmonize our understanding of the MRI-based image features of the normal TMJ. Given the paucity of pre-existing data we considered this approach as a correct first step in establishing new normal references. The approach forced us to thoroughly discuss pros and cons at every step of the reading procedure. In some settings the consensus reading has a positive connotation as it implies that the readers

strive together towards a common goal. The consensus reading however also has apparent drawbacks. In a clinical setting, in a radiology department, image reading is almost never performed as consensus reading. The consultant radiologist usually determines by himself or herself what to write in the radiology report. In most cases experienced radiologists agree substantially, but there is almost always some variability and hence a slight disagreement. The consensus reading eliminates the visualization of this variability. Nevertheless, in an early, preliminary stage of the development of a test, it can be appropriate to apply the consensus reading procedure to validate the understanding of the definitions of the test (128).

The validity of the consensus reading can also be hampered if the readers are unequal in any way, for example radiologic experience, and this inequality affects the consensus dialogue. In our setting, all three readers are consultant radiologists with long experience of clinical radiology and a special interest in musculoskeletal radiology. We therefore believe that a free-speaking, unconstrained dialogue was held under the consensus reading meetings. However, before applying a diagnostic test in a clinical setting more thorough examination of the test performance must be made (128).

In papers two and three, each observer performed the image reading alone. In many test settings the possibility to blind the readers for all relevant information is limited. All the participating children in papers two and three were diagnosed with JIA and previous evidence has shown that the TMJ often is affected in JIA. Therefore, it is not unlikely that the readers had a pre-understanding that there would be pathology present in the images. This would have constituted a significant methodological problem if the aim was to differ normal TMJs from pathologic TMJs. As our aim was to establish robust imaging features, the problem is not affecting the conclusions of the thesis. The same problem must however be thoroughly addressed in a later phase, when studying the sensitivity and specificity of the MRI- and CBCT-based image features.

5.1.5 Statistical considerations

Statistical methods are seldom perfect, and the result of a statistical method has to be seen in the light of its advantages and drawbacks. In all three papers calculations of

Kappa (Cohen's or Fleiss') were contributing heavily to the results. These methods are not without flaws as described in the section on Materials and Methods. In all three studies we encountered findings with low prevalence e.g., presence of bone marrow oedema in paper one, and position of the condyle in paper two. When we found extremely low Kappa values of a separate image feature, an extra, thorough evaluation of the distribution of findings was made. In addition, we double-checked the readers understanding of the definition of the variable.

We have not found guidance on pre-defined cut-off levels for when to refrain from Kappa calculations because of low prevalence. In some cases, one could consider dichotomizing categorical variables with three or more grades. That operation usually leads to less skewing of the distribution of findings. However, dichotomizing must be done with great care in order not to reduce the clinical importance of the variable. For example, in paper one, we tested dichotomizing the variable "shape of the glenoid fossa" from four grades to two, as the dichotomized variant still would be clinically interesting. In that specific case, the change did not improve the results.

In paper two and three, we strived to collect a dataset which was relatively balanced in terms of pathology, age, and gender. We believe achieving balance in a dataset addressing for example blood glucose, body mass index, or smoking status, is more straight forward than achieving balance in a dataset of up to 25 image features, which prevalence is close to unknown. By extracting all patients with a radiology report deviating from "normal" from the NorJIA population, and including a number of patients that is two to four times larger than other, related studies (129, 130), we assume that the statistical impact of the calculations should at least be on par. Still, as the entire data volume of the NorJIA study was not included, it cannot be ruled out that the choice to include or exclude certain examinations affected the overall prevalence of some image features. Therefore, the prevalence of the finding and hence the possible skewing of the prevalence might have affected our calculations of Kappa.

In papers two and three we carried out a set of measurements of different TMJ structures, both angles and distances. As the participants in the study ranged from young children to adolescents, we anticipated relatively large differences in

measurements depending on age. Using Bland Altman difference plots and limits of agreement give the reader an opportunity to evaluate if the disagreement is clinically significant or not. The variation of measurements between patients is not lost in the presentation. Opposite, if the same measurements were evaluated along an agreement-adjusted ICC scale, this variation would still be present, but would not be presented to the reader.

Why did we find wide LOA when measuring small distances? There are probably a series of mechanisms contributing to wide LOA. One contributing factor could be that the extensive image dataset that MRI and CBCT presents, gives large room for individual judgment of where to deploy the measuring points. The reader must first choose the most correct image slice and then the most correct points in that particular slice. Further, the spatial resolution of MRI is relatively low. There was always a need to zoom in closely on the TMJ to find the correct measuring points. This enlargement of the images combined with low spatial resolution commonly made the presentation of MRI images coarse, consequently leading to challenges in choosing points for measurements. As per today, it is challenging to find imaging systems and measurement procedures that might overcome this issue.

The clinical significance of image-based measurements of the TMJ in JIA is unclear, and evidence demonstrating the importance of measuring the anatomical structures is lacking. If and when evidence for such measurements is presented, our results could be used as a tool to guide further development.

During the consensus reading in paper one we could see that some image features tended to vary according to age group. Condylar shape in the coronal plane and condylar inclination in the sagittal/oblique plane showed acceptable kappa values and were thus included in further testing by using chi squared tests. Chi squared tests showed condylar anterior inclination to be significantly associated with age, but condylar shape in the coronal plane was not. Hierarchical multiple regression can demonstrate the influence of additional, independent factors by stepwise addition, and thus we analyzed if gender was influential on anterior inclination of the condyle, but with negative results.

5.2 Ethical considerations

In paper one, a retrospective collection of data was performed including patients undergoing clinically indicated MRI of the head. The retrospective approach gives advantages in terms of cost, time spent on collection, and availability of potentially very large datasets compared to the prospective approach. It does however also impose a large responsibility on the researcher to ensure that the data is treated correctly. The use of image data from patients who did not have the opportunity to decline participation of the study can be considered controversial. Ethical guidelines can be somewhat diverging on this topic, partly depending on the purpose and impact of the research that the data will be used for. Norwegian regional ethic committees have guidelines that approve the use of such material given that strict restriction on anonymization and data storage is upheld.

The participants in the NorJIA study were invited to a wide range of examinations, including CBCT and MRI. As per today, no evidence-based guidelines exist that confirm a positive effect of the use of advanced imaging in TMJ arthritis in JIA. From an ethical point-of-view children represent a vulnerable group of our society. Vulnerable groups can be defined as people with reduced ability to object, with reduced ability to understand the consequences of their actions, and they are prone to experience the examination as threatening and unpleasant. The latter can have implications on the child's ability to co-operate in a future examination where the clinical importance is much higher for the specific individual. Amongst other reasons, the Helsinki declaration (131) states that there must be a «reasonable likelihood that the populations in which the research is carried out stand to benefit from the results of the research».

As shown in the section on “Pathology in TMJ” there is evidence indicating that arthritis in the TMJ can be asymptomatic. There is also evidence showing that early treatment aiming at reducing or stopping inflammation generally is favourable for the JIA patient, the so-called treat-to-target paradigm (21), even though the tools for defining remission are not always clearly defined. This paradigm gives support to the use of advanced imaging to detect active inflammation even in patients without symptoms from this particular joint. One could also argue that determining whether

joint deformity is present, but no active inflammation, could be of beneficial prognostic value for the patient, in case relapse of clinical symptoms would occur.

Before carrying out research on children, a series of conditions must be fulfilled. A consent from the child must be obtained if the child is 16 years or older. If the child is between 12-16 years of age, the parents or caretakers must consent, but the child must be presented information that is adapted to the age of the child, in order to give the child a fair understanding of the research protocol. For children under 12 years of age, the parent or caretaker takes the decision for the child, based on oral and written information. The child and its caretaker must be able to withdraw from the study at any point, without fearing consequences or relevant change of treatment. During the imaging procedures, this kind of withdrawal occurred a few times, especially during the MR examination. When possible and desirable, the child and caretaker were presented with the opportunity to re-schedule the MRI. In some cases, the child and caretaker chose to continue with the other forms of data collection in the NorJIA study, and in a very small number of cases the child withdrew from the whole study. The withdrawals did not have any effect on the study population in paper two and three as the dataset was selected.

Diagnostic imaging is always associated with the risk of incidental findings. The field-of-view of the MRI examination includes the whole cranium and brain in one sequence, and parts of the brain, skull base and adjoining soft tissue on several sequences. Thus, incidental findings must be anticipated, given the size of the study population and the sensitivity of the imaging modalities. In fact, a small number of arachnoid cysts, benign parotid lesions and grey matter heterotopia was reported. This requires the researchers to implement a system for recognizing, reporting, and acting on the incidental findings in an adequate way (132). The participants of the study are also entitled to be informed of the potential, incidental findings, and their consequences as far as reasonably possible before consenting to participation. The primary investigators (O. Angenete, T. Augdal, XQ. Shi and K. Rosendahl) are clinical radiologists with experience in interpreting a wide range of paediatric imaging studies, working in an interdisciplinary environment in close collaboration with other sub-specialists. This framework secured safe and adequate management of all incidental findings.

In sum, the ethical drawbacks of exposing children in the NorJIA study to advanced imaging is considered outweighed by the potential benefit of increased knowledge for the child and the whole JIA population. The regional ethics committee of Western Norway supported this view in their decision from 2012.

5.3 Results

5.3.1 Image features of the TMJ in children without JIA

In children and adolescents without JIA we have shown that several of the features and measurements previously used to define the TMJ are imprecise. Despite active readers and meticulous deploying of the measuring points, following thorough standardization of the techniques, we could not confirm reliability of continuous measurements. These somewhat disappointing results are however not surprising. Others have also shown wide limits of agreement when measuring small distances (45, 133). Interestingly, we found very low prevalence of bone marrow oedema in both readings. The low prevalence made calculation of consensus intraobserver agreement impossible, but as such the prevalence of the feature is still interesting when comparing a cohort of children without JIA to a cohort of children with JIA. The feature anterior inclination of the condyle proved to be robust and could thus confirm the findings from previous publications (45, 80).

We noted contrast enhancement, mostly of mild degree, in nearly all TMJs in children without JIA. In her study from 2013, von Kalle described the dynamics of contrast uptake in and around the TMJ in children examined for other reasons than JIA (78). Their results are in line with ours, although the methods are somewhat different. Mild contrast uptake in the TMJ can thus be considered a normal finding.

5.3.2 Image features in the osteochondral domain

We have shown that a range of image features describing osteochondral items probably can be used to evaluate the appearance of the paediatric TMJ in JIA. The variable

condylar volume, when scored subjectively on a 0-1 scale on MRI, or on a 0-4 scale on CBCT, showed acceptable levels of agreement. As far as we know, no testing of agreement of these subjective variables have previously been published. The use of the variable has been proposed by Tamimi (134) in CBCT, but without thorough testing of its precision. Interestingly, the feature shows acceptable performance across the modalities MRI and CBCT. We speculate that the similarities in the features' definitions, combined with readers being comfortable with both techniques could indicate some transferability of the findings between the modalities. If future studies confirm the reliability of the features in a larger setting, and if the features are deemed clinically important, the ease with which the feature is used can be an advantage. Opposite, the development of automated or semiautomated techniques to calculate condylar volume intuitively seems attractive, in terms of repeatability (135, 136). However, as promising these techniques may seem, today they still require external third-party software or advanced, time-consuming procedures making them unsuitable for daily practice in a radiology department.

How the shape of the mandibular condyle and of the articular eminence and glenoid fossa is related to disease activity in JIA is unclear. As shown in the introduction, studies have shown that growth and development of these structures are intricately related to many factors, such as load and genetic expression. We found that both in the presumed normal population, and in the JIA population, a non-negligible number of children presented with shapes deviating from an S-shape in the fossa or a rounded/ovoid form of the condyle. This is not unexpected, as others have shown a development with deepening of the fossa by age as well as a slight loss of roundedness of the condyle (80). We have shown these image features to be robust in a JIA population. However, hard work remains to find the cut-off between shape alterations caused by JIA and shape alterations that can be categorized as normal variants.

Irregularities of the joint surfaces is an interesting image feature in many regards. Again, we have shown that the image feature performs well on both CBCT and MRI, although it should be noted that the MRI preferably should be obtained with an ideal setup of sequences, not a core setup. On MRI we did not aim to assess irregularities of the joint surface of the articular eminence and glenoid fossa. On CBCT we found this

image feature to be reliable and thus it could be fruitful to test the variable also on the articular eminence and glenoid fossa in the MRI dataset. As the irregularities found in this region on CBCT mainly were small or very small, one should probably anticipate difficulties detecting them on MRI, due to the lower resolution. In the population of children without JIA we found a prevalence of condylar surface irregularities somewhere between two to five percent. As such, it shows that the radiologist must be vigilant, not to unequivocally report condylar irregularities as signs of TMJ deformity. In the CBCT dataset, we also tested the image feature discontinuity of the surface. The presence of this variable theoretically indicates an aberration in the cortical surface. In terms of JIA-related pathology, this could be caused by inflammatory enzymes degrading the joint surface and is therefore a potential early biomarker for disease. It should be noted though, that the development of the condylar cortex is not finished until adulthood (137) which again requires the radiologist to be cautious. On MRI we did not aim to define the precision of the same image feature, and again the lower spatial resolution of our MRI dataset compared to CBCT probably makes the feature hard to evaluate. Considering the advances of musculoskeletal MRI in larger joints, focusing on growth plates, secondary ossifications centres and cartilage imaging (138), one can hope that the MRI techniques of the TMJ also move forward in the future. As per today however, the possibilities to examine the different layers of cortical development of the TMJ by MRI are limited.

5.3.3 Image features in the inflammatory domain

In paper two, a series of findings addressing inflammatory activity were made, with the findings in paper one as an important foundation. In line with the treat-to-target paradigm, it is essential to induce remission of inflammation as soon as possible, hopefully before structural change of the joint occurs. As the TMJ is challenging to examine clinically, MRI has emerged as an important tool for evaluating inflammation in the TMJ. Out of 13 MRI-based imaging features previously used for assessment of inflammation, four were deemed of sufficient precision to be used in a future scoring system.

5.3.3.1 Bone marrow oedema

This item with a pathophysiologically elusive content, has for long been of major importance in MRI-based assessment of inflammation in many parts of the body. On a 0-1 scale, we found relative, but not overwhelming evidence for the precision of this feature in the mandibular condyle. However, given the assumed importance of the item, and acceptable precision, it can be studied further. Others have also encountered problems with precision of this feature, in the paediatric mandibular condyle (129) and in the paediatric sacroiliac joints (139), supporting our findings.

5.3.3.2 Synovitis

Synovitis is by many seen as the imaging hallmark of arthritis, and it was tested in three slightly different variants. The image features are dependent on a series of potentially crucial factors such as serum gadolinium concentration, slice thickness, slice direction, and the quality of the pre-contrast T1-weighted sequence or fluid-sensitive sequence. Further, the feature most likely is affected by the timing and the way the data is collected in k-space (78, 79). To address as many of these factors as possible, the contrast injection and all sequences used, were highly standardized. We also explored whether dependence on a pre-contrast T1-weighted fat-saturated sequence or a T2-weighted fat-saturated sequence affected the agreement, which we cannot see has been done before. In total, a small advantage in terms of agreement, was seen for the image feature synovial enhancement, dependent on a pre-contrast T1-weighted fat-saturated sequence. Interestingly, and possibly because we used a relatively large study population, we found cases with an unexpected sequence of pathologic change e.g., presence of synovial thickening without joint effusion. This violates the logic of the progressive system (140) and could thus have affected the agreement of the readers.

5.3.3.3 Joint fluid

Joint fluid was scored in four variants, ranging from simple to more complex variants. As previous publications have shown difficulties in measuring small distances, we set

out to test a simple, binary image feature lacking all kinds of measurements and we named it overall impression of pathological joint fluid. The agreement between observers was not convincing, and as the feature probably does not differentiate well between mild and severe disease, the future use of the feature is questionable. Similar, but slightly less agreement was shown for the features regarding the amount of joint fluid in each joint compartment. Interestingly, and maybe somewhat surprising to the readers, the semiquantitative feature joint fluid on a 0-2 scale performed well. As shown in more detail in paper two, this feature is partly dependent on continuous measurements, which performed poorly as judged in a Bland-Altman plot. Still, the composite image feature performed well, both within and between observers, making it a candidate for a future scoring system. The image feature has been mentioned on several occasions, starting in the consensus scoring system from 2018 (129). In that study, the authors proposed joint fluid to be assessed on a 0-2 graded scale, based on the ICC-based results from two other variables scaled from 0-3. The 0-2 graded variable was never tested though. In subsequent studies on the perceived importance of each image feature the precision of the 0-2 score was not examined (141). This was also the case for the study testing the scoring system on radiologists and non-radiologists (142). However, our results support the recommendation by Tolend from 2018 to use the variable on a 0-2 scale.

5.3.3.4 Overall impression of inflammation

The composite variable overall impression of inflammation showed moderate levels of intraobserver and interobserver agreement, making it a candidate for a future scoring system. The variable is dependent on multiple factors including evaluation of joint fluid, synovial enhancement, and the reader's understanding of what constitutes active inflammation on MRI. The last component is deliberately constructed without measurements or very strict guidance of the constituents of the term active inflammation. As noted, it nevertheless performed well. If the feature continues to perform well in further testing in a clinical setting with multiple readers, it might represent a tool which is easy to use and understand for both radiologists and clinicians.

5.3.3.5 Synovial thickness

In their study from 2021, Tolend and co-workers let several experts share their perceived importance of a range of image features of the TMJ in JIA (141). In the inflammatory domain, synovial thickness was ranked second most important, next to the image feature joint enhancement. Considering the physiological background of synovial thickening and its probably close relation to pathological change and destruction of the joint, we agree. Nevertheless, none of the image features addressing synovial thickening did perform convincingly. The reason for this suboptimal level of agreement is not clear. One might speculate that partial volume averaging of nearby voxels results in a blurred interface between the intermediate signal returned from the thickened synovium and the normal synovium. Likewise, the interface between thickened synovium and joint fluid might be blurred, again affecting the scoring. These effects were not possible to quantify in this thesis but could probably be explored further in a larger dataset. The precision of a similar image feature on a 0-3 scale in the so-called American scoring system (143) has been tested in Tolend's work from 2018 (129) with an acceptable ICC value. The consensus-based recommendations in the same publication recommend the use of a 0-2 scaled image feature, based on continuous measurements. We have not found publications addressing the precision of this, recommended image feature, tested as a solitary variable.

5.3.4 Recommendations on a future scoring system

Based on the results from previous publications and from the present studies, the following components are considered precise enough to be included in a future scoring system:

Osteochondral domain: shape-related features of the condyle and of the articular eminence/glenoid fossa, reduction of condylar volume, impression of deformity, surface irregularities, and condylar inclination. The importance of joint surface continuity could be studied further specifically in CBCT-based imaging.

Inflammatory domain: the MRI-based features bone marrow oedema, synovial enhancement, joint fluid, and overall impression of inflammation.

5.4 Clinical implications

As stated in the introduction, it is not easy to correlate clinical examination of the TMJ, self-reported symptoms from the TMJ, and disease activity in children with JIA. A large proportion of children with JIA will undergo systemic medical treatment associated with potential, adverse events, and will have a need for long-term follow-up by an interdisciplinary team of specialists. A series of publications underscores the importance of using medical imaging as a tool to assist in the clinical decisions. When the clinician decides that there is a need for evaluation of soft tissue and osteochondral tissue of the TMJ in children with JIA, we believe the results of this thesis may be of help. The use of the scoring systems we present could facilitate understanding between the radiologist and the clinician, and most importantly, if used by the radiologist, the results can guide him or her to focus the radiology report on robust imaging features.

Recently, Collin and colleagues found correlations between TMJ symptoms, maximum mouth opening, and CBCT findings, addressing the postulate that many children with JIA develop TMJ deformity (144). However, the CBCT findings were reported according to a system constructed for radiographic techniques (46), underpinning that there is an urgent need for a specific CBCT-based scoring system, e.g., the one we propose. It is advisable, and not uncommon for children with JIA and TMJ involvement to be at least partially managed by specialists in oral health such as orthodontics and maxillofacial surgeons. These specialists usually have easier access to, and experience with CBCT as opposed to MRI. In that setting, a robust CBCT-based scoring system might contribute to a reliable framework in the treatment of children with JIA.

The proposed scoring systems for MRI and CBCT are based on a dataset of 84 to 86 children with JIA, balanced in terms of range of pathology, age, and gender. Can the results drawn from this thesis be generalized to a broader, unselected JIA population or even children under diagnostic work-up for JIA? As presented in this thesis, it is possible the results can be used in a broader, but similar JIA population to guide the radiologist and paediatric rheumatologist working with children with an established JIA diagnosis. We would also argue that the methods and the population under study probably has similarities to a JIA population found in a tertiary, paediatric hospital of other industrialized, modern countries. We believe these results represent an important

step forward for research on JIA, in line with the ESPR research strategy (1). However, we would also strongly recommend further evaluation of the scoring systems addressing use by multiple readers and in less conform settings.

5.5 Strengths and limitations

Some strengths of the thesis are worth noting. We would argue that the relatively large numbers of included patients in all three papers enhance the robustness of the results. The study population in papers two and three includes only children with JIA which increases the transferability of the results to the general JIA population. Further, efforts were made to balance the datasets with respect to age, gender, and imaging findings. Regarding the MRI examinations, thorough standardization was made concerning machines used, sequences acquired and the image presentation to the readers. In all three papers considerable effort was made to harmonize the readers understanding of the imaging features.

The results of this thesis must be seen in the light of its shortcomings and limitations, some of which have already been problematized in the discussion on methodological aspects. We acknowledge that our retrospectively collected study population in paper one does not represent healthy children, as the participants were either hospitalized for other reasons than JIA or under diagnostic work-up for suspected non-JIA disease. It is also noteworthy that not even a population of 101 children will display the whole spectrum of normal variants of the TMJ that probably exists in an unselected, much larger paediatric population. The CBCT machines used in paper three were from different manufacturers and did have somewhat different acquisition parameters, which might have caused unwanted variations in the image dataset although stratified analysis did not find differences between the machines. The use of Cohen's kappa has limitations, as discussed earlier. By presenting the absolute prevalence of each imaging feature, by each observer and by each reading, it is possible for the reader to relate each kappa value to the prevalence of each feature. However, partly due to space restrictions from the publishing journals these full datasets were not published.

6. Conclusions

In this thesis we aimed to evaluate MRI-based imaging features to identify features precise enough for the description of normal temporomandibular joints in children without JIA. We also aimed to evaluate a large set of CBCT-, and MRI-based image features, including already established measurements and scores, but also novel ones. The image features were tested in a population of children with JIA, addressing both intraobserver and interobserver agreement to identify the most precise features.

Based on the results, we conclude that:

In children and adolescents aged 2-18 years without JIA:

- Subjective assessment of anterior inclination of the mandibular condyle in the sagittal/oblique plane is a robust image feature.
- Condylar flattening in the coronal plane is a robust image feature.
- The mandibular condyle is predominantly straight in the younger age group and the anterior inclination increases by age.
- Mild flattening of the condyle in the coronal plane is a common finding.
- Mild contrast enhancement of the TMJ is a normal finding.
- Continuous measurements of different parts of the TMJ, previously used to define normal and pathological findings, are associated with wide limits of agreement, probably precluding their use in a clinical setting.

In children and adolescents with a known diagnosis of JIA:

- From a set of MRI-based image features addressing the osteochondral domain; condylar shape in the sagittal plane (on a 0-3 scale) and in the coronal plane (on a 0-2 scale), loss of condylar volume (on a 0-1 scale), condylar irregularities (on a 0-2 scale), shape of the articular eminence and glenoid fossa (on a 0-2 scale), disk abnormalities (on a 0-1 scale), and condylar inclination (on a 0-2 scale) can be used in a future scoring system.
- From a set of MRI-based image features addressing the inflammatory domain; joint fluid in the sagittal plane (on a 0-2 scale), synovial enhancement (on a 0-2

scale), overall impression of inflammation (on a 0-1 scale), and bone marrow oedema (on a 0-1 scale) can be used in a future scoring system.

- From a set of CBCT-based image features addressing the osteochondral domain; overall impression of damage, shape of the condyle and articular eminence, and glenoid fossa in both sagittal and coronal plane, reduction of condylar volume, joint surface continuity, and irregularities of the joint surfaces can be used in a future scoring system.

7. Future perspectives

The results from this thesis hopefully represent a few bricks in the on-going building project of diagnostics, treatment, and follow-up of children with JIA. However, there are many remaining bricks to be laid by us or others, to make this building higher and more robust.

In the process of recruiting volunteers without JIA, we received important information on how the volunteers experienced the data collection. It turns out that a large majority of the volunteers promote the altruistic aspect by contributing to the research society with their time and by giving access to anatomical, image-based information. Similar experiences have been drawn by Ording Müller's, Avenarius and Rosendahl's research group recruiting healthy children addressing normal standards for whole-body MRI. When communicating with ethical committees, we are also under the impression that there is an increasing understanding of the importance of normal reference standards. Thus, there could be an opportunity to engage in larger, prospective data collection of MRI-based normal standards of the TMJ in volunteers with no signs of TMJ pathology or JIA. Given the recent advances in MRI technology it is not unlikely that even an examination without gadolinium contrast could contribute to our understanding of the border between the normal and pathological TMJ.

In her publication from 2004, Obuchowski describes the development of a diagnostic test method in terms of number of cases, number of observers, and assessment of interobserver agreement (145). Accordingly, the work and results in this thesis represent the first few steps in a proposed series of steps where the next, logical advancement would be repeated testing of the scoring systems in a similar or slightly larger cohort. Preferably, a larger team of observers, between five to 10, should use the scoring systems and individual scorings of the observers should be analysed. We agree that performing such an extensive, transparent testing of the systems would give substantial knowledge of its transferability to a clinical setting. Such a test would also be in line with the recommended workflow proposed by Thornbury and Fryback, presented in the introduction.

Can MRI- and CBCT-based scoring systems of the TMJ in JIA be evaluated in terms of construct validity? Put in a different way, do the scoring systems measure presence and/or development of JIA in the TMJ? Previous publications and experiences drawn from experts on the field certainly point in that direction, but as per today, there is no golden standard to use as a comparator when evaluating medical imaging of the TMJ in JIA. This presents an inherent, fundamental challenge when construct validity of MRI or CBCT of the TMJ in JIA is to be evaluated. Possibly, studies on long-term follow-up of children with JIA, both symptomatic and asymptomatic, combined with standardized imaging, could provide further evidence on this topic.

If the results from this work are considered useful by other radiologic and paediatric rheumatologic institutions, one could consider harmonizing the existing image-based scoring systems. Important contributions have been made by others i.e., the JAMRIS-TMJ system and other ongoing initiatives from the ESPR, TMJaw, and OMERACT. These are contributions that in many ways made this thesis possible. Probably much could be gained by harmonizing the systems and by finding future ways to fruitful collaboration.

8. Errata

Summary in English, fifth section

”In the first paper we used a retrospectively collected dataset including 101 head MRI examinations, of which 36 included images before and after with intravenous contrast, performed for other reasons than JIA.”

Is changed to:

”In the first paper we used a retrospectively collected dataset including 101 head MRI examinations, of which 36 included images before and after intravenous contrast, performed for other reasons than JIA.”

Page 20, second section:

“Still, systemic treatment of TMJ arthritis is common and not controversial (22)(Stoll Ped Rheum 2014).”

Is changed to:

“Still, systemic treatment of TMJ arthritis is common and not controversial (22).”

Page 35, fifth section:

“This way of plotting the agreement (or lack thereof) gives the reader an opportunity to determine if the difference is a clinical setting relevant to him or her.”

Is changed to:

“This way of plotting the agreement (or lack thereof) gives the reader an opportunity to determine if the difference is important in a clinical setting relevant to him or her.”

Page 38, second section:

“The aim was to evaluate the reliability of established and new measurements for describing the normal MR-based anatomy of the TMJ, and based on the most robust measures, to characterize the appearances of the normal TMJ in children and adolescents.”

Is changed to:

“The aim was to evaluate the reliability of established and new measurements for describing the normal MRI-based anatomy of the TMJ, and based on the most robust measures, to characterize the appearances of the normal TMJ in children and adolescents.”

Page 39, second section:

“The study is registered on clinicaltrials.gov with identifier NCT03904459.”

Is changed to:

”The study is registered on clinicaltrials.gov with identifier NCT03904459.”

Page 40, second section:

“At the same, time inclusion of all 228 patients was not feasible due to time constraints and logistic challenges”

Is changed to:

“At the same time, inclusion of all 228 patients was not feasible due to time constraints and logistic challenges”

Page 43, third section:

“Assessment of joint fluid was made in a semiquantitative way on a 0-2 scale, ranging from no fluid to more than two mm of fluid in or two joint compartments”

Is changed to:

“Assessment of joint fluid was made in a semiquantitative way on a 0-2 scale, ranging from no fluid to more than two mm of fluid in one or two joint compartments”

Page 59, first section:

“In addition, an adequate, child-friendly environment had to be established all the way from the child entering the imaging department, staying comfortable and in the scanner and lastly, leaving the department with a feeling of being sound and taken care of.”

Is changed to:

“In addition, an adequate, child-friendly environment had to be established all the way from the child entering the imaging department, staying comfortable in the scanner and lastly, leaving the department with a feeling of being sound and taken care of.

Page 60, second section:

“Using a head coil, it is not easy to overcome this drawback of the fat saturation and technique and it is not unthinkable that this affects the visualization of bone marrow oedema”

Is changed to:

“Using a head coil, it is not easy to overcome this drawback of the fat saturation technique and it is not unthinkable that this affects the visualization of bone marrow oedema”

Page 66, second section:

“A consent from the child must be obtain if the child is 16 years or older.”

Is changed to:

“A consent from the child must be obtained if the child is 16 years or older.”

9. References

1. Arthurs OJ, van Rijn RR, Granata C, Porto L, Hirsch FW, Rosendahl K. European Society of Paediatric Radiology 2019 strategic research agenda: improving imaging for tomorrow's children. *Pediatric radiology*. 2019;49(8):983-9.
2. Keats TE, Smith TH. An atlas of normal developmental roentgen anatomy 2nd edition. Chicago: Year book medical publisher; 1987.
3. Anderson MW, Keats TE. Atlas of normal roentgen variants that may simulate disease: Saunders; 2012.
4. Prahald S, O'Brien E, Fraser AM, Kerber RA, Mineau GP, Pratt D, et al. Familial aggregation of juvenile idiopathic arthritis. *Arthritis and rheumatism*. 2004;50(12):4022-7.
5. Hinks A, Cobb J, Marion MC, Prahald S, Sudman M, Bowes J, et al. Dense genotyping of immune-related disease regions identifies 14 new susceptibility loci for juvenile idiopathic arthritis. *Nat Genet*. 2013;45(6):664-9.
6. Alberdi-Saugstrup M, Enevold C, Zak M, Nielsen S, Nordal E, Berntson L, et al. Non-HLA gene polymorphisms in juvenile idiopathic arthritis: associations with disease outcome. *Scandinavian journal of rheumatology*. 2017;46(5):369-76.
7. Murray KJ, Moroldo MB, Donnelly P, Prahald S, Passo MH, Giannini EH, et al. Age-specific effects of juvenile rheumatoid arthritis-associated HLA alleles. *Arthritis and rheumatism*. 1999;42(9):1843-53.
8. Nigrovic PA, Martínez-Bonet M, Thompson SD. Implications of juvenile idiopathic arthritis genetic risk variants for disease pathogenesis and classification. *Current opinion in rheumatology*. 2019;31(5):401-10.
9. Gonzalez B, Larrañaga C, León O, Díaz P, Miranda M, Barría M, et al. Parvovirus B19 may have a role in the pathogenesis of juvenile idiopathic arthritis. *The Journal of rheumatology*. 2007;34(6):1336-40.
10. Lehmann HW, Knöll A, Küster RM, Modrow S. Frequent infection with a viral pathogen, parvovirus B19, in rheumatic diseases of childhood. *Arthritis and rheumatism*. 2003;48(6):1631-8.
11. Massa M, Mazzoli F, Pignatti P, De Benedetti F, Passalia M, Viola S, et al. Proinflammatory responses to self HLA epitopes are triggered by molecular mimicry to Epstein-Barr virus proteins in oligoarticular juvenile idiopathic arthritis. *Arthritis and rheumatism*. 2002;46(10):2721-9.
12. Ellis JA, Munro JE, Ponsonby AL. Possible environmental determinants of juvenile idiopathic arthritis. *Rheumatology (Oxford, England)*. 2010;49(3):411-25.
13. Clarke SLN, Mageean KS, Maccora I, Harrison S, Simonini G, Sharp GC, et al. Moving from nature to nurture: a systematic review and meta-analysis of environmental factors associated with juvenile idiopathic arthritis. *Rheumatology (Oxford, England)*. 2021.
14. Gattorno M, Gerloni V, Morando A, Comanducci F, Buoncompagni A, Picco P, et al. Synovial membrane expression of matrix metalloproteinases and tissue inhibitor 1 in juvenile idiopathic arthritides. *The Journal of rheumatology*. 2002;29(8):1774-9.
15. Petty RE, Southwood TR, Manners P, Baum J, Glass DN, Goldenberg J, et al. International League of Associations for Rheumatology classification of juvenile

- idiopathic arthritis: second revision, Edmonton, 2001. *The Journal of rheumatology*. 2004;31(2):390-2.
16. Ravelli A, Martini A. Juvenile idiopathic arthritis. *Lancet*. 2007;369(9563):767-78.
 17. Thierry S, Fautrel B, Lemelle I, Guillemin F. Prevalence and incidence of juvenile idiopathic arthritis: a systematic review. *Joint Bone Spine*. 2014;81(2):112-7.
 18. Berntson L, Andersson Gäre B, Fasth A, Herlin T, Kristinsson J, Lahdenne P, et al. Incidence of juvenile idiopathic arthritis in the Nordic countries. A population based study with special reference to the validity of the ILAR and EULAR criteria. *The Journal of rheumatology*. 2003;30(10):2275-82.
 19. Glerup M, Rypdal V, Arnstad ED, Ekelund M, Peltoniemi S, Aalto K, et al. Long-Term Outcomes in Juvenile Idiopathic Arthritis: Eighteen Years of Follow-Up in the Population-Based Nordic Juvenile Idiopathic Arthritis Cohort. *Arthritis care & research*. 2020;72(4):507-16.
 20. Nordal E, Zak M, Aalto K, Berntson L, Fasth A, Herlin T, et al. Ongoing disease activity and changing categories in a long-term nordic cohort study of juvenile idiopathic arthritis. *Arthritis and rheumatism*. 2011;63(9):2809-18.
 21. Ravelli A, Consolaro A, Horneff G, Laxer RM, Lovell DJ, Wulfraat NM, et al. Treating juvenile idiopathic arthritis to target: recommendations of an international task force. *Annals of the rheumatic diseases*. 2018;77(6):819-28.
 22. Stoll ML, Cron RQ. Treatment of juvenile idiopathic arthritis: a revolution in care. *Pediatric rheumatology online journal*. 2014;12:13.
 23. Schaller JG. The history of pediatric rheumatology. *Pediatr Res*. 2005;58(5):997-1007.
 24. Giannini EH, Brewer EJ, Kuzmina N, Shaikov A, Maximov A, Vorontsov I, et al. Methotrexate in resistant juvenile rheumatoid arthritis. Results of the U.S.A.-U.S.S.R. double-blind, placebo-controlled trial. The Pediatric Rheumatology Collaborative Study Group and The Cooperative Children's Study Group. *N Engl J Med*. 1992;326(16):1043-9.
 25. Scott C, Meiorin S, Filocamo G, Lanni S, Valle M, Martinoli C, et al. A reappraisal of intra-articular corticosteroid therapy in juvenile idiopathic arthritis. *Clin Exp Rheumatol*. 2010;28(5):774-81.
 26. Jennings H, Hennessy K, Hendry GJ. The clinical effectiveness of intra-articular corticosteroids for arthritis of the lower limb in juvenile idiopathic arthritis: a systematic review. *Pediatric rheumatology online journal*. 2014;12:23.
 27. Ravelli A, Davì S, Bracciolini G, Pistorio A, Consolaro A, van Dijkhuizen EHP, et al. Intra-articular corticosteroids versus intra-articular corticosteroids plus methotrexate in oligoarticular juvenile idiopathic arthritis: a multicentre, prospective, randomised, open-label trial. *Lancet*. 2017;389(10072):909-16.
 28. Giancane G, Muratore V, Marzetti V, Quilis N, Benavente BS, Bagnasco F, et al. Disease activity and damage in juvenile idiopathic arthritis: methotrexate era versus biologic era. *Arthritis research & therapy*. 2019;21(1):168.
 29. Klein A, Klotsche J, Hügler B, Minden K, Hospach A, Weller-Heinemann F, et al. Long-term surveillance of biologic therapies in systemic-onset juvenile idiopathic arthritis: data from the German BIKER registry. *Rheumatology (Oxford, England)*. 2020;59(9):2287-98.

30. Klein A, Becker I, Minden K, Hospach A, Schwarz T, Foeldvari I, et al. Biologic Therapies in Polyarticular Juvenile Idiopathic Arthritis. Comparison of Long-Term Safety Data from the German BIKER Registry. *ACR Open Rheumatol.* 2020;2(1):37-47.
31. Schmidt C, Ertel T, Arbogast M, Hügler B, Kalle TV, Neff A. The Diagnosis and Treatment of Rheumatoid Arthritis and Juvenile Idiopathic Arthritis of the Temporomandibular Joint. *Dtsch Arztebl Int.* 2022(Forthcoming).
32. Stoll ML, Cron RQ, Saurenmann RK. Systemic and intra-articular anti-inflammatory therapy of temporomandibular joint arthritis in children with juvenile idiopathic arthritis. *Seminars in Orthodontics.* 2015;21(2):125-33.
33. Resnick CM, Pedersen TK, Abramowicz S, Twilt M, Stoustrup PB. Time to Reconsider Management of the Temporomandibular Joint in Juvenile Idiopathic Arthritis. *Journal of oral and maxillofacial surgery : official journal of the American Association of Oral and Maxillofacial Surgeons.* 2018.
34. Cannizzaro E, Schroeder S, Muller LM, Kellenberger CJ, Saurenmann RK. Temporomandibular joint involvement in children with juvenile idiopathic arthritis. *The Journal of rheumatology.* 2011;38(3):510-5.
35. Billiau AD, Hu Y, Verdonck A, Carels C, Wouters C. Temporomandibular joint arthritis in juvenile idiopathic arthritis: prevalence, clinical and radiological signs, and relation to dentofacial morphology. *The Journal of rheumatology.* 2007;34(9):1925-33.
36. Glerup M, Stoustrup P, Hauge L, Rypdal V, Nordal E, Frid P, et al. Long-term Outcomes of Temporomandibular Joints in Juvenile Idiopathic Arthritis. *The Journal of rheumatology.* 2019.
37. Ringold S, Cron RQ. The temporomandibular joint in juvenile idiopathic arthritis: frequently used and frequently arthritic. *Pediatric rheumatology online journal.* 2009;7:11.
38. Smartt JM, Jr., Low DW, Bartlett SP. The pediatric mandible: I. A primer on growth and development. *Plastic and reconstructive surgery.* 2005;116(1):14e-23e.
39. Hinton RJ. Genes that regulate morphogenesis and growth of the temporomandibular joint: a review. *Dev Dyn.* 2014;243(7):864-74.
40. Stocum DL, Roberts WE. Part I: Development and Physiology of the Temporomandibular Joint. *Curr Osteoporos Rep.* 2018;16(4):360-8.
41. Roberts WE, Stocum DL. Part II: Temporomandibular Joint (TMJ)-Regeneration, Degeneration, and Adaptation. *Curr Osteoporos Rep.* 2018;16(4):369-79.
42. Nickel JC, McLachlan KR, Smith DM. Eminence development of the postnatal human temporomandibular joint. *Journal of dental research.* 1988;67(6):896-902.
43. Katsavrias EG. Changes in articular eminence inclination during the craniofacial growth period. *The Angle orthodontist.* 2002;72(3):258-64.
44. Junhasavasdikul T, Abadeh A, Tolend M, Doria AS. Developing a reference MRI database for temporomandibular joints in healthy children and adolescents. *Pediatric radiology.* 2018;48(8):1113-22.
45. Karlo CA, Stolzmann P, Habernig S, Muller L, Saurenmann T, Kellenberger CJ. Size, shape and age-related changes of the mandibular condyle during childhood. *European radiology.* 2010;20(10):2512-7.
46. Arvidsson LZ, Flato B, Larheim TA. Radiographic TMJ abnormalities in patients with juvenile idiopathic arthritis followed for 27 years. *Oral Surg Oral Med Oral Pathol Oral Radiol Endod.* 2009;108(1):114-23.

47. Twilt M, Moberg SM, Arends LR, ten Cate R, van Suijlekom-Smit L. Temporomandibular involvement in juvenile idiopathic arthritis. *The Journal of rheumatology*. 2004;31(7):1418-22.
48. Koos B, Twilt M, Kyank U, Fischer-Brandies H, Gassling V, Tzaribachev N. Reliability of clinical symptoms in diagnosing temporomandibular joint arthritis in juvenile idiopathic arthritis. *The Journal of rheumatology*. 2014;41(9):1871-7.
49. Stoustrup P, Resnick CM, Pedersen TK, Abramowicz S, Michelotti A, Kuseler A, et al. Standardizing Terminology and Assessment for Orofacial Conditions in Juvenile Idiopathic Arthritis: International, Multidisciplinary Consensus-based Recommendations. *The Journal of rheumatology*. 2019;46(5):518-22.
50. Stoustrup P, Lerman MA, Twilt M. The Temporomandibular Joint in Juvenile Idiopathic Arthritis. *Rheum Dis Clin North Am*. 2021;47(4):607-17.
51. Skeie MS, Gil EG, Cetrelli L, Rosén A, Fischer J, Åström AN, et al. Oral health in children and adolescents with juvenile idiopathic arthritis - a systematic review and meta-analysis. *BMC Oral Health*. 2019;19(1):285.
52. Rahimi H, Twilt M, Herlin T, Spiegel L, Pedersen TK, Kuseler A, et al. Orofacial symptoms and oral health-related quality of life in juvenile idiopathic arthritis: a two-year prospective observational study. *Pediatric rheumatology online journal*. 2018;16(1):47.
53. Stoustrup P, Glerup M, Bilgrau AE, Kuseler A, Verna C, Christensen AE, et al. Cumulative Incidence of Orofacial Manifestations in Early Juvenile Idiopathic Arthritis: A Regional, Three Year Cohort Study. *Arthritis care & research*. 2019.
54. El Assar de la Fuente S, Angenete O, Jellestad S, Tzaribachev N, Koos B, Rosendahl K. Juvenile idiopathic arthritis and the temporomandibular joint: A comprehensive review. *Journal of cranio-maxillo-facial surgery : official publication of the European Association for Cranio-Maxillo-Facial Surgery*. 2016;44(5):597-607.
55. Petersson A. What you can and cannot see in TMJ imaging--an overview related to the RDC/TMD diagnostic system. *Journal of oral rehabilitation*. 2010;37(10):771-8.
56. Adams GL, Gansky SA, Miller AJ, Harrell WE, Jr., Hatcher DC. Comparison between traditional 2-dimensional cephalometry and a 3-dimensional approach on human dry skulls. *American journal of orthodontics and dentofacial orthopedics : official publication of the American Association of Orthodontists, its constituent societies, and the American Board of Orthodontics*. 2004;126(4):397-409.
57. Hechler BL, Phero JA, Van Mater H, Matthews NS. Ultrasound versus magnetic resonance imaging of the temporomandibular joint in juvenile idiopathic arthritis: a systematic review. *International journal of oral and maxillofacial surgery*. 2018;47(1):83-9.
58. Hemke R, Herregods N, Jaremko JL, Åström G, Avenarius D, Becce F, et al. Imaging assessment of children presenting with suspected or known juvenile idiopathic arthritis: ESSR-ESPR points to consider. *European radiology*. 2020;30(10):5237-49.
59. Karlo CA, Patcas R, Kau T, Watzal H, Signorelli L, Muller L, et al. MRI of the temporo-mandibular joint: which sequence is best suited to assess the cortical bone of the mandibular condyle? A cadaveric study using micro-CT as the standard of reference. *European radiology*. 2012;22(7):1579-85.
60. Navallas M, Inarejos EJ, Iglesias E, Cho Lee GY, Rodriguez N, Anton J. MR Imaging of the Temporomandibular Joint in Juvenile Idiopathic Arthritis: Technique

and Findings. *Radiographics* : a review publication of the Radiological Society of North America, Inc. 2017;37(2):595-612.

61. Chan BY, Gill KG, Rebsamen SL, Nguyen JC. MR Imaging of Pediatric Bone Marrow. *Radiographics* : a review publication of the Radiological Society of North America, Inc. 2016;36(6):1911-30.
62. Maraghelli D, Brandi ML, Matucci Cerinic M, Peired AJ, Colagrande S. Edema-like marrow signal intensity: a narrative review with a pictorial essay. *Skeletal radiology*. 2021;50(4):645-63.
63. Blum A, Roch D, Loeuille D, Louis M, Batch T, Lecocq S, et al. [Bone marrow edema: definition, diagnostic value and prognostic value]. *J Radiol*. 2009;90(12):1789-811.
64. Tanturri de Horatio L, Damasio MB, Barbuti D, Bracaglia C, Lambot-Juhan K, Boavida P, et al. MRI assessment of bone marrow in children with juvenile idiopathic arthritis: intra- and inter-observer variability. *Pediatric radiology*. 2012;42(6):714-20.
65. Del Grande F, Santini F, Herzka DA, Aro MR, Dean CW, Gold GE, et al. Fat-suppression techniques for 3-T MR imaging of the musculoskeletal system. *Radiographics* : a review publication of the Radiological Society of North America, Inc. 2014;34(1):217-33.
66. Baumbach SF, Pfahler V, Bechtold-Dalla Pozza S, Feist-Pagenstert I, Fürmetz J, Baur-Melnyk A, et al. How We Manage Bone Marrow Edema-An Interdisciplinary Approach. *J Clin Med*. 2020;9(2).
67. McQueen FM. Bone marrow edema and osteitis in rheumatoid arthritis: the imaging perspective. *Arthritis research & therapy*. 2012;14(5):224.
68. Bøyesen P, Haavardsholm EA, van der Heijde D, Østergaard M, Hammer HB, Sesseng S, et al. Prediction of MRI erosive progression: a comparison of modern imaging modalities in early rheumatoid arthritis patients. *Annals of the rheumatic diseases*. 2011;70(1):176-9.
69. Hetland ML, Ejbjerg B, Hørslev-Petersen K, Jacobsen S, Vestergaard A, Jurik AG, et al. MRI bone oedema is the strongest predictor of subsequent radiographic progression in early rheumatoid arthritis. Results from a 2-year randomised controlled trial (CIMESTRA). *Annals of the rheumatic diseases*. 2009;68(3):384-90.
70. Avenarius DFM, Ording Muller LS, Rosendahl K. Joint Fluid, Bone Marrow Edemalike Changes, and Ganglion Cysts in the Pediatric Wrist: Features That May Mimic Pathologic Abnormalities-Follow-Up of a Healthy Cohort. *AJR American journal of roentgenology*. 2017;208(6):1352-7.
71. Bracken J, Nandurkar D, Radhakrishnan K, Ditchfield M. Normal paediatric bone marrow: magnetic resonance imaging appearances from birth to 5 years. *J Med Imaging Radiat Oncol*. 2013;57(3):283-91.
72. Shah LM, Hanrahan CJ. MRI of spinal bone marrow: part I, techniques and normal age-related appearances. *AJR American journal of roentgenology*. 2011;197(6):1298-308.
73. Laor T, Jaramillo D. MR imaging insights into skeletal maturation: what is normal? *Radiology*. 2009;250(1):28-38.
74. Smith MD. The normal synovium. *Open Rheumatol J*. 2011;5:100-6.
75. Rieter JF, de Horatio LT, Nusman CM, Muller LO, Hemke R, Avenarius DF, et al. The many shades of enhancement: timing of post-gadolinium images strongly

- influences the scoring of juvenile idiopathic arthritis wrist involvement on MRI. *Pediatric radiology*. 2016.
76. Barendregt AM, van Gulik EC, Groot PFC, Dolman KM, van den Berg JM, Nassar-Sheikh Rashid A, et al. Prolonged time between intravenous contrast administration and image acquisition results in increased synovial thickness at magnetic resonance imaging in patients with juvenile idiopathic arthritis. *Pediatric radiology*. 2019.
 77. Stoll ML, Sharpe T, Beukelman T, Good J, Young D, Cron RQ. Risk factors for temporomandibular joint arthritis in children with juvenile idiopathic arthritis. *The Journal of rheumatology*. 2012;39(9):1880-7.
 78. von Kalle T, Winkler P, Stuber T. Contrast-enhanced MRI of normal temporomandibular joints in children--is there enhancement or not? *Rheumatology (Oxford, England)*. 2013;52(2):363-7.
 79. von Kalle T, Stuber T, Winkler P, Maier J, Hospach T. Early detection of temporomandibular joint arthritis in children with juvenile idiopathic arthritis - the role of contrast-enhanced MRI. *Pediatric radiology*. 2015;45(3):402-10.
 80. Kellenberger CJ, Junhasavasdikul T, Tolend M, Doria AS. Temporomandibular joint atlas for detection and grading of juvenile idiopathic arthritis involvement by magnetic resonance imaging. *Pediatric radiology*. 2018;48(3):411-26.
 81. Buch K, Peacock ZS, Resnick CM, Rothermel H, Kaban LB, Caruso P. Regional differences in temporomandibular joint inflammation in patients with juvenile idiopathic arthritis: a dynamic post-contrast magnetic resonance imaging study. *International journal of oral and maxillofacial surgery*. 2020;49(9):1210-6.
 82. Kellenberger CJ, Abramowicz S, Arvidsson LZ, Kirkhus E, Tzaribachev N, Larheim TA. Recommendations for a Standard Magnetic Resonance Imaging Protocol of Temporomandibular Joints in Juvenile Idiopathic Arthritis. *Journal of oral and maxillofacial surgery : official journal of the American Association of Oral and Maxillofacial Surgeons*. 2018;76(12):2463-5.
 83. Kottke R, Saurenmann RK, Schneider MM, Muller L, Grotzer MA, Kellenberger CJ. Contrast-enhanced MRI of the temporomandibular joint: findings in children without juvenile idiopathic arthritis. *Acta radiologica (Stockholm, Sweden : 1987)*. 2014.
 84. Keller H, Muller LM, Markic G, Schraner T, Kellenberger CJ, Saurenmann RK. Is early TMJ involvement in children with juvenile idiopathic arthritis clinically detectable? Clinical examination of the TMJ in comparison with contrast enhanced MRI in patients with juvenile idiopathic arthritis. *Pediatric rheumatology online journal*. 2015;13:56.
 85. Malattia C, Tolend M, Mazzoni M, Panwar J, Zlotnik M, Otober T, et al. Current status of MR imaging of juvenile idiopathic arthritis. *Best Pract Res Clin Rheumatol*. 2020;34(6):101629.
 86. Kadesjö N, Lynds R, Nilsson M, Shi XQ. Radiation dose from X-ray examinations of impacted canines: cone beam CT vs two-dimensional imaging. *Dento maxillo facial radiology*. 2018;47(3):20170305.
 87. Larheim TA, Abrahamsson AK, Kristensen M, Arvidsson LZ. Temporomandibular joint diagnostics using CBCT. *Dento maxillo facial radiology*. 2015;44(1):20140235.

88. Zain-Alabdeen EH, Alsadhan RI. A comparative study of accuracy of detection of surface osseous changes in the temporomandibular joint using multidetector CT and cone beam CT. *Dento maxillo facial radiology*. 2012;41(3):185-91.
89. Cohnen M, Kemper J, Möbes O, Pawelzik J, Mödder U. Radiation dose in dental radiology. *European radiology*. 2002;12(3):634-7.
90. Kadesjö N, Benchimol D, Falahat B, Näsström K, Shi XQ. Evaluation of the effective dose of cone beam CT and multislice CT for temporomandibular joint examinations at optimized exposure levels. *Dento maxillo facial radiology*. 2015;44(8):20150041.
91. atomsikkerhet Dfso. Direktoratet for strålevern og atomsikkerhet [Direktoratet for strålevern og atomsikkerhet]. Available from: <https://radnett.dsa.no/?doc=faq>.
92. Honey OB, Scarfe WC, Hilgers MJ, Klueber K, Silveira AM, Haskell BS, et al. Accuracy of cone-beam computed tomography imaging of the temporomandibular joint: comparisons with panoramic radiology and linear tomography. *American journal of orthodontics and dentofacial orthopedics : official publication of the American Association of Orthodontists, its constituent societies, and the American Board of Orthodontics*. 2007;132(4):429-38.
93. Caruso S, Storti E, Nota A, Ehsani S, Gatto R. Temporomandibular Joint Anatomy Assessed by CBCT Images. *BioMed research international*. 2017;2017:2916953.
94. Tominna M, Vega-Fernandez P, McLaurin W, Meyers AB. Imaging of the Pediatric Temporomandibular Joint. *Seminars in Roentgenology*. 2021;56(3):307-24.
95. Bianchi J, Roberto Gonçalves J, Carlos de Oliveira Ruellas A, Vieira Pastana Bianchi J, Ashman LM, Yatabe M, et al. Radiographic interpretation using high-resolution Cbct to diagnose degenerative temporomandibular joint disease. *PLoS One*. 2021;16(8):e0255937.
96. Patel A, Tee BC, Fields H, Jones E, Chaudhry J, Sun Z. Evaluation of cone-beam computed tomography in the diagnosis of simulated small osseous defects in the mandibular condyle. *American journal of orthodontics and dentofacial orthopedics : official publication of the American Association of Orthodontists, its constituent societies, and the American Board of Orthodontics*. 2014;145(2):143-56.
97. Zhang ZL, Shi XQ, Ma XC, Li G. Detection accuracy of condylar defects in cone beam CT images scanned with different resolutions and units. *Dento maxillo facial radiology*. 2014;43(3):20130414.
98. Fryback DG, Thornbury JR. The efficacy of diagnostic imaging. *Med Decis Making*. 1991;11(2):88-94.
99. Leeftang MM, Rutjes AW, Reitsma JB, Hooft L, Bossuyt PM. Variation of a test's sensitivity and specificity with disease prevalence. *Cmaj*. 2013;185(11):E537-44.
100. Crewson PE. Reader agreement studies. *AJR American journal of roentgenology*. 2005;184(5):1391-7.
101. Ranganathan P, Pramesh CS, Aggarwal R. Common pitfalls in statistical analysis: Measures of agreement. *Perspect Clin Res*. 2017;8(4):187-91.
102. Watson PF, Petrie A. Method agreement analysis: a review of correct methodology. *Theriogenology*. 2010;73(9):1167-79.
103. Cohen J. Weighted kappa: Nominal scale agreement provision for scaled agreement or partial credit. *Psychological Bulletin*. 1960;70(4):213-20.

104. Cohen J. Weighted kappa: nominal scale agreement with provision for scaled disagreement or partial credit. *Psychol Bull.* 1968;70(4):213-20.
105. Landis JR, Koch GG. The measurement of observer agreement for categorical data. *Biometrics.* 1977;33(1):159-74.
106. Fleiss JL. Measuring nominal scale agreement among many raters. *Psychological bulletin.* 1971;76(5):378.
107. Feinstein AR, Cicchetti DV. High agreement but low kappa: I. The problems of two paradoxes. *Journal of clinical epidemiology.* 1990;43(6):543-9.
108. Gwet KL. Computing inter-rater reliability and its variance in the presence of high agreement. *Br J Math Stat Psychol.* 2008;61(Pt 1):29-48.
109. Bland JM, Altman DG. Statistical methods for assessing agreement between two methods of clinical measurement. *Lancet.* 1986;1(8476):307-10.
110. de Vet HC, Terwee CB, Knol DL, Bouter LM. When to use agreement versus reliability measures. *Journal of clinical epidemiology.* 2006;59(10):1033-9.
111. McGraw KO, & Wong, S. P. . Forming inferences about some intraclass correlation coefficients. *Psychological Methods.* 1996;1(1):30-46.
112. Rothwell PM. Analysis of agreement between measurements of continuous variables: general principles and lessons from studies of imaging of carotid stenosis. *J Neurol.* 2000;247(11):825-34.
113. Arthurs OJ, Bjørkum AA. Safety in pediatric imaging: an update. *Acta radiologica (Stockholm, Sweden : 1987).* 2013;54(9):983-90.
114. Avenarius DM, Ording Muller LS, Eldevik P, Owens CM, Rosendahl K. The paediatric wrist revisited--findings of bony depressions in healthy children on radiographs compared to MRI. *Pediatric radiology.* 2012;42(7):791-8.
115. Grobner T. Gadolinium – a specific trigger for the development of nephrogenic fibrosing dermopathy and nephrogenic systemic fibrosis? *Nephrology Dialysis Transplantation.* 2006;21(4):1104-8.
116. Kanda T, Ishii K, Kawaguchi H, Kitajima K, Takenaka D. High signal intensity in the dentate nucleus and globus pallidus on unenhanced T1-weighted MR images: relationship with increasing cumulative dose of a gadolinium-based contrast material. *Radiology.* 2014;270(3):834-41.
117. Blumfield E, Swenson DW, Iyer RS, Stanescu AL. Gadolinium-based contrast agents - review of recent literature on magnetic resonance imaging signal intensity changes and tissue deposits, with emphasis on pediatric patients. *Pediatric radiology.* 2019;49(4):448-57.
118. McDonald RJ, Weinreb JC, Davenport MS. Symptoms Associated with Gadolinium Exposure (SAGE): A Suggested Term. *Radiology.* 0(0):211349.
119. Jones SR, Carley S, Harrison M. An introduction to power and sample size estimation. *Emerg Med J.* 2003;20(5):453-8.
120. Orr KE, Andronikou S, Bramham MJ, Holjar-Erlc I, Menegotto F, Ramanan AV. Overcoming two technical pitfalls in MRI of paediatric and adolescent sacroiliitis. *Clinical radiology.* 2019;74(3):235-41.
121. Fritz J, Ahlawat S, Fritz B, Thawait GK, Stern SE, Raithel E, et al. 10-Min 3D Turbo Spin Echo MRI of the Knee in Children: Arthroscopy-Validated Accuracy for the Diagnosis of Internal Derangement. *Journal of magnetic resonance imaging : JMRI.* 2019;49(7):e139-e51.

122. Delfaut EM, Beltran J, Johnson G, Rousseau J, Marchandise X, Cotten A. Fat suppression in MR imaging: techniques and pitfalls. *Radiographics : a review publication of the Radiological Society of North America, Inc.* 1999;19(2):373-82.
123. Ma J. Dixon techniques for water and fat imaging. *Journal of magnetic resonance imaging : JMRI.* 2008;28(3):543-58.
124. Kutanzi KR, Lumen A, Koturbash I, Miousse IR. Pediatric Exposures to Ionizing Radiation: Carcinogenic Considerations. *Int J Environ Res Public Health.* 2016;13(11).
125. Yeh JK, Chen CH. Estimated radiation risk of cancer from dental cone-beam computed tomography imaging in orthodontics patients. *BMC Oral Health.* 2018;18(1):131.
126. Jha N, Kim YJ, Lee Y, Lee JY, Lee WJ, Sung SJ. Projected lifetime cancer risk from cone-beam computed tomography for orthodontic treatment. *Korean J Orthod.* 2021;51(3):189-98.
127. Geiger D, Bae WC, Statum S, Du J, Chung CB. Quantitative 3D ultrashort time-to-echo (UTE) MRI and micro-CT (μ CT) evaluation of the temporomandibular joint (TMJ) condylar morphology. *Skeletal radiology.* 2014;43(1):19-25.
128. Bankier AA, Levine D, Halpern EF, Kressel HY. Consensus interpretation in imaging research: is there a better way? *Radiology.* 2010;257(1):14-7.
129. Tolend MA, Twilt M, Cron RQ, Tzaribachev N, Guleria S, von Kalle T, et al. Toward Establishing a Standardized Magnetic Resonance Imaging Scoring System for Temporomandibular Joints in Juvenile Idiopathic Arthritis. *Arthritis care & research.* 2018;70(5):758-67.
130. Koos B, Tzaribachev N, Bott S, Ciesielski R, Godt A. Classification of temporomandibular joint erosion, arthritis, and inflammation in patients with juvenile idiopathic arthritis. *J Orofac Orthop.* 2013;74(6):506-19.
131. World Medical Association Declaration of Helsinki: ethical principles for medical research involving human subjects. *Jama.* 2013;310(20):2191-4.
132. Booth TC, Jackson A, Wardlaw JM, Taylor SA, Waldman AD. Incidental findings found in "healthy" volunteers during imaging performed for research: current legal and ethical implications. *The British journal of radiology.* 2010;83(990):456-65.
133. Engesæter I, Laborie LB, Lehmann TG, Sera F, Fevang J, Pedersen D, et al. Radiological findings for hip dysplasia at skeletal maturity. Validation of digital and manual measurement techniques. *Skeletal radiology.* 2012;41(7):775-85.
134. Tamimi D, Jalali E, Hatcher D. Temporomandibular Joint Imaging. *Radiol Clin North Am.* 2018;56(1):157-75.
135. Lo Giudice A, Quinzi V, Ronsivalle V, Farronato M, Nicotra C, Indelicato F, et al. Evaluation of Imaging Software Accuracy for 3-Dimensional Analysis of the Mandibular Condyle. A Comparative Study Using a Surface-to-Surface Matching Technique. *Int J Environ Res Public Health.* 2020;17(13).
136. Huntjens E, Kiss G, Wouters C, Carels C. Condylar asymmetry in children with juvenile idiopathic arthritis assessed by cone-beam computed tomography. *European journal of orthodontics.* 2008;30(6):545-51.
137. Lei J, Liu MQ, Yap AU, Fu KY. Condylar subchondral formation of cortical bone in adolescents and young adults. *Br J Oral Maxillofac Surg.* 2013;51(1):63-8.

138. Nguyen JC, Markhardt BK, Merrow AC, Dwek JR. Imaging of Pediatric Growth Plate Disturbances. *Radiographics : a review publication of the Radiological Society of North America, Inc.* 2017;37(6):1791-812.
139. Orr KE, Andronikou S, Bramham MJ, Holjar-Erlic I, Menegotto F, Ramanan AV. Magnetic resonance imaging of sacroiliitis in children: frequency of findings and interobserver reliability. *Pediatric radiology.* 2018;48(11):1621-8.
140. Kellenberger CJ, Arvidsson LZ, Larheim TA. In: Øgaard B, editor. *Seminars in ortodontics.* 212015. p. 111-20.
141. Tolend M, Junhasavasdikul T, Cron RQ, Inarejos Clemente EJ, von Kalle T, Kellenberger CJ, et al. Discrete Choice Experiment on a Magnetic Resonance Imaging Scoring System for Temporomandibular Joints in Juvenile Idiopathic Arthritis. *Arthritis care & research.* 2021.
142. Tolend M, Doria AS, Meyers AB, Larheim TA, Abramowicz S, Aguet J, et al. Assessing the Reliability of the OMERACT Juvenile Idiopathic Arthritis Magnetic Resonance Scoring System for Temporomandibular Joints (JAMRIS-TMJ). *Journal of Clinical Medicine.* 2021;10(18):4047.
143. Vaid YN, Dunnivant FD, Royal SA, Beukelman T, Stoll ML, Cron RQ. Imaging of the temporomandibular joint in juvenile idiopathic arthritis. *Arthritis care & research.* 2014;66(1):47-54.
144. Collin M, Hagelberg S, Ernberg M, Hedenberg-Magnusson B, Christidis N. Temporomandibular joint involvement in children with juvenile idiopathic arthritis-Symptoms, clinical signs and radiographic findings. *Journal of oral rehabilitation.* 2022;49(1):37-46.
145. Obuchowski NA. How many observers are needed in clinical studies of medical imaging? *AJR American journal of roentgenology.* 2004;182(4):867-9.
146. Miller E, Inarejos Clemente EJ, Tzaribachev N, Guleria S, Tolend M, Meyers AB, et al. Imaging of temporomandibular joint abnormalities in juvenile idiopathic arthritis with a focus on developing a magnetic resonance imaging protocol. *Pediatric radiology.* 2018;48(6):792-800.

10. Appendices

Appendix A. Acquisition parameters for the MRI sequences used in paper two

Sequence	Plane	Fat saturation	TR	TE	Slice thickness	Interslice gap	Field of view	Matrix	NSA	Flip angle	ETL
T1-MPRAGE	Sagittal	No	2000	2.26	1		250x250	256x256	1	8	
T1-TSE	Coronal	No	826	7.9	2	2.2	179x179	448x359	3	131	4
T2-TSE	Sagittal/oblique	Yes	3530	71	2	2.2	150x150	448x314	2	150	9
PD-TSE	Sagittal/oblique	No	3470	22	2	2.2	150x150	448x314	2	139	10
T1-TSE	Sagittal/oblique	Yes	774	8.1	2	2.2	150x150	384x269	3	122	4
T1-TSE, after intravenous contrast	Sagittal/oblique	Yes	774	8.1	2	2.2	150x150	384x269	2	122	4
PD-TSE, open mouth	Sagittal/oblique	No	3470	22	2	2.2	150x150	448x314	2	139	10

Appendix B. Scoring protocol of paper one

Image feature	Plane	Grade
Shape of the condyle	Sagittal/oblique	0= rounded 1= mildly flattened 2= moderately flattened 3= severely flattened
Presence of an anterior beak	Sagittal/oblique	0= absent 1= present
Anterior condylar inclination	Sagittal/oblique	0= no inclination 1= mild 2= moderate
Shape of the glenoid fossa and articular eminence	Sagittal/oblique	0= S-shaped 1= slightly flattened or widened fossa 2= clear widening of the fossa or flattening of the eminence 3= J-shaped, extensive abnormality
Shape of the condyle	Coronal	0= rounded 1= mildly flattened 2= moderately to severely flattened
Condylar surface irregularities	Coronal	0= absent 1= present
Joint space	Sagittal/oblique	mm
Temporal fossa angle	Sagittal/oblique	degrees
Condylar inclination	Sagittal/oblique	degrees
Joint fluid	All available	0= none 1= a fine, hyperintense line in the upper or lower compartment or small dots in an articular recess 2= moderate >2 mm fluid in one or more of abovementioned locations
Bone marrow oedema	All available	0= absent 1= present

Joint enhancement	Transverse	0= none 1= mild, immediately around the condyle 2= moderate, exceeding the joint tissue
-------------------	------------	---

Appendix C. Scoring protocol paper 2. Imaging features for scoring of temporomandibular joints in the osteochondral domain by magnetic resonance imaging

	Image plane	Grade 0	Grade 1	Grade 2	Grade 3
Condylar shape	Sagittal/oblique	Rounded/ovoid	Very subtle anterior flattening	Mild flattening; involves part of the surface of the condyle	Moderate/severe flattening; involves the entire surface of the condyle, or loss of height of the condyle
Condylar shape	Coronal T1	Convex throughout	Mild/partial flattening	Moderately or severely flattened throughout	
Condylar inclination	Sagittal/oblique	Straight	Mild anterior inclination	Moderate/significant anterior inclination	
Shape of the articular eminence and glenoid fossa	Sagittal/oblique	S-shaped	Mild to moderate widening or flattening	Severely flattened fossa-eminence	
Loss of condylar volume	All available	None	Clearly deformed condyle		
Condylar irregularities, core and ideal protocol, adapted from (146)	Coronal and sagittal/oblique	No irregularities or deep breaks of the bony joint surface	Mild irregularities involving only part of the articular surface of the condyle	Moderate/ severe; presence of deep breaks in the subchondral bone seen in two planes, or irregularities involving the entire articular surface	
Condylar flattening, adapted from (129)	Sagittal/oblique	No loss of the round/slightly angular shape of the condyle	Mild; extent of flattening involves parts of the surface of the condyle	Moderate/severe; extent of flattening involves the entire surface of the condyle, or loss of the height of the condyle	
Disk abnormalities	Sagittal/oblique	None	Presence of flattening, displacement or destruction		

Appendix D. Scoring protocol paper 2. Imaging features for scoring of temporomandibular joints in the inflammatory domain by magnetic resonance imaging

Imaging feature	Definition/image plane	Grading
Overall impression of inflammation	All available images	0=Normal; includes normal synovial enhancement and a thin line of joint fluid 1=Mild inflammation; considered pathological 2=Moderate to severe inflammation
Overall impression of pathological joint fluid	All available images	0=No 1=Yes
Synovial enhancement	Signal intensity of the synovium, based on sagittal/ oblique T1-fs pre contrast and sagittal/oblique T1-fs post-contrast images	0= Subtle synovial enhancement, what is believed as normal 1= Mildly increased synovial enhancement 2= Moderately to severely increased synovial enhancement (signal intensity \geq nearby vessel)
Subjective impression of joint fluid, upper compartment	Sagittal/ oblique T2-fat saturated images	0=No signal 1=A thin line of signal 2=More than a thin line
Subjective impression of joint fluid, lower compartment	Sagittal/ oblique T2-fat saturated images	0=No signal 1=A thin line of signal 2=More than a thin line
Joint enhancement, adapted from (129)	Signal intensity of the synovium, capsule and joint fluid higher than that of muscle on post contrast T1-fat saturated images	0=Normal; high signal intensity confined to signal perimeter of normal amount of fluid on corresponding fluid-sensitive image 1=Mild; high signal intensity focally exceeding signal perimeter of physiologic amount of joint fluid on corresponding fluid-sensitive image 2= Moderate/ severe; high signal intensity diffusely involving 1 or both joint compartments
Joint fluid, adapted from (129)	Increased joint fluid with isointense signaling of joint space compared to that of cerebrospinal fluid on fluid-sensitive images	0=Absent; \leq 1mm fluid in recess 1=Small; >1 and ≤ 2 mm in recess or involving entire joint compartment 2=Large; > 2 mm fluid in recess or involving entire joint compartment

Synovial enhancement	Sagittal/ oblique T1-fat saturated images post iv contrast	0=Subtle synovial enhancement 1=Mildly increased synovial enhancement 2=Moderate to severe synovial enhancement (signal intensity \geq nearby vessel)
Synovial thickening, adapted from (129)	Sagittal/oblique T2 fat-saturated images	0=Absent; no synovium visible (apparent joint compartment \leq 1 mm width) 1=Mild; >1 and <2 mm thickness at the point of maximum synovial thickening, 2=Moderate/severe; >2 mm thickness at the point of maximum synovial thickening
Joint enhancement, adapted from (129)	Sagittal/ oblique T1-fat saturated images post iv contrast and sagittal/oblique T2 fat-saturated images	0=Normal; high signal intensity confined to signal perimeter of normal amount of fluid on corresponding fluid-sensitive image 1=Mild; high signal intensity focally exceeding signal perimeter of physiologic amount of joint fluid on corresponding fluid-sensitive image 2=Moderate/severe; high signal intensity diffusely involving 1 or both joint compartments
Subjective impression of synovial thickening	Sagittal/oblique T2 fat-saturated images	0=No thickening 1=Mild thickening 2=Moderate/severe thickening
Bone marrow oedema	Coronal T1 images and sagittal/oblique T2 fat-saturated images	0=Absent 1=Present
Bone marrow enhancement	Sagittal/ oblique T1-fat saturated images before and post iv contrast	0=No enhancement 1=Subtle enhancement, considered normal 2=Increased, pathological enhancement

Appendix E. Scoring protocol paper 2. Progressive scoring system for assessing inflammation and osseous deformity of temporomandibular joint by magnetic resonance imaging, adapted from reference (80)

Inflammation		Osseous deformity	
Grade 0	No inflammation: No or small amounts of fluid in any recess with ≤ 1 mm width. No enhancement or enhancement confined to physiological joint fluid.	Grade 0	Normal shape of temporal bone and mandibular condyle according to age: S-shaped articular eminence/glenoid fossa. Round condyle (young patient) Less rounded, more angular appearing condyle (older patient) Smooth subchondral bone contour
Grade 1	Mild inflammation: Extension of joint enhancement exceeds that of physiological joint fluid but does not involve entire joint compartment and/or presence of bone marrow oedema.	Grade 1	Mild flattening of the mandibular condyle and/or temporal bone.
Grade 2	Moderate inflammation: Joint enhancement involves entire joint compartment or there is an enhancing joint effusion	Grade 2	Moderate flattening of the mandibular condyle and/or temporal bone
Grade 3	Severe inflammation: Detectable synovial thickening in addition to increased joint enhancement or effusion.	Grade 3	Severe flattening of the mandibular condyle with loss of height, and/or completely flat temporal bone, and/or presence of small erosions/irregularities
Grade 4	Joint space filled with and enlarged by pannus	Grade 4	“Destruction” of temporomandibular joint by large erosions, fragmentation of the mandibular condyle, intra-articular ossification or bone apposition on mandibular condyle or temporal bone.

Appendix F. Scoring protocol paper 2. Grading of position of the mandibular condyle and disc displacement

	Position of the condyle in the glenoid fossa		Disc displacement
Grade 0	Neutral	Grade 0	None
Grade 1	Anterior	Grade 1	Anterior
Grade 2	Posterior	Grade 2	Posterior
Grade 3	Medial	Grade 3	Lateral
Grade 4	Lateral	Grade 4	Medial
Grade 5	Superior	Grade 5	Disc cannot be defined
Grade 6	Inferior		

Appendix G. Scoring protocol paper 3

CBCT SCORING OF TMJs. Nor-JIA			
Study number/ID:	“Fødselsnummer”	Examination date:	Institution: 1= Bergen 2= Trondheim 3= Tromsø
Surname:	Accessionnumber:		
<p>NOTES ON SCORING</p> <ol style="list-style-type: none"> 1. If in doubt, be conservative. 2. Standardised environment (diagnostic screens w/adequate settings, ambient light etc). 3. Two sets per scoring session: Set B (variable names end with “B”), with the ramus-based alternative assessment plane, is to be scored appr. 3 weeks after set A to avoid recall bias. 4. Second session (TA only) to take place appr. 3 weeks after the first session. <p>CORRECTED ASSESSMENT PLANES</p> <p>A. CONDYLE-BASED (condyle-based sagittal plane) In an axial plane through the centre of the condyle, the sagittal plane is defined by a line perpendicular to the long axis of the condyle. No further adjustments.</p> <p>B. RAMUS-BASED (sagittal-oblique) In the axial plane, the sagittal plane is defined by a line through the centre of the condyle and the coronoid process. In the coronal plane the sagittal plane is approximated to the (assumed) longitudinal axis of the condyle.</p> <p>SCORING OF THE TEMPORAL JOINT COMPONENT</p> <p>CONTOUR OF THE GLENOID FOSSA AND THE POSTERIOR PART OF THE TUBERCULUM ARTICULARE</p> <p>T1. Continuity of the surface (condyle-based) Defined as the integrity of the surface itself. Note that an irregularity as scored in 1b can be either continuous or discontinuous. 0 = continuous 1 = discontinuous 2 = not applicable (due to sclerotic underlying bone)</p> <p>T2-4. Surface irregularity (both planes) Defined as an irregularity that is more distinct and demarcated than changes of shape. Scored for the: T2. medial third T3. central third T4. lateral third as: And scored as: 0 = none (smooth) 1 = single depression/lesion</p>			

2 = mild (involving only part of the articular surface, including multiple depressions/lesions)
3 = moderate/severe (involving the entire articular surface, or presence of deep brakes in the subchondral bone seen in two planes)

T5-7. SHAPE OF THE POSTERIOR PART OF THE TUBERCULUM ARTICULARE IN THE SAGITTAL PLANE (BOTH PLANES)

Defined as a (flattening) change from the expected appearance. Scored for the:

T5. medial third

T6. central third

T7. lateral third

as:

0 = none (convex as expected, incl. a less prominent convexity in the medial third)

1 = mild (straight)

2 = moderate/severe (incl. concave)

T8-10. DIMENSIONS OF THE GLENOID FOSSA (BOTH PLANES)

To be measured in mm (one decimal) in the sagittal plane at the medial border of the postglenoid process.

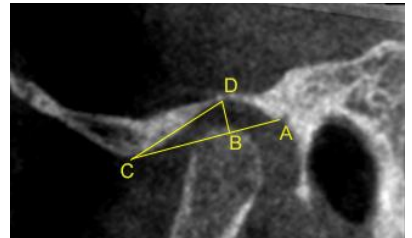
The following points are identified for measurements

A: The postglenoid process/sutura postglenoidalis

B: The point of intersection between the anterior-posterior and cranio-caudal diameter.

C: The most inferior/caudal point of the posterior part of the tuberculum articulare/articular eminence.

D: The most superior/cranial point of the mandibular fossa (perpendicular to the ap-diameter).



T8. Anterior-posterior diameter, A to C.

T9. Cranio-caudal diameter (height). B to D, drawn perpendicular to 3a.

T10. Posterior part of the fossa. A to B.

T11. FOSSA / TUBERCLE INCLINATION (BOTH PLANES)

The fossa/tubercle inclination angle in degrees (one decimal). Defined by the angle between the fossa AP-diameter line and the slope of the tubercle given as a straight line between C and D. I.e. the angle A-C-D.

T12-14. Secondary osteoarthrosis (condyle-based plane)

T12. Subchondral pseudocyst (all planes):

0 = absent

1 = present

T13. Subchondral sclerosis (all planes):

0 = absent

1 = present

T14. Osteophyte (all planes):

0 = absent

1 = present



SCORING OF THE MANDIBULAR JOINT COMPONENT

CONTOUR OF THE MANDIBULAR CONDYLE (BOTH PLANES)

M1. Continuity of the surface (condyle-based plane)

Defined as the integrity of the surface itself. Note that an irregularity as scored in 1b can be either continuous or discontinuous.

0 = continuous

1 = discontinuous

M2-6. Surface irregularity (both planes)

Defined as an irregularity that is more distinct and demarcated than changes of shape.

Scored for the regions:

M2. anterior

M3. posterior

M4. medial

M5. lateral

M6. central

as:

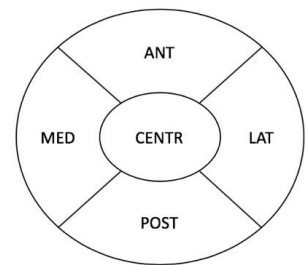
And scored as:

0 = none (smooth)

1 = single depression/lesion

2 = mild (involving only part of the articular surface, including multiple depressions/lesions)

3 = moderate/severe (involving the entire articular surface, or presence of deep brakes in the subchondral bone seen in two planes)



M7. Joint surface cortex visibility (condyle-based plane)

Defined as a thin high-density lining of the joint surface of the condyle. Assessed in areas not affected by discontinuity or surface irregularity.

0 = invisible

1 = thin line

2 = line thicker than expected

M8-12. SHAPE OF THE MANDIBULAR CONDYLE (BOTH PLANES)

Defined as a (flattening) change from the expected appearance: In the sagittal-oblique plane rounded to oval; in the coronal plane oval and convex throughout.

Scored for each of the regions

M8. anterior

M9. posterior

M10. medial

M11. lateral

M12. central

as:

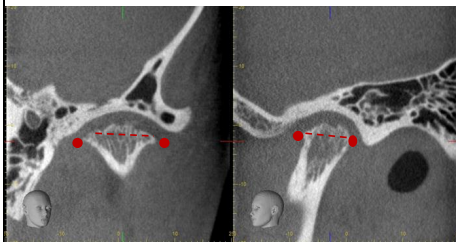
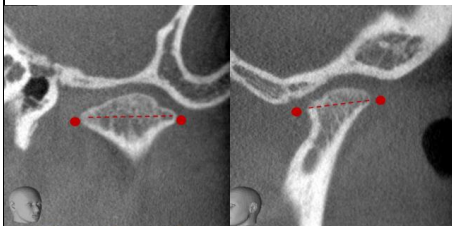
- 0 = no flattening
- 1 = mild flattening (straight)
- 2 = moderate/severe (incl. concave)

M13. GENERAL LOSS OF VOLUME AS DEFINED BY TAMIMI (CONDYLE-BASED PLANE)

Defined as a general loss of volume of the condyle. The condyle is here defined cranial to the 'maximum anterior/posterior/medial/lateral heights of contour' (as defined by Tamimi). These "heights" are the points of maximum convexity when the condyle and neck is viewed in the sagittal and coronal plane, respectively. The posterior is assumed to be inferior to the anterior and they are all assumed to coincide with the change of cortex thickness between the mandibular neck and the condyle. The four points define the 'equator'.

Scored as:

- 0 = no loss of volume/height
- 1 = mild loss of volume/height (clearly above 'equator'-level)
- 2 = moderate loss of volume/height (does not cross 'equator'-level)
- 3 = severe loss of volume/height ('equator'-level or lower, yet still fan shape in coronal view)
- 4 = cylinder shape in coronal view



M14-16. MAXIMUM DIMENSIONS OF THE CONDYLE IN THE AXIAL VIEW (APPR. MID-SECTION) (CONDYLE-BASED PLANE)

M14. Maximum anterior-posterior diameter measured in millimeters (one decimal).

M15. Maximum mesio-lateral diameter in millimeters (one decimal).

M16. Ratio (computer based calculation)

M17-19. secondary osteoarthritis (condyle-based plane)

M17. Subchondral pseudocyst (all views):

0 = absent

1 = present

M18. Subchondral sclerosis (all planes):

0 = absent

1 = present

M19. Osteophyte (all planes):

0 = absent

1 = present

SCORING OF THE TEMPORAL-MANDIBULAR COUPLING (RAMUS-BASED PLANE)

C1. Overall position of the condyle in the temporal fossa

Defined as the position of the majority of the mandibular condyle in the mandibular fossa and scored as:

- 0 = neutral
- 1 = anterior
- 2 = posterior
- 3 = medial
- 4 = lateral
- 5 = superior
- 6 = inferior

C2. Bone apposition

- 0 = absent
- 1 = present

C3. Ankylosis

- 0 = absent
- 1 = fibrous ankylosis
- 2 = bony ankylosis

OTHER FINDINGS

O1. Joint mice (all planes): defined as intraarticular loose bodies, and scored as:

- 0 = absent
- 1 = present

O2. Heterotopic calcification (all planes):

- 0 = absent
- 1 = present

O3. Comments:

CBCT SCORING OF TMJs. Nor-JIA

Study number/ID:	"Fødselsnummer"	Examination date:	Institution:
			1= Bergen
Surname:	Accessionnumber:		2= Trondheim
			3= Tromsø

NOTES ON SCORING

1. If in doubt, be conservative.
2. If the variable cannot be assessed due to f.i. abysmal image quality or insufficient field of view it is to be graded "999", i.e. "missing".
3. Standardised environment (diagnostic screens w/adequate settings, ambient light etc).
4. Two sets per scoring session: Set B (variable names end with "B"), with the ramus-based alternative assessment plane, is to be scored appr. 3 weeks after set A to avoid recall bias.
5. XS and OA to score variables as noted in text. TA to score all variables.
6. Second session (TA only) to take place appr. 3 weeks after the first session.

CORRECTED ASSESSMENT PLANES

A. CONDYLE-BASED (condyle-based sagittal plane)

In an axial plane through the centre of the condyle, the sagittal plane is defined by a line perpendicular to the long axis of the condyle. No further adjustments.

B. RAMUS-BASED (sagittal-oblique)

In the axial plane, the sagittal plane is defined by a line through the centre of the condyle and the coronoid process. In the coronal plane the sagittal plane is approximated to the (assumed) longitudinal axis of the condyle.

IMAGE QUALITY

OPTIONAL COMMENTARY FIELD

SCORING OF THE TEMPORAL JOINT COMPONENT

CONTOUR OF THE GLENOID FOSSA AND THE POSTERIOR PART OF THE TUBERCULUM ARTICULARE

T31. Surface irregularity (ramus-based)

Defined as an irregularity that is more distinct and demarcated than changes of shape and scored as:

0 = none (smooth)

1 = mild (involving only part of the articular surface, including multiple depressions/lesions)

2 = moderate/severe (involving the entire articular surface, or presence of deep brakes in the subchondral bone seen in two planes)

T32. SHAPE OF THE POSTERIOR PART OF THE TUBERCULUM ARTICULARE IN THE SAGITTAL VIEW (RAMUS-BASED)

Defined as a (flattening) change from the expected appearance and scored as:

0 = s-shaped

1 = slight to moderate widening or flattening

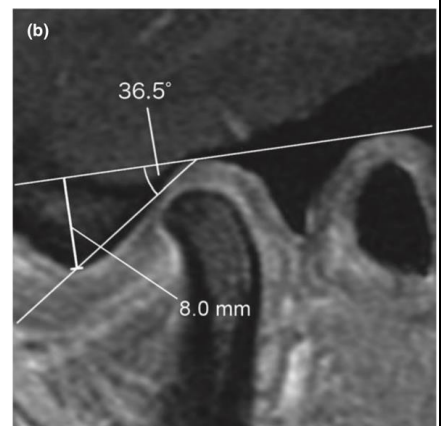
2 = severely flattened fossa-eminence

T. DIMENSIONS OF THE GLENOID FOSSA

T33. Fossa height Kellenberger (mm. one decimal) (ramus-based):

Plane: (...) 2-mm-thick slices in the sagittal-oblique planes aligned perpendicular to the long axis of the respective mandibular condyle (...).

Our modification: Same image as var. T8-T11.



«(..) The depth of the glenoid fossa was measured from the apex of the articular eminence to a horizontal line through the upper border of the external auditory canal and the deepest point of the fossa (Figure 1B) (...).»

FOSSA / TUBERCLE INCLINATION

T34. Inclination angle Kellenberger (one decimal) (ramus-based):

«(...) A fossa-eminence inclination angle between the horizontal line and a line from the deepest point of the glenoid fossa to the apex of the articular eminence was constructed (Figure 1B) (...).

T35-37. secondary osteoarthritis (condyle-based plane)

T35. Subchondral pseudocyst - cyst appearance, more than a variation of trabecular bone (all views):

0 = absent

1 = present

T36. Subchondral sclerosis (all views):

Defined as a thickening of the cortical bone and unequivocal involvement of the subchondral bone. Scored as:

0 = none

1 = thickened cortical bone (more than what may be explained by normal variation and technical quality)

2 = subchondral sclerosis)

T37. Osteophyte (all views):

0 = absent

1 = present

SCORING OF THE MANDIBULAR JOINT COMPONENT

CONTOUR OF THE MANDIBULAR CONDYLE (BOTH PLANES)

M31. Surface irregularity (ramus-based)

Defined as an irregularity that is more distinct and demarcated than changes of shape and scored as:

0 = none (smooth)

1 = mild (involving only part of the articular surface, including multiple depressions/lesions)

2 = moderate/severe (involving the entire articular surface, or presence of deep cracks in the subchondral bone seen in two planes)

SHAPE OF THE MANDIBULAR CONDYLE (RAMUS-BASED)

Defined as a (flattening) change from the expected appearance: In the coronal view oval and convex throughout; in the sagittal-oblique view rounded to oval.

M33. Flattening/changed shape of the condyle coronal view (ramus-based plane):

0 = absent, i.e. convex throughout

1 = slight or partial flattening

2 = moderately or severely flattened, or flattened throughout

M34. Flattening/changed shape of the condyle sagittal view (ramus-based plane):

0 = absent, i.e. rounded/ovoid

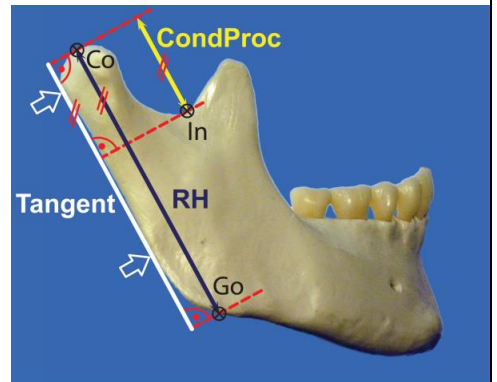
1 = very subtle anterior flattening

2 = mild flattening, involving part of the surface of the condyle

3 = moderate/severe involving entire surface or loss of height

M35. LENGTH OF THE CONDYLE (RAMUS-BASED)

As outlined by Markic et al 2015, the length in mm (one decimal) from the top of the condyle to the lowest point of the incisura mandibulae (/mandibular notch), parallel to the 'tangent'.



Tangent: Posterior margin condyle + lowermost point of ramus in our FOV.

M36-8. secondary osteoarthritis (condyle-based)

M36. Subchondral pseudocyst – cyst appearance, clearly more than a variation of trabecular bone (all views):

- 0 = absent
- 1 = present

M37. Subchondral sclerosis (all views):

Defined as a thickening of the cortical bone and unequivocal involvement of the subchondral bone. Scored as:

- 0 = none
- 1 = thickened cortical bone (more than what may be explained by normal variation and technical quality)
- 2 = subchondral sclerosis)

M38. Osteophyte (all views):

- 0 = absent
- 1 = present

SCORING OF THE TEMPORAL-MANDIBULAR COUPLING (RAMUS-BASED PLANE)

OTHER FINDINGS

O3. Comments:

O4. OVERALL IMPRESSION OF CHANGES TMJ

0 = none

1 = minimal (for example minor irregularity or minor change of shape)

2 = mild

3 = moderate/severe

11. Papers

Paper I



Normal magnetic resonance appearances of the temporomandibular joints in children and young adults aged 2–18 years

Oskar W. Angenete^{1,2} · Thomas A. Augdal^{3,4} · Stig Jellestad⁵ · Marite Rygg^{2,6} · Karen Rosendahl^{7,8}

Received: 9 August 2017 / Revised: 4 October 2017 / Accepted: 23 November 2017
© Springer-Verlag GmbH Germany, part of Springer Nature 2017

Abstract

Background Knowledge of normal appearances of the temporomandibular joint (TMJ) is paramount when assessing the joint for disease in juvenile idiopathic arthritis. Reliable features defining normal TMJs in children are limited.

Objective To establish reliable normal standards for the TMJ at magnetic resonance imaging (MRI).

Materials and methods We included children and young adults aged 2–18 years undergoing a head MRI for reasons not believed to affect the TMJs. We assessed TMJ anatomy and contrast enhancement using a high-resolution 3-D T1-weighted sequence. We noted joint fluid and bone marrow oedema based on a T2-weighted sequence. Three experienced radiologists read all examinations twice in consensus and defined intraobserver consensus agreement.

Results We evaluated the TMJs in 101 children and young adults (45 female), mean age 10.7 years (range 2–18 years). The intraobserver consensus agreement for the assessment of anterior condylar inclination in the sagittal/oblique plane was moderate to good (Cohen $\kappa=0.7$ for the right side). Cohen κ for intraobserver consensus agreement for condylar shape in the coronal plane on a 0–2 scale was 0.4 for the right and 0.6 for the left. Intraobserver agreement for measurement of joint space height and assessment of bone marrow oedema was poor. There was a statistically significant increase in anterior inclination by age in the sagittal plane on a 0–2 scale ($P<0.0001$). Eighty percent of the condyles showed a rounded shape in the coronal plane while 20% showed mild flattening. Thirty-five of 36 right TMJs showed contrast enhancement (mild enhancement in 32 joints, moderate in 3 joints).

Conclusion Subjective assessment of the anterior condylar inclination in the sagittal/oblique plane and condylar flattening in the coronal plane can be considered precise features for describing TMJ anatomy in healthy children. There is an increasing anterior inclination by age. Mild contrast enhancement of the TMJs should be considered a normal finding.

Keywords Bone marrow · Child · Contrast enhancement · Joint fluid · Juvenile idiopathic arthritis · Magnetic resonance imaging · Observer variability

✉ Oskar W. Angenete
oskar.angenete@stolav.no

Thomas A. Augdal
thomas.angell.augdall@unn.no

Stig Jellestad
stig.jellestad@helse-bergen.no

¹ Department of Radiology and Nuclear Medicine, St Olav Hospital HF, Trondheim University Hospital Postboks 3250, Sluppen, 7006 Trondheim, Norway

² Department of Circulation and Medical imaging, Faculty of Medicine and Health Sciences

Norwegian University of Science and Technology
Trondheim, Norway

³ Department of Radiology, University Hospital of North Norway, Tromsø, Norway

⁴ Department of Clinical Medicine, UiT The Arctic University of Norway, Tromsø, Norway

⁵ Department of Radiology, Haukeland University Hospital, Bergen, Norway

⁶ Department of Pediatrics, St. Olavs Hospital, Trondheim, Norway

⁷ Department of Clinical Medicine, University of Bergen, Bergen, Norway

⁸ Department of Radiology, Haukeland University hospital, Bergen, Norway

Introduction

Involvement of the temporomandibular joint (TMJ) has been reported in a high percentage of children with juvenile idiopathic arthritis, ranging 17–93% depending on study design, juvenile idiopathic arthritis categories, diagnostic method and criteria used [1–4]. Left untreated, TMJ arthritis can lead to growth disturbances or destruction, which can result in orofacial deformity [3, 5]. Because clinical and laboratory findings are often insufficient to detect and monitor TMJ disease [1, 6–8], focus has been directed to imaging studies [7–9]. During the last decade, MRI has emerged as the method of choice for evaluating TMJ disease [10–12]. However knowledge on the normal MRI-based appearances of TMJs during childhood is limited. Although the normal anatomy of TMJs has been addressed by several authors, the studies are heterogeneous with respect to numbers, age, ethnicity, imaging methods, imaging planes and measurements used [13–18]. Some studies are based on CT [13, 15, 18, 19], some on cadavers including children aged 3–6 years [15], and others on silicone impressions from cadavers to assess morphology [15, 16]. Important contributions on MRI-based appearances of healthy individuals have been published [14, 17]; however morphologic features are only briefly described and one study excluded individuals with presumed pathological changes such as synovial enhancement and mandibular changes, leading to selection bias [17]. Moreover, recent studies have addressed the utility of MRI in diagnosing active TMJ disease in children with juvenile idiopathic arthritis because findings suggestive of inflammation have been reported in healthy children without juvenile idiopathic arthritis [14, 17, 20, 21]. Some of the studies evaluated contrast enhancement [14, 21–23] and others bone marrow oedema-like changes [14, 17, 20]. In their study on 46 children who had a total of 100 contrast-enhanced MRIs of the brain, von Kalle and co-workers [21] also discussed the complexity of contrast enhancement, underpinning the importance of correct measurements and timing of the post-contrast images.

Our aim was to evaluate the reliability of established and new measurements for describing the normal MR-based anatomy of the temporomandibular joints in children and adolescents aged 2–18 years, and, based on the most robust measures, to characterize the appearances for the normal TMJ.

Materials and methods

In this retrospective cross-sectional study, we included children and young adults aged 2–18 years who had a head MRI during the period 2005–2015 at Haukeland University Hospital. The examinations were performed for reasons other than juvenile idiopathic arthritis or diseases known to involve the TMJs. The patients were identified by record review and

were included if MRI was performed on a 1.5- or a 3-T MR machine, using a dedicated head coil and including the following sequences: high-resolution 3-D T1-weighted sequence (T1 MP-RAGE) with or without intravenous contrast agent and a fluid-sensitive sequence (T2-weighted sequence with or without fat suppression).

Patients were excluded from the study if they had systemic inflammatory diseases including juvenile idiopathic arthritis, tumors affecting the brain or head, hydrocephalus, syndromes involving cerebral malformations or skeletal dysplasia, sub-optimal MRI images and MRI examinations showing other pathologies involving or in close proximity to the TMJs. Benign lesions such as arachnoid cysts and small white-matter cysts were not considered as exclusion criteria. Furthermore, indications such as follow-up after treatment of intracranial infection, intracranial haemorrhage and thrombosis were included. To ensure a balanced dataset, the sample was stratified by age and gender.

The study was approved by the regional ethics committee (2016/257/REK vest). No MRI examinations were performed for the purpose of this study alone.

Imaging sequences

Ninety-six of the 101 MRI examinations were performed on a 1.5-T scanner (Symphony Vision; Siemens Healthcare, Erlangen, Germany), using a 64-channel head coil. All 96 had a sagittal high-resolution (3-D) T1-weighted sequence with slice thickness 1.1 mm, repetition time (TR)/echo time (TE) = 2,110/3.93 ms, number of signal averages (NSA) 1, flip angle 15° and matrix 256 × 240. In 47/96 patients the T1 sequence was performed after injection of intravenous gadolinium (0.2 mL/kg body weight of gadoterate meglumine [Dotarem, Guerbet, France]); 36 of these 47 also had pre-contrast T1-weighted images. In 87/101 patients, a T2-weighted turbo spin-echo sequence in axial or coronal plane with slice thickness 5 mm, TR/TE 3,240/86 ms, NSA 2 and matrix 256 × 190 was performed.

Five of the MRI examinations were performed using a 3-T MRI scanner (Signa HDxt; GE Medical Systems, Milwaukee, WI) with a 32-channel head coil. A sagittal high-resolution (3-D) T1-weighted sequence with slice thickness 1 mm, TR/TE 7.816/2.952 ms, NSA 1 and matrix 256 × 192, and a T2-weighted spin-echo sequence with slice thickness 3 mm, TR/TE 4,700/99 ms, NSA 1.5 and matrix 416 × 416 were performed. The examinations were performed in a closed-mouth position.

Imaging analysis

All 3-D MRI scans were exported to a post-processing program (SyngoVia; Siemens Healthcare) to ensure identical imaging planes. Based on the high-resolution T1-weighted

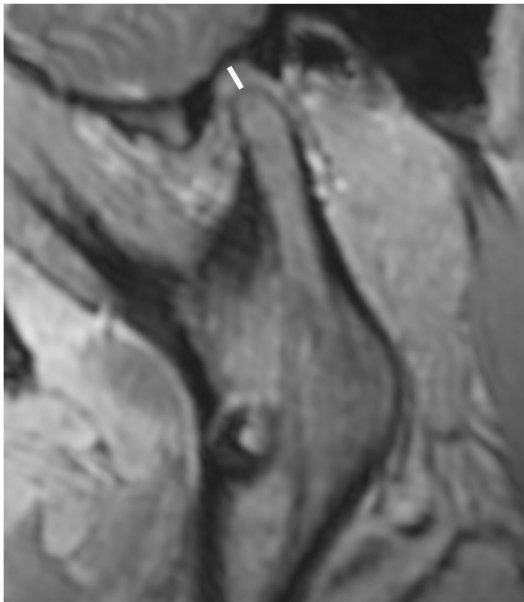


Fig. 1 Sagittal/oblique reconstruction of high-resolution T1-weighted MR images in a 16-year-old girl with no evidence of juvenile idiopathic arthritis, undergoing follow-up after sinus venous thrombosis. Image demonstrates a straight condyle and measurement of the joint space height (*line*). The joint space was measured between the top of the condyle and the deepest part of the glenoid fossa

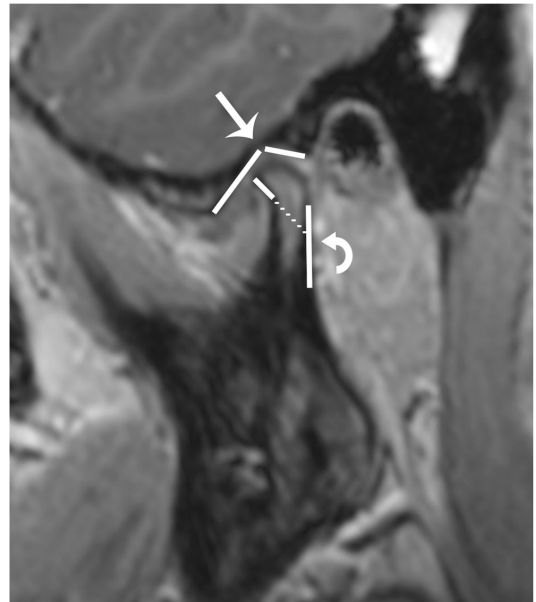


Fig. 2 Sagittal/oblique reconstruction of high-resolution T1-weighted MR images in a 17-year-old girl with no evidence of juvenile idiopathic arthritis, undergoing neurologic workup. Image shows the temporal fossa angle (*straight arrow*) as defined by a line between the deepest point of the fossa and the top of the articular eminence and a line from the deepest part of the fossa parallel to the tympanic part of the temporal bone. The inclination angle (*curved arrow*) is defined by a line parallel to the anterior part of the mandibular condyle and a line parallel to the posterior cortex of the mandibular ramus

images, a new stack of T1-weighted images was reconstructed in the sagittal/oblique plane, aligned along the mandible (1-mm slice thickness, 1-mm increments) for assessment of the following features: (a) condylar shape (0=rounded, 1=mildly flattened, 2=moderately flattened or 3=severely flattened); (b) presence of an anterior, condylar beak [13] (no/yes); (c) anterior condylar inclination (0=no inclination, 1=mild, 2=moderate); (d) shape of glenoid fossa eminence (0=normal S-shape, 1=slightly flattened or widened fossa eminence, 2=clear widening of the fossa or flattening of the eminence, 3=extensive abnormality) [24]; (e) measurements of the joint space, temporal fossa angle and condylar inclination (Figs. 1 and 2).

From the T1-weighted coronal plane, the following features were registered: (a) shape of the condyle (0=rounded, 1=mildly flattened, 2=moderate to severely flattened); and (b) presence of condylar surface irregularities (no/yes; Figs. 3 and 4). We assessed the following features based on T2-weighted images: (a) amount of joint fluid at a 0–2 scale (0=none, 1=a mild amount, defined as a fine, hyperintense line in the upper or lower joint compartment or as small dots in an articular recess, and 2=a moderate amount, defined as >2 mm fluid in one or more of the of abovementioned locations; Fig. 5); and (b) presence of bone marrow oedema (no/yes). Bone marrow

oedema was defined as a lesion within the trabecular bone with ill-defined margins and signal characteristics consistent with increased water content, returning high signal on T2-weighted and low signal on T1-weighted images. We used T1-weighted sequences with intravenous gadolinium contrast agent in the transverse plane to score the degree of enhancement on a 0–2 scale (0=none, 1=mild, 2=moderate), as compared to pre-contrast images. The degree of contrast enhancement was scored as mild when seen immediately around the condyle, or as moderate when seen exceeding the joint tissue [21].

On axial T1-weighted images without intravenous gadolinium we scrutinized the joint tissue for hyperintense areas that could confound the assessment of post-contrast enhancement (yes/no). The examinations were read twice, using high-resolution diagnostic screens (Agfa PACS for the first reading and Sectra PACS for the second reading). In the first session, all images were read by three radiologists in consensus (O.W.A., T.A.A. and K.R., with 9, 10 and 25 years of experience in paediatric musculoskeletal imaging, respectively). During this first session, the readers thoroughly discussed all findings for calibration issues. After an interval of 3 months,

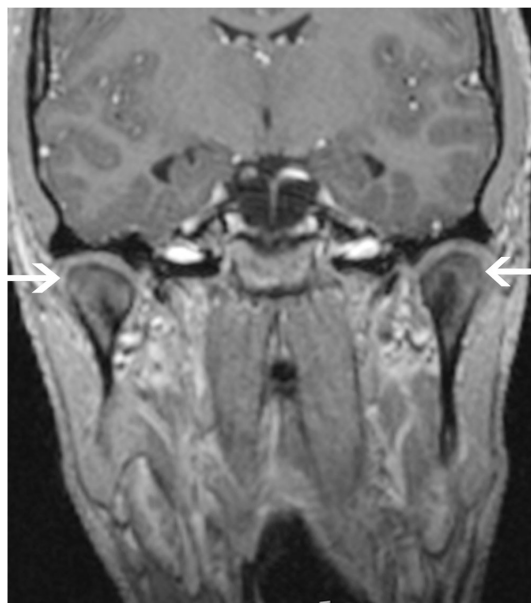


Fig. 3 Coronal reconstruction of high-resolution T1-weighted post-contrast MR images in an 18-year-old man with no evidence of juvenile idiopathic arthritis. Image demonstrates rounded, smooth condyles bilaterally (arrows). The condyles were scored as rounded, given their upward convex contour

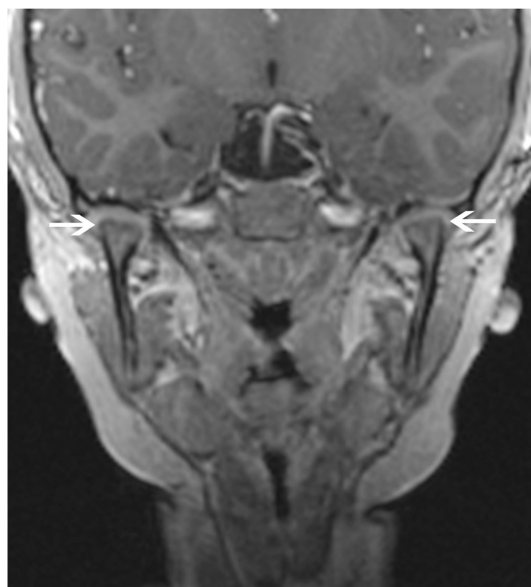


Fig. 4 Coronal reconstruction of high-resolution T1-weighted post-contrast MR images in an 8-year-old girl undergoing MRI because of a headache, with no evidence of juvenile idiopathic arthritis. Image shows mildly flattened, smooth condyles (arrows). The condyles were scored to be mildly flattened when the upward convexity was between rounded and entirely flat

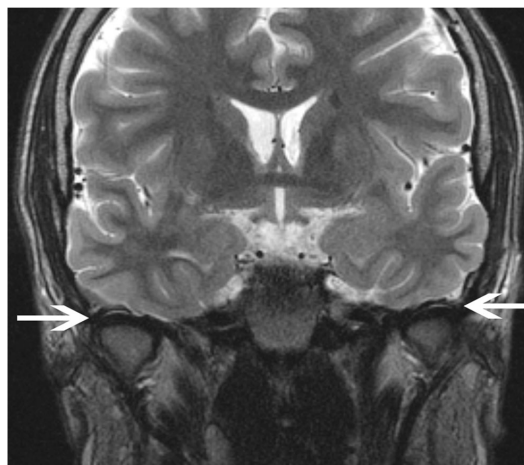


Fig. 5 Coronal T2-weighted turbo spin echo MR image in a 17-year-old boy undergoing brain workup because of disease in other parts of the body, with no evidence of juvenile idiopathic arthritis. Image shows mild amounts of joint fluid (arrows) defined by fine hyperintense lines within the joint compartment

two of the radiologists (O.W.A. and T.A.A. in consensus) re-read all examinations to assess intraobserver agreement. Anatomical features that could not be precisely assessed were not used in the description of normal anatomy.

Statistics

Continuous data are presented as means (\pm standard deviation [SD]), ordinal data as medians (ranges) and dichotomous data as proportions. Intraobserver consensus agreement for the assessment of condylar and fossa eminence shape was performed using a simple Cohen κ coefficient [25]. A κ score of <0.2 is considered poor, 0.21–0.40 fair, 0.41–0.60 moderate, 0.61–0.80 good and 0.81–1.00 very good. We analyzed differences in measurements by establishing 95% limits of agreement (termed repeatability coefficient when used for repeat measurements) as per Bland and Altman [26]. Bland–Altman plots are generally interpreted informally, and a clinically acceptable agreement was set at 15%. We grouped the patients and adolescents into six age groups (2–5, 6–9, 10–13, 14–16 and 17–18 years of age). We used chi-squared tests to examine possible associations between age and anterior condylar inclination in the sagittal/oblique plane and condylar flattening in the coronal plane. Moreover, we used hierarchical multiple regression to assess the utility of age in predicting the anterior condylar inclination, after controlling for the influence of gender. A significance level of 0.05 was decided a priori and all the reported P -values are two-tailed. Statistical analyses were performed using SPSS Statistics, version 23 (IBM, Armonk, NY).

Table 1 Clinical indications for performing head MRI in 101 children and young adults (45 females) in the study, ages 2–18 years

Clinical indication	Number of children (females in parentheses)
Epilepsy	49 (21)
Benign brain tumour	12 (5)
Headache	11 (11)
Intracranial infection, follow-up	7 (1)
Intracranial haemorrhage or thrombosis, follow-up	6 (3)
Psychiatric workup	3 (0)
Brain workup related to disease in other part of the body	3 (1)
Nausea	2 (1)
Others	8 (2)

Results

We evaluated TMJs in 101 children and young adults ages 2–18 years (45 females) with a mean age of 10.7 (SD=5.3) years. Indications for the examinations are presented in Table 1. There were no differences according to gender or side for any of the variables; thus we report the results for both genders merged, right side.

Intraobserver agreement

The mean right joint space height was 3.8 mm, with a mean difference of 0.2 mm between the first and second readings (95% limits of agreement –1.5 to 1.1 mm). The mean right condylar angle was 20.4°, with a mean difference of 5.5° between the first and second readings (95% limits of agreement –17.4° to 23.2°). The mean right fossa angle was 101.3°, with a mean difference of 0.7° between the first and second readings (95% limits of agreement –21.8° to 19.9°).

A scoring system consisting of three categories resulted in moderate to good intraobserver consensus agreement for the assessment of anterior condylar inclination in the sagittal/oblique plane, with a κ value of 0.7 (95% confidence interval [CI] 0.6–0.8) for the right side. The intraobserver consensus agreement for condylar shape in the coronal plane on a 0–2 scale was 0.4 (95% CI 0.2–0.6) for the right side, and 0.6 (95% CI 0.4–0.8) for the left side. The assessment of condylar flattening and shape of the glenoid fossa-eminence in the sagittal/oblique plane (Figs. 6 and 7), right side, showed fair levels of consensus agreement on a 0–3 scale, with κ values of 0.3 (95% CI 0.2–0.4) and 0.2 (95% CI 0.1–0.3), respectively. Dichotomizing the variables did not improve the results.

The agreement for assessment of an anterior condylar beak, condylar surface irregularities, bone marrow oedema and joint fluid could not be adequately tested because of a severely skewed distribution of the findings (Fig. 8).

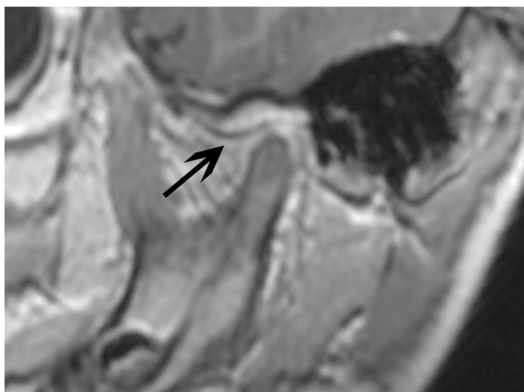


Fig. 6 Sagittal/oblique reconstruction of high-resolution T1-weighted post-contrast MR images in a 2-year-old boy undergoing follow-up after sinus venous thrombosis, with no evidence of juvenile idiopathic arthritis. Image shows clear flattening of the eminence (arrow) as proposed by Arvidsson et al. [24]

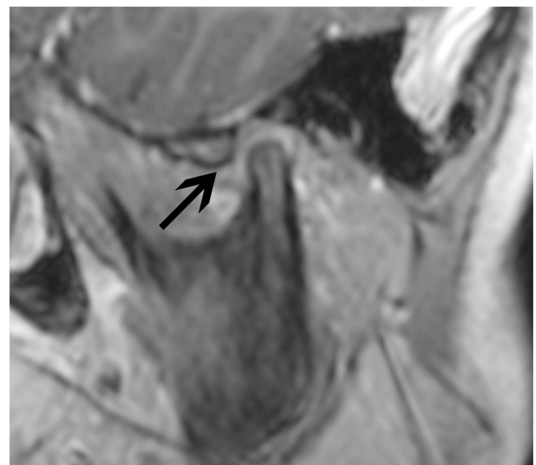
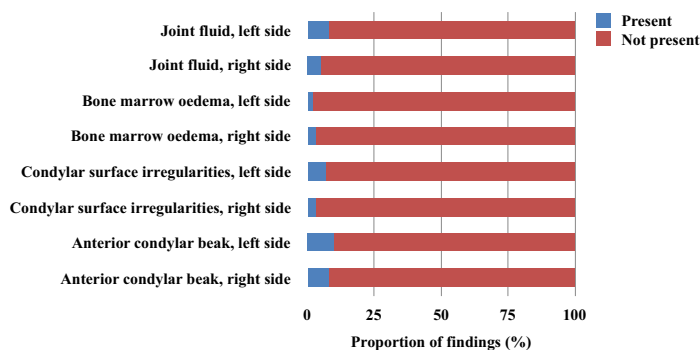


Fig. 7 Sagittal/oblique reconstruction of high-resolution T1-weighted post-contrast MR images in an 8-year-old boy undergoing MRI because of headache, with no evidence of juvenile idiopathic arthritis. Image shows an S-shape fossa/eminence (arrow) as proposed by Arvidsson et al. [24]

Fig. 8 The distribution of findings for a set of variables as judged by the three observers (consensus) during the first reading session. As a result of skewed datasets, kappa statistics could not be applied



Normal anatomy

On a 0–2 scale, assessed in the sagittal/oblique plane 34 (34%) of 101 right condyles were straight, while 47 (47%) showed mild anterior inclination and 20 (20%) showed moderate anterior inclination (Table 2). There was a statistically significant increase in inclination by age ($P < 0.0001$), with 78% of the condyles in the 2–5 years age group showing straight condyles and none of the condyles in the group aged 17–18. None of the condyles in the 2–5 years group showed moderate anterior inclination in comparison to 45% and 40% of the condyles in the 14–16 and 17–18 years groups, respectively. Hierarchical multiple regression did not add to the results.

Subjective classification of the shape of the mandibular condyle in the coronal plane showed that 81 (80%) of the condyles were rounded, 20 (20%) were slightly flattened and none was clearly flattened (Table 2). The presence and degree of flattening was not associated with age ($P = 0.94$).

Thirty-five of 36 right TMJs showed contrast enhancement, of which 32 were judged to be mild and 3 moderate

(Table 3). There was no association between the presence and degree of enhancement and age ($P = 0.44$). Bilateral mild enhancement was shown in 29 of the 36 patients (81%) and bilateral moderate enhancement in 2. In two patients there was moderate synovial enhancement in one TMJ and mild enhancement in the other TMJ while in two patients only mild unilateral enhancement was seen. The indications for MR imaging in the patients with moderate enhancement did not differ from indications for the other patients (headache, white-matter cyst, epilepsy and follow-up after thrombosis or intracranial haemorrhage).

Discussion

In a cohort of children and young adults examined for reasons other than TMJ disease, we identified two imaging features of sufficient precision to describe parts of the anatomy, namely ordinal classification of anterior condylar inclination in the sagittal/oblique plane and flattening of the condyle in the coronal plane. Several other features and measures commonly used to describe TMJ anatomy, such as the condylar and

Table 2 Temporomandibular joint (TMJ) anatomy on MRI in 101 children and young adults ages 2–18 years (45 females)

Characteristics ^a	Age groups (years)					P-value ^b
	2–5 (n=23)	6–9 (n=20)	10–13 (n=16)	14–16 (n=29)	17–18 (n=13)	
Anterior condylar inclination ^c						<0.0001
Straight	18	8	4	4	0	
Mild	5	12	9	16	5	
Moderate	0	0	3	9	8	
Condylar flattening, coronal plane ^c						0.94
Rounded	19	17	13	22	10	
Slightly flattened	4	3	3	7	3	
Clearly flattened	0	0	0	0	0	

^a Right TMJs, based on the first reading. Only robust measures have been included

^b Pearson chi-square test

^c Based on subjective assessment

Table 3 Enhancement of the right temporomandibular joint (TMJ) in 36 patients^a with no evidence of TMJ disease by age group, based on immediate post-contrast T1-weighted images as compared to pre-contrast T1-weighted images, first reading

	Age groups (years)					<i>P</i> -value ^b
	2–5 (<i>n</i> =3)	6–9 (<i>n</i> =4)	10–13 (<i>n</i> =5)	14–16 (<i>n</i> =17)	17–18 (<i>n</i> =7)	
Contrast enhancement						0.44
No enhancement	0	0	0	1	0	
Mild enhancement	2	3	4	16	7	
Moderate enhancement	1	1	1	0	0	

^aOne MR examination was excluded because of artefacts

^bPearson chi-square test

glenoid fossa eminence shapes in the sagittal/oblique plane, performed poorly. One might argue that 0–3-scale scoring systems, ranging from a rounded to a severely flattened condyle or from a normal S-shape to an extensively abnormal glenoid fossa eminence, can be applied on pathological joints only (Fig. 6). However collapsing score categories 1–3 into one category did not change the results even though one-third was categorized as flattened by at least one of the two observers. The same was true for the glenoid fossa eminence, suggesting that a subjective assessment is hampered with difficulties.

Continuous measurements of the joint space height, fossa eminence and anterior condylar inclination angles also performed poorly, with values unacceptable for clinical purposes. The latter findings are disappointing, given the thorough standardisation work performed prior to the first reading session. Similar results have, however, been reported by others [27]. In a CT-based study of 420 TMJs in 210 children without juvenile idiopathic arthritis, Karlo and co-workers [13] found relatively poor interobserver agreement for measurements of condylar size, with 95% limits of agreement at about 30–50% of the mean condylar width and length. As for condylar anteversion, the mean angle was 27°, with 95% limits of agreement being 60–100% of the mean anteversion angle, indicating methodological difficulties with measuring small structures and angles. Opposite, they found very good agreement for the assessment of anterior condylar inclination on a 0–2 scale, with a κ of 0.67, which is similar to the intraobserver consensus agreement found in our MR-based study. Those authors did not examine interobserver variability of condylar flattening.

In a study by Weiss et al. [7] including 32 patients with juvenile idiopathic arthritis, interobserver agreement was assessed in 8 of 32 patients. For any findings of disease, the κ coefficient was 1.0 but for specific findings the κ was lower, including effusion ($\kappa=0.38$) and synovial thickening ($\kappa=0.33$). In sum, although studies addressing the repeatability of features and measurements used for describing normal TMJ anatomy are sparse, assessment of anterior condylar inclination in the sagittal/oblique plane on a 0–2 scale seems to be sufficiently

precise. Based on our results, we would add a second feature, namely condylar flattening on a 0–2 scale on coronal images.

In the present study, all except for 2 of 36 examinations showed bilateral contrast enhancement of the TMJs. The precision of assessing contrast enhancement of the TMJs in healthy children has been addressed in a few studies [21, 22]. In a study of 100 contrast-enhanced MRIs in 46 children without juvenile idiopathic arthritis, von Kalle and co-workers [21] reported relatively poor interobserver agreement for the assessment of dynamic enhancement. Two experienced radiologists independently drew regions of interest for analysis of signal-intensity curves. Similar results were obtained when the same observer did repeat measurements of 20 cases. Because of their wide limits of agreement, they combined the findings of both observers for description of TMJ enhancement in children without juvenile idiopathic arthritis [21]. In another paper, Ma and co-workers [22] reported on 67 children with juvenile idiopathic arthritis and 24 children without juvenile idiopathic arthritis, focusing on contrast enhancement in both synovial tissue and in the mandibular condyle. Although the authors performed subjective assessment of the degree of enhancement, they did not report on the precision of their findings [22]. Quantitative assessment was also performed by two radiologists independently drawing regions of interest for calculation of two different types of signal-intensity ratios. Repeatability of these ratios was assessed with intraclass correlation in the juvenile idiopathic arthritis cohort, showing interobserver values of 0.93–0.98 and intraobserver values of 0.97–0.98 [22]. They did not report separately on repeatability in the healthy cohort.

We found that the condylar inclination in the sagittal/oblique plane increased by age, and that 60% of children younger than 10 years had straight condyles while the majority of those aged 17–18 years had marked anterior inclination. In the CT-based study by Karlo et al. [13] including 210 children without juvenile idiopathic arthritis, the authors described three condylar shapes based on a sagittal view: a smooth round shape most frequently seen in children ages 0–5 years, and an intermediate type with development of an anterior beak, together with an anterior flattening of the

condyle, were primarily observed in children older than 10 years. Our findings support those of Karlo and colleagues, demonstrating an association between age and increasing anterior inclination. Although the assessment of condylar flattening on sagittal view performed poorly in our study, some condyles were definitely judged to be flattened on both assessments, offering support for the findings by Karlo et al.

In our study, one of five condyles was slightly flattened in the coronal plane. In contrast, Tzaribachev and colleagues [17] found none with condylar flattening in 96 children aged 3–13 years without juvenile idiopathic arthritis. This discrepancy might be explained in part by the fact that we used a high-resolution T1 sequence reconstructed along the mandible while Tzaribachev and colleagues used a 3-mm coronal T2-weighted sequence. In the present study some condyles were judged to have an irregular surface when based on the sagittal/oblique view; however the finding could not be confirmed on the coronal view. Moreover, the repeatability of that study was poor, leaving the credibility of this finding in question. In their study of children with no evidence of juvenile idiopathic arthritis, Tzaribachev and colleagues did not observe any condylar erosions, defined as abnormal irregularity of the osseous cortex or loss of normal mushroom-like shape of the mandibular condyle [17].

We found that some condyles had features suggestive of bone marrow oedema, but again the precision of this finding was poor for estimating rates. Other authors have shown similar results: Kottke et al. [14] reported mild oedema-like bone marrow in 10% of TMJs while Tzaribachev and co-workers [17] found no TMJs with bone marrow oedema in a study on 96 non-rheumatic children.

Joint fluid, as assessed on axial and coronal images, was seen in 6 and 10 of 202 TMJs based on the first and second readings; however, similar to bone marrow oedema-like change, the precision of this finding was poor. Kottke et al. [14], in their study of 27 children without juvenile idiopathic arthritis, reported on small amounts of intra-articular fluid in 31% when based on axial T2-weighted images without fat saturation and in 83% on sagittal-oblique T2-weighted images with fat saturation, appearing as fine lines in the upper or lower joint compartment or as small dots in an articular recess. Taken together, the results are diverging, probably reflecting the increased conspicuity of joint fluid in TMJ in the sagittal-oblique plane, which probably would be the preferred plane for joint fluid assessment in the TMJ. Tzaribachev et al. [17], also using axial and coronal images, found small amounts of joint fluid in 3 of 96 children and as such the results are consistent with our study.

In a few previous studies [1, 8, 12], any degree of contrast enhancement of the joint tissue was considered suggestive of active inflammatory disease. In the present study, mild or even moderate enhancement of the joint

tissue was seen in all but one of the patients who had contrast agent administered intravenously. Although most of the post-contrast images were obtained immediately after contrast injection, one might speculate that the more pronounced enhancement was a result of delayed images, with diffusion of contrast agent into the joint space.

Our findings are in accordance with those of Kottke and co-workers [14], showing that 79% of the TMJs enhanced. Their findings were based on subjective and objective assessment of T1-weighted fat-saturated images taken immediately after contrast administration, as compared to pre-contrast T1-weighted images in 27 children aged 1–16 years without any known TMJ disease. Our results are also supported by two other recent publications. In 46 children without TMJ disease von Kalle and colleagues [21] showed 73% (± 2 S.D.=23-123) mean increase in signal intensity in synovial tissue while Ma and co-workers [22] showed 66% 95% CI 0.40-0.92 mean increase in 24 children without rheumatologic disease.

There are some limitations to this study. The retrospective nature of our study might have influenced the results. However, we scrutinized the referrals and the reports of the included children for information that might be associated with TMJ pathology. Further, exact details on the timing of post-contrast images were unavailable, although most post-contrast series were performed immediately after contrast injection. According to a recent study, timing of post-contrast images has a significant impact on the degree of enhancement [21]. Although we cannot entirely rule out that contrast enhancement of joint tissue is related to the underlying disease or treatment of the children, the wide spectrum of indications for MRI in the included cohort makes this somewhat unlikely. Mild contrast enhancement of joint tissue should therefore be considered a normal finding. All of the examinations were performed with a 32- or 64-channel head coil. One might argue that a dedicated surface coil would have added to image quality regarding both spatial resolution and signal-to-noise ratio. Finally, most of the T2-weighted sequences were performed with 5-mm slice thickness, which could lead to an underestimation of the amount of bone marrow oedema and joint fluid because of volume averaging.

Conclusion

We have identified two robust features to describe parts of the TMJ anatomy as assessed on MRI in children without evidence of TMJ disease, namely a subjective assessment of anterior inclination in the sagittal/oblique plane and condylar flattening in the coronal plane. The shape of the mandibular condyle is straight in the younger age group, with an increasing anterior inclination according to age. Mild flattening of the

condyle, shown in the coronal plane, is a common finding and not necessarily indicative of chronic inflammatory disease. Mild contrast enhancement of the TMJs should be considered a normal finding.

Acknowledgements Parts of this study were funded by the Liaison Committee between the Central Norway Regional Health Authority (RHA) and the Norwegian University of Science and Technology (NTNU).

Compliance with ethical standards

Conflicts of interest None

References

1. Stoll ML, Sharpe T, Beukelman T et al (2012) Risk factors for temporomandibular joint arthritis in children with juvenile idiopathic arthritis. *J Rheumatol* 39:1880–1887
2. Cannizzaro E, Schroeder S, Muller LM et al (2011) Temporomandibular joint involvement in children with juvenile idiopathic arthritis. *J Rheumatol* 38:510–515
3. Ringold S, Cron RQ (2009) The temporomandibular joint in juvenile idiopathic arthritis: frequently used and frequently arthritic. *Pediatr Rheumatol Online J* 7:11
4. Abramowicz S, Cheon JE, Kim S et al (2011) Magnetic resonance imaging of temporomandibular joints in children with arthritis. *J Oral Maxillofac Surg* 69:2321–2328
5. Arvidsson LZ, Smith HJ, Flato B et al (2010) Temporomandibular joint findings in adults with long-standing juvenile idiopathic arthritis: CT and MR imaging assessment. *Radiology* 256:191–200
6. Twilt M, Moberg SM, Arends LR et al (2004) Temporomandibular involvement in juvenile idiopathic arthritis. *J Rheumatol* 31:1418–1422
7. Weiss PF, Arabshahi B, Johnson A et al (2008) High prevalence of temporomandibular joint arthritis at disease onset in children with juvenile idiopathic arthritis, as detected by magnetic resonance imaging but not by ultrasound. *Arthritis Rheum* 58:1189–1196
8. Kuseler A, Pedersen TK, Gelineck J et al (2005) A 2 year followup study of enhanced magnetic resonance imaging and clinical examination of the temporomandibular joint in children with juvenile idiopathic arthritis. *J Rheumatol* 32:162–169
9. Moe JS, Desai NK, Aiken AH et al (2016) Magnetic resonance imaging of temporomandibular joints of children. *J Oral Maxillofac Surg* 74:1723–1727
10. Arabshahi B, Cron RQ (2006) Temporomandibular joint arthritis in juvenile idiopathic arthritis: the forgotten joint. *Curr Opin Rheumatol* 18:490–495
11. Muller L, Kellenberger CJ, Cannizzaro E et al (2009) Early diagnosis of temporomandibular joint involvement in juvenile idiopathic arthritis: a pilot study comparing clinical examination and ultrasound to magnetic resonance imaging. *Rheumatology* 48:680–685
12. Kuseler A, Pedersen TK, Herlin T et al (1998) Contrast enhanced magnetic resonance imaging as a method to diagnose early inflammatory changes in the temporomandibular joint in children with juvenile chronic arthritis. *J Rheumatol* 25:1406–1412
13. Karlo CA, Stolzmann P, Habernig S et al (2010) Size, shape and age-related changes of the mandibular condyle during childhood. *Eur Radiol* 20:2512–2517
14. Kottke R, Saurenmann RK, Schneider MM et al (2014) Contrast-enhanced MRI of the temporomandibular joint: findings in children without juvenile idiopathic arthritis. *Acta Radiol* 56:1145–1152
15. Meng F, Liu Y, Hu K et al (2008) A comparative study of the skeletal morphology of the temporo-mandibular joint of children and adults. *J Postgrad Med* 54:191–194
16. Katsavrias EG (2002) Changes in articular eminence inclination during the craniofacial growth period. *Angle Orthod* 72:258–264
17. Tzaribachev N, Fritz J, Horger M (2009) Spectrum of magnetic resonance imaging appearances of juvenile temporomandibular joints (TMJ) in non-rheumatic children. *Acta Radiol* 50:1182–1186
18. Christiansen EL, Chan TT, Thompson JR et al (1987) Computed tomography of the normal temporomandibular joint. *Scand J Dent Res* 95:499–509
19. Kinniburgh RD, Major PW, Nebbe B et al (2000) Osseous morphology and spatial relationships of the temporomandibular joint: comparisons of normal and anterior disc positions. *Angle Orthod* 70:70–80
20. Kottke RST, Grotzer M, Kellenberger C (2008) MRI of paediatric temporomandibular joints, normal findings. *Pediatr Radiol* 38: S534–S569
21. von Kalle T, Winkler P, Stuber T (2013) Contrast-enhanced MRI of normal temporomandibular joints in children — is there enhancement or not? *Rheumatology* 52:363–367
22. Ma GM, Amirabadi A, Inarejos E et al (2015) MRI thresholds for discrimination between normal and mild temporomandibular joint involvement in juvenile idiopathic arthritis. *Pediatr Rheumatol Online J* 13:53
23. Resnick CM, Vakilian PM, Breen M et al (2016) Quantifying temporomandibular joint synovitis in children with juvenile idiopathic arthritis. *Arthritis Care Res* 68:1795–1802
24. Arvidsson LZ, Flato B, Larheim TA (2009) Radiographic TMJ abnormalities in patients with juvenile idiopathic arthritis followed for 27 years. *Oral Surg Oral Med Oral Pathol Oral Radiol Endod* 108:114–123
25. Cohen J (1960) Weighted kappa: nominal scale agreement provision for scaled agreement or partial credit. *Psychol Bull* 70:213–220
26. Bland JM, Altman DG (1986) Statistical methods for assessing agreement between two methods of clinical measurement. *Lancet* 1:307–310
27. Engesaeter IO, Laborie LB, Lehmann TG et al (2012) Radiological findings for hip dysplasia at skeletal maturity. Validation of digital and manual measurement techniques. *Skelet Radiol* 41:775–785

Paper II

MRI in the Assessment of TMJ-Arthritis in Children with JIA; Repeatability of a Newly Devised Scoring System

Oskar W. Angenete, MD, Thomas A. Augdal, MD, Marite Rygg, MD, PhD, Karen Rosendahl, MD, PhD

Rationale and Objectives: The temporomandibular joint (TMJ) is commonly involved in children with juvenile idiopathic arthritis. The diagnosis and evaluation of the disease progression is dependent on medical imaging. The precision of this imaging is under debate. Several scoring systems have been proposed but transparent testing of the precision of the constituents of the scoring systems is lacking. The present study aims to test the precision of 25 imaging features based on magnetic resonance imaging (MRI).

Materials and Methods: Clinical data and imaging were obtained from the Norwegian juvenile idiopathic arthritis study, The NorJIA study. Twenty-five imaging features of the TMJ in MRI datasets from 86 study participants were evaluated by two experienced radiologists for inter- and intraobserver agreement. Agreement of ordinal variables was measured with Cohen's linear or weighted Kappa as appropriate. Agreement of continuous measurements was assessed with 95% limit of agreement according to Bland-Altman.

Results: In the osteochondral domain, the ordinal imaging variables "loss of condylar volume," "condylar shape," "condylar irregularities," "shape of the eminence/fossa," "disk abnormalities," and "condylar inclination" showed inter- and intraobserver agreement above Kappa 0.5. In the inflammatory domain, the ordinal imaging variables "joint fluid," "overall impression of inflammation," "synovial enhancement" and "bone marrow oedema" showed inter- and intraobserver agreement above Kappa 0.5. Continuous measurements performed poorly with wide limits of agreement.

Conclusion: A precise MRI-based scoring system for assessment of TMJ in JIA is proposed consisting of seven variables in the osteochondral domain and four variables in the inflammatory domain. Further testing of the clinical validity of the variables is needed.

Key Words: arthritis; juvenile; observer variation; scoring system; precision.

© 2021 The Association of University Radiologists. Published by Elsevier Inc. This is an open access article under the CC BY license (<http://creativecommons.org/licenses/by/4.0/>)

Acad Radiol 2021; ■:1-16

From the Department of Radiology and Nuclear Medicine (O.W.A.), St Olav University Hospital, Postboks 3250 Sluppen, Trondheim 7006, Norway. Institute for Circulation and Medical Imaging, Faculty of Medicine and Health Sciences (O.W.A.), Norwegian University of Science and Technology, Trondheim, Norway. Section of Paediatric Radiology (T.A.A.), University Hospital North Norway, Tromsø, Norway. Department of Clinical Medicine (T.A.A.), UiT The Arctic University of Norway, Faculty of Health Sciences, Tromsø, Norway. Department of Clinical and Molecular Medicine (M.R.), NTNU - Norwegian University of Science and Technology, Trondheim, Norway. Department of Pediatrics (M.R.), St Olav University Hospital, Trondheim, Norway. Section of Paediatric Radiology (K.R.), University Hospital North Norway, Tromsø, Norway. Department of Clinical Medicine (K.R.), UiT The Arctic University of Norway, Faculty of Health Sciences, Tromsø, Norway. Received August 18, 2021; revised September 16, 2021; accepted September 26, 2021. **Address correspondence to:** O.W.A. e-mail: oskar.angenete@stolav.no

© 2021 The Association of University Radiologists. Published by Elsevier Inc. This is an open access article under the CC BY license (<http://creativecommons.org/licenses/by/4.0/>) <https://doi.org/10.1016/j.acra.2021.09.024>

INTRODUCTION

Juvenile idiopathic arthritis (JIA) is a chronic rheumatic disease of unknown origin, with an onset before the age of 16 and a reported incidence of 15 (7-23) per 100,000 children/year in the Nordic countries (1). In patients with JIA, the temporomandibular joint (TMJ) is affected in 39-78% (2-5) depending on definitions used for involvement, disease duration, and on the methods used for ascertainment. On imaging, TMJ arthritis is characterized by synovial inflammation, bone marrow- and soft tissue oedema and joint effusion, subsequently followed by destructive changes of cartilage and bone. Left untreated, or in treatment-resistant cases, arthritis of the TMJ can lead to facial asymmetry, orofacial pain and reduced quality of life (6-10).

The diagnosis of TMJ involvement in JIA is based on clinical findings, magnetic resonance imaging (MRI), cone beam computed tomography (CBCT) or a combination of these (11-15). The accuracy of clinical findings and clinical

monitoring of the disease course, both active inflammation and permanent damage, is under debate (16,17) and much effort has been made during the past years to establish a valid, MRI-based imaging protocol and classification system. However, methodological difficulties, including lack of references for normal findings, low image resolution and imprecise scoring systems have led to both over- and underreporting of signs of pathology (18,19). For example, Stoll and colleagues, in a study of 35 patients with JIA and 122 controls without JIA, demonstrated a significant overlap between the two groups with respect to MR findings thought to be suggestive of active disease (20).

In 2013, Koos et al (21) proposed a classification system addressing both structural changes and inflammation, applicable on JIA-related findings in the TMJ for both MRI and CBCT. The authors reported that the system was not hampered with significant intra- or inter-reader differences but did not present any data to confirm their statement. Vaid and colleagues (22) proposed an MRI-based scoring system based on 20 patients, classifying changes into acute or chronic (structural damage). The grading system included measurements of small, intraarticular components under 3 mm in size, however, the precision of these measurements was not presented. The overall interobserver agreement for acute and chronic changes, based on composite variables, was moderate to good, with weighted kappa values of 0.51 and 0.68, respectively.

In 2015, a third MRI-based scoring system was published by Kellenberger and co-authors (13). The system is progressive on a 0–4 scale and divided into an inflammatory domain and a deformity domain. The system is in part built on the experiences drawn from the publications by Koos and Vaid, but in the publication from 2015, a full scale, adequate test of intra- and interobserver agreement is lacking. In 2018, Tolend et al proposed an MRI-based scoring system (23) founded on the experiences drawn from the systems published by Koos, Vaid and Kellenberger. The system was developed by a multi-institutional consensus process finally proposing eight imaging items including both the inflammatory and osteochondral damage domains. Each item was assigned either a binary, ordinal grade (0–1) or a 3-graded, ordinal grade (0–2). The grades of each, individual item were then added, resulting in a total score. The authors performed a reliability exercise of the system in 21 selected cases and chose to measure reliability along an intra-class correlation scale (ICC). However, measuring agreement of ordinal variables with ICC is debatable (24). Furthermore, the selection of patients and low number of patients ($n = 21$) leaves unanswered questions on the transferability of the results to the JIA population.

In 2018, Kellenberger published a pictorial essay on JIA-related, temporomandibular changes on MRI (14). This publication presents a thorough explanation of the scoring systems already proposed by Tolend and Kellenberger, both through written explanations and through a wide range of MRI examples. Used as a common ground-reference this publication might help reduce interobserver variability.

To date, however, no MRI-based scoring system of the TMJ is proven precise and valid. We therefore aimed to examine the precision of MRI-based measurements and scores used to describe anatomy, structural damage and inflammation of the TMJ in a large cohort of children and adolescents with JIA. Next, to indicate markers holding sufficient precision to be included in a future scoring system for active arthritis and structural deformity.

MATERIAL AND METHODS

Patients

The participants in this study constitute a subset of 86 children and adolescents selected from a prospective, longitudinal observational study addressing TMJ involvement in children with JIA ($n = 228$), the Norwegian JIA Study (NorJIA), NCT number NCT03904459 in www.clinicaltrials.gov. Participants in the NorJIA study were recruited from three tertiary pediatric university hospitals (Haukeland University hospital, Bergen, St Olav University hospital, Trondheim and University hospital of North Norway, Tromsø). Inclusion criteria were a diagnosis of JIA according to the ILAR criteria (25) performed by experienced pediatric rheumatologists, and age between 4 and 16 years at inclusion. According to the study protocol, all of the included participants in the NorJIA study were referred to MRI of the TMJ, regardless of clinical symptoms from the TMJ. In cases of clinical TMJ symptoms, and when an MRI was judged to be of specific clinical importance, sedation was used for the younger children. For this particular sub-study, we included MRIs performed between March 2015 and May 2018. Exclusion criteria for this study were suboptimal examinations due to artefacts and the use of braces.

To test the scoring system regarding skeletal development and varied pathology, an a priori, balanced selection of patients from the NorJIA cohort was made, based on the radiology report and patient age. The selection consisted of approximately 33% participants with moderate/severe findings, 33% participants with mild findings and 33% participants with subtle or no findings.

Imaging

All MRI examinations were performed on a 3 Tesla system (Skyra, Siemens healthineers, Erlangen, Germany), using a 64-channel head coil (32-channel at St Olav). An extensive protocol, including nine sequences was performed to allow for comparisons of different sequences, either alone or in combination, in the assessment of pathology. The MRI protocol takes into account the recommendations given by Miller (26) and Kellenberger (27), including sagittal T1-weighted MPRAGE, sagittal/oblique proton density-weighted, sagittal/oblique fat-saturated T2-weighted, sagittal/oblique fat-saturated T1-weighted, coronal T1-weighted and coronal T1-weighted two-point Dixon sequences.

Following intravenous gadolinium contrast injection, a dynamic coronal sequence, a sagittal/oblique fat-saturated T1-weighted sequence and a sagittal/oblique proton density-weighted sequence (open mouth) were performed. Intravenous gadolinium contrast was injected in a standardized way in an antecubital vein (Dotarem 279,3 mg/ml, 0,2 ml/kg body weight, 2 ml/s with 20 ml saline chaser). A detailed protocol description is provided in [Appendix A](#).

Image Review

For the present study, the following seven sequences were used; coronal T1-weighted, sagittal T1-weighted MPRAGE, sagittal/oblique fat-saturated T2-weighted, sagittal/oblique fat-saturated T1-weighted, sagittal/oblique proton density-weighted with closed and open mouth and sagittal/oblique fat-saturated T1-weighted after intravenous contrast. The images were assessed independently by two consultant radiologists, twice (at an interval of at least 4 weeks) by O.A. (12 years of experience) and once by T.A.A. (13 years of experience), without any additional information available. Before scoring was performed, previous publications on scoring protocols and imaging atlas were thoroughly studied ([14,21-23](#)). The readers calibrated their interpretation of the chosen scoring protocol during two 1-day meetings and 2 video conferences, followed by consensus scoring of five TMJ MR examinations from a cohort of children with JIA, not included in the present study.

Five imaging markers describing anatomical features, seven describing structural changes (damage) and 13 markers describing inflammation were analyzed for the right and for the left TMJ, separately ([Appendix B, C, D and E](#)). To explore the usefulness of an extended MRI protocol, assessment of condylar irregularities was made, first on a minimal (core) set of sequences and second, on an extended (ideal) set of sequences, as suggested by Miller et al ([26](#)).

Statistical Analysis

Continuous data were presented as means (\pm SD), ordinal data as medians (ranges) and dichotomous data as proportions. Intra- and interobserver agreement were analyzed using a simple or a weighted (linear) Cohen's Kappa coefficient with 95% confidence interval. A kappa score of <0.2 was considered poor, 0.21-0.40 fair, 0.41-0.60 moderate, 0.61-0.80 good and 0.81-1.00 very good. Absolute agreement was reported as proportions. Differences in measurements were analyzed using 95% limits of agreement (termed repeatability coefficient, when used for repeat measurements) as per Bland-Altman. Bland-Altman plots are generally interpreted informally, and a clinically acceptable agreement was set at 15%. A significance level of 0.05 was decided a priori and all the reported p values are two-tailed. Statistical analyses were performed using IBM SPSS Statistics, version 26.

Ethics

The NorJIA study was approved by the Regional Ethics Committee; REK nr 2012/542. Informed consents were given by the children if ≥ 16 years, and by the parents if the child were <16 years. Data was collected and stored according to the General Data Protection Regulation.

RESULTS

One set of MRIs from a total of 86 children (51 females) with JIA, median age 13 years (IQR 5), were included. Median age at diagnosis was 6 years (IQR 8) and the median duration of disease at the time of MRI imaging was 4,5 years (IQR 6) ([Table 1](#)). The distribution of findings for each of the 25 MRI-features assessed are shown in [Figure 1 and 2](#) (right side first reading).

Osteochondral Domain

Assessment of loss of condylar volume on a 0-1 scale, condylar shape/flattening in the sagittal (0-3 and 0-2 scale) and in the coronal plane (0-2 scale), condylar irregularities on a 0-2 scale (both based on a core and an ideal protocol), disk abnormalities on a 0-1 scale and the shape of the articular eminence and glenoid fossa on a 0-2 scale showed good to very good agreement for the same reader, with kappa values of 0.67-0.80 ([Table 2](#)) ([Fig 3](#)). The inter-reader agreement was also good to very good except for condylar irregularities (both the ideal and the core protocols) and shape of the articular eminence and glenoid fossa, showing moderate agreement with kappa values of 0.57, 0.47 and 0.55, respectively ([Table 2](#)) ([Figs 4a-b](#) and [Figure 5a-b](#)).

Assessment of condylar inclination on a 0-2 scale showed good intra- and interobserver agreement, with kappa values of 0.74 and 0.61.

TABLE 1. Characteristics of the 86 Children with a Known Diagnosis of Juvenile Idiopathic Arthritis (JIA), Included in the Current Study

Characteristics	Values
Girls, n (%)	51 (59%)
Age at MRI examination, median years (IQR)	13,0 (5)
Age at JIA diagnosis, median years (IQR)	6,0 (8)
Disease duration, median years (IQR)	4,5 (6)
JIA categories	
<i>Systemic</i>	3 (3%)
<i>Oligoarticular persistent</i>	25 (29%)
<i>Oligoarticular extended</i>	8 (9%)
<i>Polyarticular RF negative</i>	27 (31%)
<i>Psoriatic arthritis</i>	3 (3%)
<i>Enthesitis-related arthritis</i>	11 (13%)
<i>Undifferentiated arthritis</i>	9 (10%)

ILAR, International League of Association for Rheumatology; IQR, interquartile range (25th-75th percentile); JIA, juvenile idiopathic arthritis; MRI, Magnetic resonance imaging; RF, Rheumatoid factor.

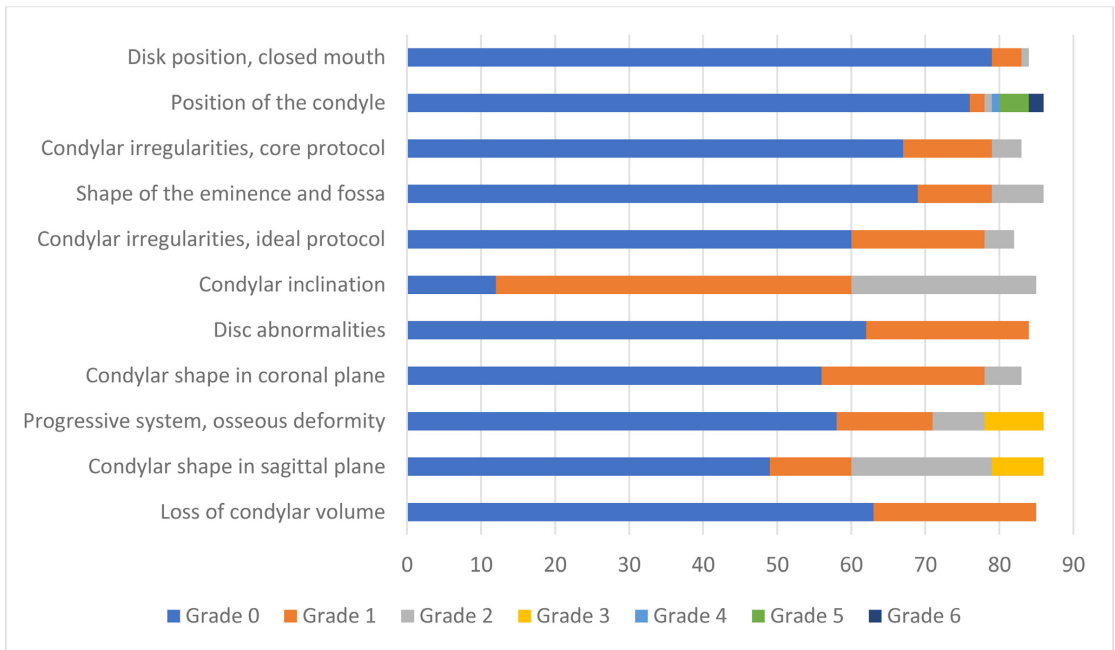


Figure 1. Distribution of findings in the osteochondral domain, right side, first reading. The x-axis denotes number of patients.

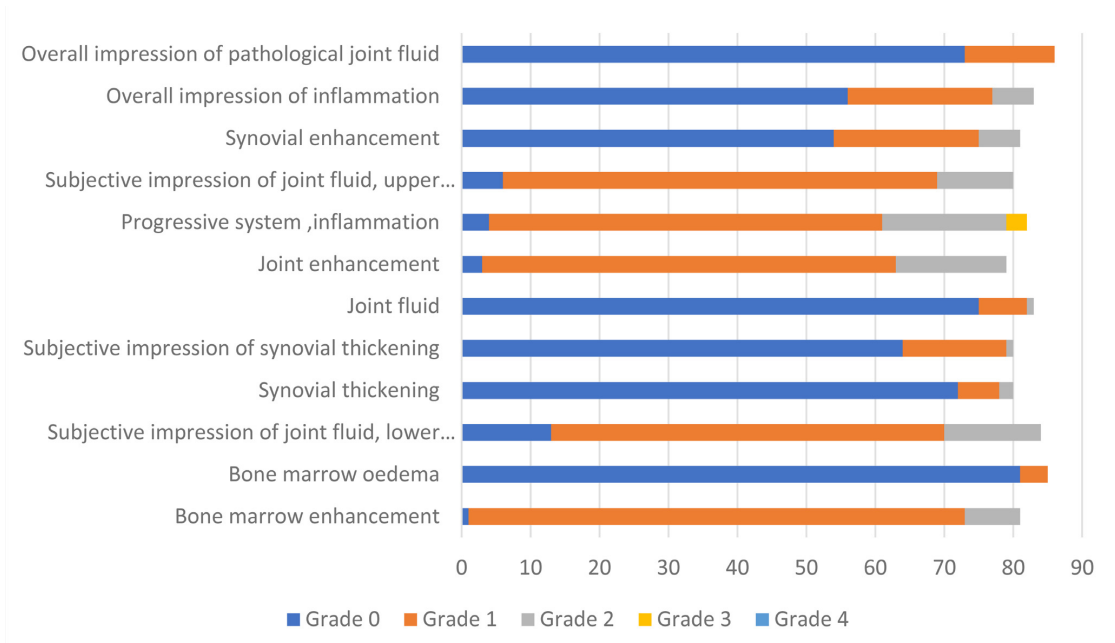


Figure 2. Distribution of findings in the inflammatory domain, right side, first reading. The x-axis denotes number of patients.

TABLE 2. MRI-scoring of the TMJs – osteochondral domain. Cohen’s kappa values and proportion of absolute, interobserver agreement for TMJ imaging variables defining osteochondral damage in a cohort of 86 patients (51 girls) with JIA, right TMJ. Simple kappa for dichotomized variables and linear, weighted kappa for variables with 3 or more grades. Scoring systems are detailed below.

Imaging feature	Intraobserver kappa value (95% CI)	Interobserver kappa value (95% CI)	Interobserver absolute agreement (%)
Loss of condylar volume (0-1) ¹	0.79 (0.63-0.94)	0.78 (0.62-0.94)	77/84 (92%)
Condylar shape in sagittal plane (0-3) ²	0.72 (0.60-0.83)	0.68 (0.58-0.79)	58/85 (68%)
Condylar flattening in sagittal plane, (0-2) ³	0.68 (0.54-0.82)	0.66 (0.54-0.79)	65/85 (76%)
Progressive system, osseous deformity (0-4) ⁴	0.73 (0.61-0.85)	0.66 (0.54-0.79)	52/73 (71%)
Condylar shape in coronal plane (0-2) ⁵	0.80 (0.67-0.92)	0.62 (0.47-0.78)	65/83 (78%)
Disk abnormalities (0-1) ⁶	0.74 (0.58-0.90)	0.61 (0.41-0.81)	72/83 (87%)
Condylar inclination (0-2) ⁷	0.74 (0.61-0.87)	0.61 (0.48-0.74)	59/84 (70%)
Condylar irregularities, ideal protocol (0-2) ⁸	0.67 (0.49-0.85)	0.57 (0.39-0.74)	62/79 (78%)
Shape of the articular eminence and glenoid fossa (0-2) ⁹	0.76 (0.62-0.90)	0.55 (0.37-0.74)	64/85 (75%)
Condylar irregularities, core protocol (0-2) ¹⁰	0.69 (0.49-0.88)	0.47 (0.27-0.68)	61/79 (77%)
Position of the condyle (0-6) ¹¹	0.31 (0.02-0.59)	0.20 (-0.09-0.50)	66/84 (79%)
Disk position, closed mouth (0-5) ¹²	0.34 (0.02-0.67)	0.17 (0.00-0.34)	66/81 (81%)

Abbreviations: JIA juvenile idiopathic arthritis; MRI, magnetic resonance imaging; TMJ, temporomandibular joint;

1 0=none, 1=present

2 0=rounded/ovoid, 1=subtle anterior flattening, 2=mild flattening, involves part of the surface of the condyle, 3= moderate/severe flattening involves the entire surface of the condyle, or loss of height of the condyle

3 0=Absent; round/slightly angular shape of the condyle, 1=Mild, extent of flattening involves part of the surface of the condyle. 2=Moderate/severe, extent of flattening involves the entire surface of the condyle, or loss of height of the condyle. According to reference 23

4 0=Normal shape of temporal bone and mandibular condyle according to age: S-shaped articular eminence/glenoid fossa. Round condyle (young patient). Less rounded, more angular appearing condyle (older patient). Smooth subchondral bone contour, 1=Mild flattening of the mandibular condyle and/or temporal bone. 2=Moderate flattening of the mandibular condyle and/or temporal bone. 3=Severe flattening of the mandibular condyle with loss of height, and/or completely flat temporal bone, and/or presence of small erosions/irregularities. 4= "Destruction" of temporomandibular joint by large erosions, fragmentation of the mandibular condyle, intra-articular ossification or bone apposition on mandibular condyle or temporal bone. According to reference 13

5 0=Convex throughout, 1=mild/partial flattening, 2=moderately or severely flattened throughout

6 0=absent, 1=present

7 0=Straight, 1=mild anterior inclination, 2=moderate/significant anterior inclination

8 Based on coronal T1, Sagittal/oblique T2fs, Sagittal/oblique T1fs, Sagittal/oblique PD and Sagittal/oblique T1-fs with Gd; 0=none, 1=mild (involving only part of the articular surface of the condyle), 2=moderate/severe (presence of deep breaks in the subchondral bone seen in two planes, or irregularities involving the entire articular surface)

9 0=S-shaped, 1= mild to moderate widening or flattening, 2= severely flattened fossa-eminence

10 Based on coronal T1, Sagittal/oblique T2fs, Sagittal/oblique T1-fs with Gd; 0=none, 1=mild (involving only part of the articular surface of the condyle), 2=moderate/severe (presence of deep breaks in the subchondral bone seen in two planes, or irregularities involving the entire articular surface). Right side excluded due to skewed distribution of findings.

11 Overall position of the condyle in the temporal fossa; 0=neutral, 1=anterior, 2=posterior, 3=medial, 4=lateral, 5=superior, 6=inferior

12 0=none, 1=displaced anteriorly, 2=displaced posteriorly, 3=displaced laterally, 4=displaced medially, 5=Not applicable, disc cannot be defined

Assessment of the position of the condyle on a 0–6–point location scale showed fair agreement for the same reader and poor inter-reader agreement (Table 2).

As for disk position on a 0–5 scale, with the mouth closed, there was a fair intra-reader and a poor inter-reader agreement (Table 2).

Inflammatory Domain

Joint fluid: The intra-observer agreement for assessment of joint fluid on a 0–2 scale was good, both for the whole joint, and for the lower compartment, with kappa values of 0.74 and 0.69, respectively, while the agreement for upper

compartment was moderate (kappa 0.51) (Table 3) (Fig 6). Agreement between observers was good for the whole joint, moderate for the upper and poor for the lower compartment (Table 3). Assessment of pathological fluid on a 0–1 scale performed well for the same observer, and moderately between observers.

Synovial inflammation/enhancement/thickening: There was moderate agreement for grading overall impression of inflammation on a 0–2 scale, with a kappa value of 0.59 for the same reader and 0.57 between readers (Table 3).

Assessing synovial enhancement on a 0–2 scale showed good to moderate agreement, with kappa values of 0.68 for the same reader and 0.54 between readers (Fig 7). Similar, the

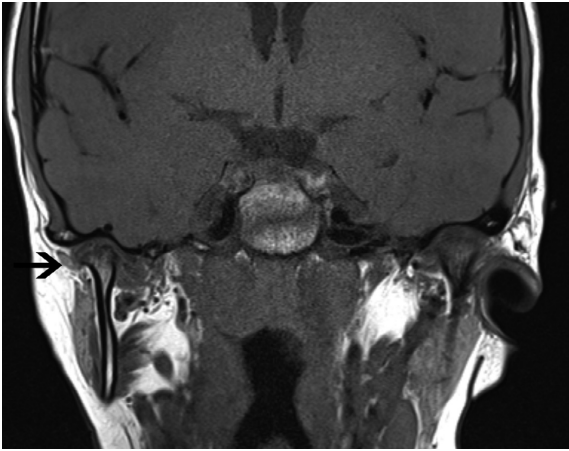


Figure 3. Coronal T1 weighted image of a 12-year-old boy with oligoarthritic JIA and disease duration 11 years, showing loss of volume of the right condyle (arrow).

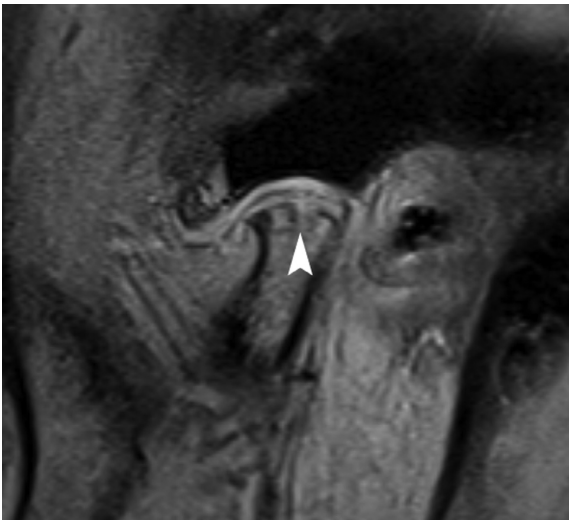


Figure 4a. Sagittal/oblique T1 weighted image with fat saturation after intravenous contrast of a 15-year-old boy with polyarthritic, rheumatoid factor (RF) negative JIA, and disease duration 4 years, showing grade 2 condylar irregularity (arrow-head).

agreement for grading inflammation on a 0–4 scale according to the progressive system as suggested by Kellenberger (13) was good to moderate, with kappa values of 0.61 for the same reader and 0.45 between readers. The agreement for assessment of synovial thickening on a 0–2 scale and joint enhancement on a 0–2 scale, as suggested by Tolend (23), was moderate with kappa values of 0.43–0.44 both between readers and for the same reader. Subjective impression of thickened synovium was assessed with moderate agreement for the same reader and fair agreement between readers (Kappa 0.23).

Bone marrow oedema/enhancement: Assessment of bone marrow oedema on a 0–1 scale showed fair to moderate agreement, with kappa values of 0.35 for the same reader and 0.54 between readers.

The analysis of agreement of the variable bone marrow enhancement on a 0–2 scale was hampered by severely

skewed distribution in one of the readings. Therefore, kappa analysis could not be performed. The variable showed a high proportion of absolute agreement (89%).

Direct measurements of joint fluid: The mean measurement of joint fluid in the upper compartment was 0.2 mm (median 0.1), with 95% limits of agreement of –0.6 to 0.4 mm between readers. The mean measurement of joint fluid in the lower compartment was 0.3 mm (median 0.1) with 95% limits of agreement of –1.0 to 0.7 mm between readers.

Based on the presented results a scoring system consisting of the following, precise imaging features could be considered (Table 4).

DISCUSSION

Of 25 commonly used MRI-based markers for TMJ changes in children with JIA, 13 showed sufficient precision, of which

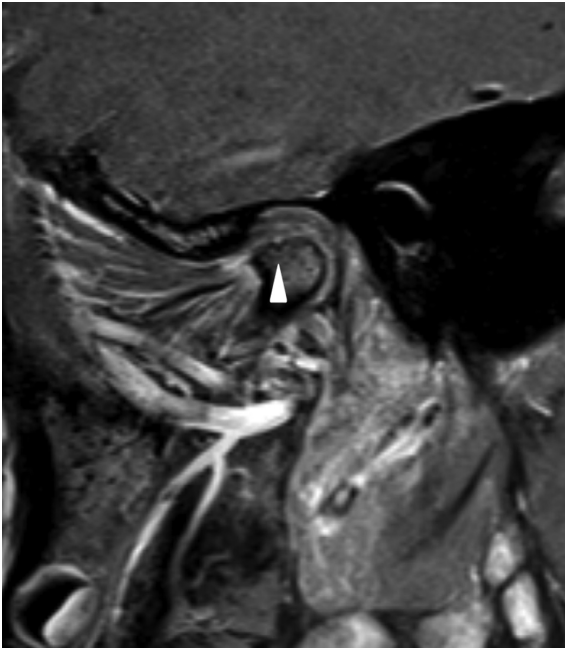


Figure 4b. Sagittal/oblique T1 weighted image with fat saturation after intravenous contrast of a 15-year-old girl with enthesitis-related JIA and disease duration 14 years, showing grade 1 condylar irregularity (arrowhead).

11 were judged the more relevant to be included in a robust scoring system; seven within the osteochondral domain and four within the inflammatory domain (Table 4). An additional six markers performed well for the same reader, indicating that these be used with caution. Interestingly, several of the commonly used markers performed poorly, in

particular assessment of synovial thickness and joint enhancement, as well as measurements of joint fluid.

Osteochondral Domain

In the present study, the most precise MRI marker suggestive of osteochondral damage was condylar volume on a 0-1 scale;

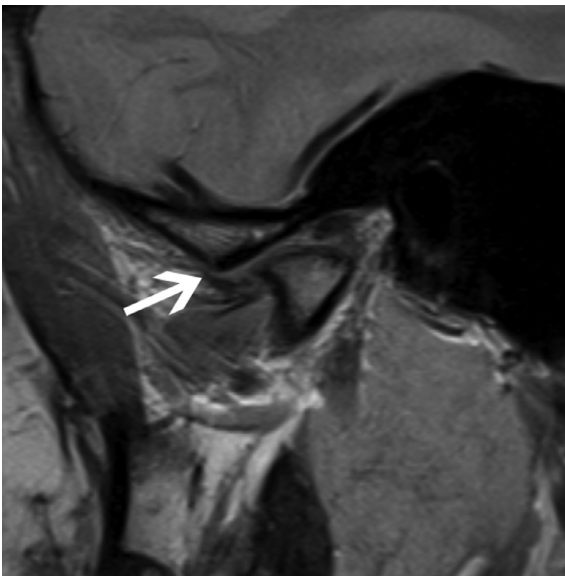


Figure 5a. Sagittal/oblique PD weighted image of a 15-year-old girl with undifferentiated JIA and disease duration 13 years, showing severely flattened articular eminence/ glenoid fossa (grade 2) (white arrow).

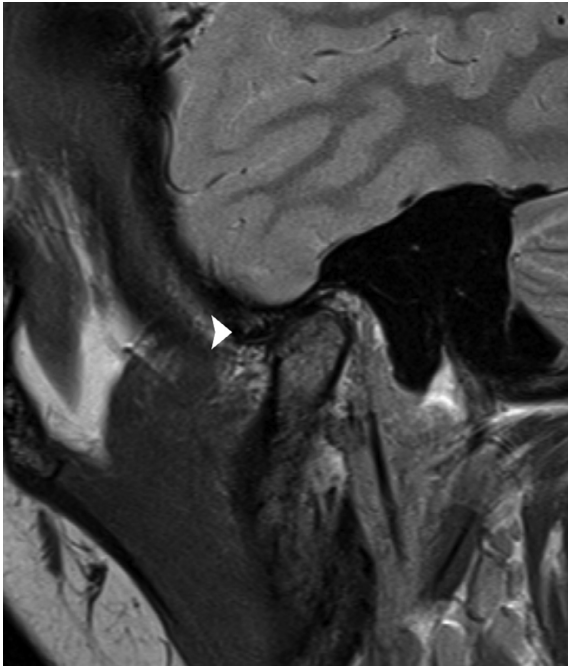


Figure 5b. Sagittal/oblique PD weighted image of a 12-year-old girl with polyarthritic, rheumatoid factor (RF) negative JIA and disease duration 10 years, showing mild to moderate widening or flattening of the articular eminence and glenoid fossa (grade 1) (white arrowhead).

0 being within normal and 1 representing a clearly deformed condyle in the sagittal and/or coronal views, a feature not seen in children without JIA (14,19,28).

Likewise, assessment of osseous deformity as suggested by Tolend and Kellenberger using a progressive scoring system performed well, however, this grading system is based on a sequence of pathological changes, starting with a mildly flattened mandibular condyle and/or temporal bone (grade 1), followed by moderate flattening of the same structures (grade 2). Grade 3 is characterized by severe flattening of the mandibular condyle with loss of height, and/or completely flat temporal bone, and/or presence of small erosions/irregularities while grade 4 is defined as destruction of the temporomandibular joint by large erosions, fragmentation of the mandibular condyle, intra-articular ossification or bone apposition on mandibular condyle or temporal bone (13).

We have previously shown that a mildly flattened condyle is seen in around 20% of children without JIA, and as such represents a normal variation rather than early destructive change (19). Moreover, we experienced that both condylar irregularities and erosions may be present before severe condylar flattening, thus biasing a progressive system.

To overcome the abovementioned challenges, we suggest that the different markers are scored separately, and summarized. More specifically, that the most precise markers, such as loss of condylar volume, condylar shape and irregularities, and shape of articular eminence and glenoid fossa are used to construct a total damage score. Ideally, each of these

components should be weighted, for example by using CBCT scores that are more fine-meshed in the osteochondral domain.

Several authors have explored the importance and incidence of disk abnormalities in TMJ (29–32), however, without addressing the precision of findings. We have now shown that assessing the disk as either normal or pathological represents a precise variable.

Subjective assessment of the condylar inclination showed good intra- and interobserver agreement. Previous studies have shown that the condylar inclination is symmetrical, and that it normally increases with age (14,19,28). Thus, the finding of asymmetric condylar inclination in a child with JIA could indicate growth disturbances secondary to the disease.

Inflammation

Four markers within the inflammation domain were considered of sufficient precision, both within and between readers, to be included in a future scoring system, namely joint fluid on a 0–2 scale, overall impression of inflammation on a 0–2 scale, synovial enhancement on a 0–2 scale and bone marrow oedema on a 0–1 scale (Table 4).

As for evaluation of joint fluid, the hybrid assessment with both continuous measurements and semi-qualitative evaluation suggested by Tolend (23) performed well in contrast to the subjective grading of the upper and lower compartments

TABLE 3. MRI-scoring of the TMJs - inflammatory domain. Cohen's kappa values and proportion of absolute, interobserver agreement for variables describing TMJ-inflammation in 86 patients (51 girls) with JIA, right TMJs. Simple kappa for dichotomized variables and linear, weighted kappa for variables with 3 or more grades. Scoring systems are detailed below.

MRI-feature	Intraobserver Kappa value (95% CI)	Interobserver Kappa value (95% CI)	Interobserver proportion absolute agreement
Joint fluid			
Joint fluid (0-2) ¹	0.74 (0.55-0.93)	0.71 (0.48-0.95)	76/81 (94%)
Subjective impression of joint fluid, upper compartment (0-2) ²	0.51 (0.29-0.73)	0.40 (0.20-0.59)	60/81 (74%)
Subjective impression of joint fluid, lower compartment (0-2) ³	0.69 (0.53-0.85)	0.29 (0.14-0.44)	41/81 (51%)
Overall impression of pathological joint fluid (0-1) ⁴	0.71 (0.50-0.91)	0.40 (0.14-0.66)	68/82 (83%)
Synovial inflammation/enhancement/thickening			
Overall impression of inflammation (0-2) ⁵	0.59 (0.41-0.76)	0.57 (0.43-0.72)	59/79 (75%)
Synovial enhancement (0-2) ⁶	0.68 (0.52-0.83)	0.54 (0.40-0.69)	53/78 (68%)
Inflammation, progressive system (0-4) ⁷	0.61 (0.43-0.79)	0.45 (0.31-0.60)	49/74 (66%)
Synovial thickening (0-2) ⁸	0.44 (0.22-0.65)	0.44 (0.22-0.66)	63/78 (81%)
Joint enhancement (0-2) ⁹	0.43 (0.23-0.62)	0.44 (0.25-0.62)	58/78 (74%)
Subjective impression of synovial thickening (0-2) ¹⁰	0.51 (0.32-0.70)	0.23 (0.08-0.38)	46/78 (59%)
Bone marrow oedema/enhancement			
Bone marrow oedema (0-1) ¹¹	0.35 (0.18-0.51)	0.54 (0.28-0.80)	76/85 (89%)
Bone marrow enhancement (0-2) ¹²	0.85 (0.64-1.00)	n/a	62/70 (89%)

Abbreviations: JIA juvenile idiopathic arthritis; MRI, magnetic resonance imaging; TMJ, temporomandibular joint.

1 0=absent; ≤ 1 mm fluid in joint recess, 1=small; > 1 mm and ≤ 2 mm fluid in recess or involving entire joint compartment, 2=large; > 2 mm fluid in recess or involving entire joint compartment. Adapted from reference 23

2 0=no joint fluid, 1=a thin line of fluid, 2=more than a thin line of fluid

3 0=no joint fluid, 1=a thin line of fluid, 2=more than a thin line of fluid

4 0=no, 1=yes

5 0=normal, includes normal synovial enhancement and a thin line of joint fluid, 1=mild inflammation, considered pathological, 2=moderate/severe inflammation

6 0=subtle synovial enhancement, 1=mildly increased synovial enhancement, 2=moderately to severe synovial enhancement (signal intensity \geq nearby vessel)

7 0= no inflammation: No or small amounts of joint fluid in any recess, with ≤ 1 mm width. No enhancement or enhancement confined to physiological joint fluid. 1= mild inflammation: Extension of joint enhancement exceeds that of physiological joint fluid but does not involve entire joint compartment and/or presence of bone marrow oedema. 2= moderate inflammation: Joint enhancement involves entire joint compartment or there is an enhancing joint effusion, 3= severe inflammation: Detectable synovial thickening in addition to increased joint enhancement or effusion, 4= joint space filled with and enlarged by pannus. Adapted from reference 13

8 0=absent; no synovium visible (apparent joint compartment ≤ 1 mm width), 1=mild; > 1 and < 2 mm thickness at the point of maximum synovial thickening, 2=Moderate/severe; > 2 mm thickness at the point of maximum synovial thickening. Adapted from reference 23

9 0=normal; high signal intensity confined to signal perimeter of normal amount of fluid on corresponding fluid-sensitive image, 1=mild; high signal intensity focally exceeding signal perimeter of physiologic amount of joint fluid on corresponding fluid-sensitive image, 2=moderate/severe; high signal intensity diffusely involving 1 or both joint compartments. Adapted from reference 23

10 0=no thickening, 1=mild thickening, 2=moderate/severe thickening

11 0=absent, 1=present

12 0=No enhancement, 1=subtle enhancement, what is considered normal, 2=increased, pathological enhancement

separately. However, direct continuous measurement of joint fluid turned out to be rather inaccurate, with significant variation between observers. These results are in line with others (33,34), reflecting difficulties in measuring small distances. To overcome the challenges associated with continuous measurements, we tested the subjective variable "overall impression of joint fluid," although with disappointing results between readers. In conclusion, the mechanisms providing high precision to the variable "joint fluid" are not fully understood, but probably depends on a thorough understanding of the normal appearances of fluid in the recesses and joint compartments.

The variable "overall impression of inflammation 0-2" depends explicitly on the subjective understanding of normal, age-related and physiologic findings in the TMJ. At the same time the variable demands the reader to define, from his/her own understanding, the difference between normal findings and inflammation. Like the binary variables "overall impression of pathological joint fluid" and "loss of condylar volume" this type of variables has not been tested in other publications. This study shows that the variable as such is precise enough to be studied further.

Opposite to the marker *synovial enhancement*, which was based on pre and post T1-fat suppressed images only,

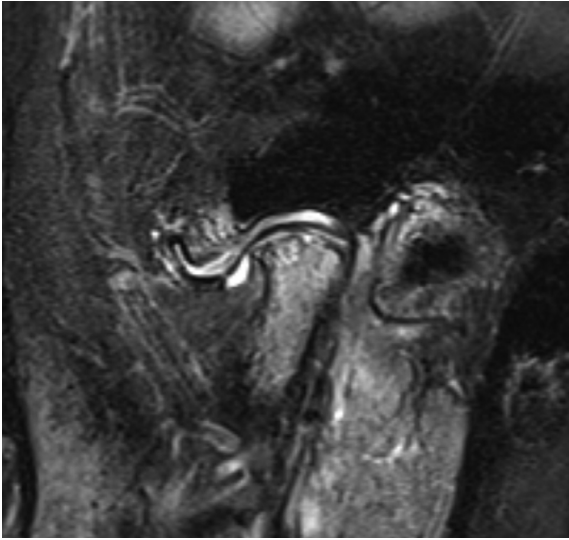


Figure 6. Sagittal/oblique T2 weighted image with fat saturation of a 15-year-old boy with persistent oligoarthritic JIA and disease duration 4 years, showing large amount of joint fluid (grade 2) in the right temporomandibular joint.

assessment of *joint enhancement*, as suggested by Tolend et al (23), is based on both fluid-sensitive images as well as post-contrast T1-weighted fat-suppressed images. According to

their 0–2 score, mild inflammation is defined as high signal intensity focally exceeding signal perimeter of physiologic amount of joint fluid on corresponding fluid-sensitive image



Figure 7. Sagittal/oblique T1 weighted image with fat saturation after intravenous contrast of a 6-year-old girl with polyarthritic JIA and disease duration 4 years, showing moderate to severe synovial enhancement (grade 2) (white arrow).

TABLE 4. Proposed Scoring System for MRI-Based Evaluation of Osteochondral Damage and Inflammatory Change in the Pediatric Temporomandibular Joint in Children with Juvenile Idiopathic Arthritis (JIA)

MRI Imaging Feature	Imaging Plane	Grading
<i>Osteochondral domain</i>		
Loss of condylar volume	All available	0-1
Condylar shape	Sagittal/oblique	0-3
Condylar shape	Coronal	0-2
Condylar irregularities, ideal protocol	All available	0-2
Shape of the eminence/fossa	Sagittal/oblique	0-2
Disk abnormalities	Sagittal/oblique	0-1
Condylar inclination	Sagittal/oblique	0-2
<i>Inflammatory domain</i>		
Joint fluid	Sagittal/oblique	0-2
Overall impression of inflammation	All available	0-2
Synovial enhancement	Sagittal/oblique	0-2
Bone marrow oedema	All available	0-1

JIA, juvenile idiopathic arthritis; MRI, magnetic resonance imaging; TMJ, temporomandibular joint.

while moderate to severe inflammation is characterized by high signal intensity diffusely involving one or both joint compartments. We observed numerous cases showing subtle, focal, synovial contrast enhancement on T1-weighted fat-suppressed images, with no fluid seen on T2-weighted images, i.e., a grade 0 according to the synovial enhancement score and a grade 1 according to the joint enhancement score. Thus, it seems that combining pre-gadolinium fluid-sensitive images with post-gadolinium fat-suppressed T1-weighted images tends to overestimate pathology, possibly accentuated by slightly different imaging parameters on T1- and T2-weighted images. These difficulties are reflected in the slightly lower agreement between readers for the joint enhancement score as compared to the synovial enhancement score.

We found acceptable agreement between readers for the assessment of condylar bone marrow oedema. In adults with rheumatoid arthritis of the wrist, the precision of this variable is addressed in numerous publications (35–37) with results supporting the findings in our study. However, the precision in these studies is measured as a sum of scores along an ICC-scale so the transferability of the results to the mandibles of a pediatric population is questionable. In their study on MRI and CBCT Koos and colleagues report “no relevant interobserver differences” which per se supports our findings, even though their statement could be more elaborated (21). In 2014, Vaid studied the composite variable including contrast enhancement, joint fluid, synovial thickening and bone marrow oedema with a weighted kappa of 0.51. The complexity of their composite variable makes it hard to say if their results support or contradict our findings (22). Lastly, Tolend tested both a binary and a 4-graded version of the variable bone marrow oedema with ICC-results that do not support our

findings (sICC 0.01 and 0.06, avICC 0.61 and 0.57). Still, bone marrow oedema is considered an important marker, as oedema/osteitis is believed to represent relevant pathology in rheumatology. Taken together, we suggest the variable should be part of a future scoring system.

As for the progressive inflammation score, this is based on a fixed sequence of changes, like that described for the osteochondral domain. We experienced, in a small number of TMJs, that this sequence was violated, in that subtle synovial thickening was present without synovial enhancement or joint effusion. Thus, according to the progressive system, these joints should be scored as a grade 3 inflammation. Seen together with the difficulties in defining synovial thickening this represents a bias in the progressive system. As in the osteochondral domain, we suggest that each variable be scored separately, and subsequently summarized.

Similar to bone marrow oedema, the variable “bone marrow enhancement” aims to describe an important and closely related part of the rheumatologic pathology, namely osteitis and increased perfusion of the intraosseous part of the condyle. However, we noted that virtually all condyles demonstrated some degree of enhancement, also when compared to the mandibular ramus, which corresponds to a grade 1 in the binary system as proposed by Tolend. The 3-graded system proposed in this study shows a slight differentiation between assumed normal and pathological enhancement with a high proportion of absolute agreement, although kappa analysis could not be performed due to skewed distribution of the findings. We note that Tolend and co-workers do not present data on the repeatability of the binary variant of this variable. The assumed importance of the pathological process, in combination with the paucity of data on the precision of the variable makes it an interesting topic for further research, but as per today it should not be included in a robust scoring system.

Except for the inflammation score in the progressive system, all these scores are relatively crude, however, previous studies have demonstrated difficulties in establishing reliable, fine-meshed imaging markers for the inflammatory domain (23).

In general, we found that the intra-observer agreement was better than agreement between observers, despite thorough calibration and the use of a reference atlas. This is not unexpected and similar results has been shown in numerous earlier publications. Still, we assume that this finding underscores the importance of performing clinical, JIA-related radiology reporting in a small environment of subspecialists with a special interest in JIA.

Limitations and Strengths

We acknowledge that our study has shortcomings. First, the use of Cohens Kappa has limitations especially in analysis of datasets with skewed distribution (38,39). To compensate for this, we chose to both present the proportion of absolute agreement and the distribution of findings for each variable. We assume this to

APPENDIX A. MRI Protocol for TMJ Imaging in the NorJIA-Study

Sequence	Plane	Fat Saturation	TR ^a (ms)	TE ^b (ms)	Slice Thickness (mm)	Gap (mm)	FOV ^c (mm)	Matrix	Number of Averages	Flip Angle	ETL ^d
T1-MPRAGE ^e	Sagittal	No	2000	2.26	1		250 × 250	256 × 256	1	8	
T1-TSE ^f	Coronal	No	826	7.9	2	2.2	179 × 179	448 × 359	3	131	4
T2-TSE	Sagittal/oblique	Yes (CHES) ^g	3530	71	2	2.2	150 × 150	448 × 314	2	150	9
PD ^h -TSE	Sagittal/oblique	No	3470	22	2	2.2	150 × 150	448 × 314	2	139	10
T1-TSE	Sagittal/oblique	Yes	774	8.1	2	2.2	150 × 150	384 × 269	3	122	4
T1-TSE-Dixon	Coronal	2-point Dixon	650	12	2	2.2	180 × 180	448 × 358	1	144	4
Vibe-Twist	Coronal	No	3.78	1.03	2		210 × 210	160 × 144	1	9	1
T1-TSE	Sagittal/oblique	Yes (CHES)	774	8.1	2	2.2	150 × 150	384 × 269	2	122	4
PD-TSE, open mouth	Sagittal/oblique	No	3470	22	2	2.2	150 × 150	448 × 314	2	139	10

MRI, magnetic resonance imaging; NorJIA, the Norwegian juvenile idiopathic arthritis study; TMJ, temporomandibular joint.

^a Repetition time (TR)

^b Echo time (TE)

^c Field of view (FOV)

^d Echo train length (ETL)

^e Magnetization prepared rapid gradient echo (MPRAGE)

^f Turbo spin-echo (TSE)

^g Chemical shift selective fat saturation (CHES)

^h Proton density (PD)

APPENDIX B. Imaging Features for Scoring of Temporomandibular Joints in the Osteochondral Domain by Magnetic Resonance Imaging

	Image Plane	Grade 0	Grade 1	Grade 2	Grade 3
Condylar shape	Sagittal/oblique	Rounded/ovoid	Very subtle anterior flattening	Mild flattening; involves part of the surface of the condyle	Moderate/severe flattening; involves the entire surface of the condyle, or loss of height of the condyle
Condylar shape	Coronal T1	Convex throughout	Mild/partial flattening	Moderately or severely flattened throughout	
Condylar inclination	Sagittal/ oblique	Straight	Mild anterior inclination	Moderate/ significant anterior inclination	
Shape of the articular eminence and glenoid fossa	Sagittal/ oblique	S-shaped	Mild to moderate widening or flattening	Severely flattened fossa-eminence	
Loss of condylar volume	All available	None	Clearly deformed condyle		
Condylar irregularities, core and ideal protocol ^{a,b}	Coronal and sagittal/oblique	No irregularities or deep breaks of the bony joint surface	Mild irregularities involving only part of the articular surface of the condyle	Moderate/ severe; presence of deep breaks in the subchondral bone seen in two planes, or irregularities involving the entire articular surface	
Condylar flattening ^c	Sagittal/oblique	No loss of the round/slightly angular shape of the condyle	Mild; extent of flattening involves parts of the surface of the condyle	Moderate/severe; extent of flattening involves the entire surface of the condyle, or loss of the height of the condyle	
Disk abnormalities	Sagittal/oblique	None	Presence of flattening, displacement or destruction		

^a Core protocol based on coronal T1, sagittal/oblique T2-fat suppressed, sagittal/ oblique contrast enhanced fat-suppressed T1-weighted images. Adapted from reference 26.

^b Ideal protocol based on the same images as Core protocol + sagittal/oblique T1 fat-suppressed and sagittal/ oblique proton density weighted images. Adapted from reference 26.

^c Adapted from reference 23.

be a more correct and transparent way of presenting the data than other statistical models which would introduce other sources of error. Next, the study was performed with two readers only, aiming to examine the potential of a scoring system given optimal conditions, rather than assessing its performance in a clinical setting. And lastly, the distribution of findings for some of the variables under investigation was skewed, thus hindering statistical analysis to be performed. The strengths of our study include the high numbers, the meticulous standardization of scoring systems and measurements, and the construction of an atlas for optimizing precision.

CONCLUSION

We propose a robust scoring system for the assessment of TMJ involvement in children with JIA including four variables in the inflammatory domain and seven variables in the osteochondral domain. Further studies on clinical validity of these markers are needed.

ACKNOWLEDGMENTS

This work was partially funded by the Liaison Committee between the Central Norway Regional Health Authority

APPENDIX C. Imaging Features for Scoring of Temporomandibular Joints in the Inflammatory Domain by Magnetic Resonance Imaging

Imaging Feature	Definition/Image Plane	Grading
Overall impression of inflammation	All available images	0=Normal; includes normal synovial enhancement and a thin line of joint fluid 1=Mild inflammation; considered pathological 2=Moderate to severe inflammation
Overall impression of pathological joint fluid	All available images	0=No 1=Yes
Synovial enhancement	Signal intensity of the synovium, based on sagittal/ oblique T1-fs pre contrast and sagittal/oblique T1-fs post-contrast images	0= Subtle synovial enhancement, what is believed as normal 1= Mildly increased synovial enhancement 2= Moderately to severely increased synovial enhancement (signal intensity \geq nearby vessel)
Subjective impression of joint fluid, upper compartment	Sagittal/ oblique T2-fat saturated images	0=No signal 1=A thin line of signal 2=More than a thin line
Subjective impression of joint fluid, lower compartment	Sagittal/ oblique T2-fat saturated images	0=No signal 1=A thin line of signal 2=More than a thin line
Joint enhancement ^a	Signal intensity of the synovium, capsule and joint fluid higher than that of muscle on post contrast T1-fat saturated images	0=Normal; high signal intensity confined to signal perimeter of normal amount of fluid on corresponding fluid-sensitive image 1=Mild; high signal intensity focally exceeding signal perimeter of physiologic amount of joint fluid on corresponding fluid-sensitive image 2= Moderate/ severe; high signal intensity diffusely involving 1 or both joint compartments
Joint fluid ^a	Increased joint fluid with isointense signaling of joint space compared to that of cerebrospinal fluid on fluid-sensitive images	0=Absent; ≤ 1 mm fluid in recess 1=Small; > 1 and ≤ 2 mm in recess or involving entire joint compartment 2=Large; > 2 mm fluid in recess or involving entire joint compartment
Synovial enhancement	Sagittal/ oblique T1-fat saturated images post iv contrast	0=Subtle synovial enhancement 1=Mildly increased synovial enhancement 2=Moderate to severe synovial enhancement (signal intensity \geq nearby vessel)
Synovial thickening ^a	Sagittal/oblique T2 fat-saturated images	0=Absent; no synovium visible (apparent joint compartment ≤ 1 mm width) 1=Mild; > 1 and < 2 mm thickness at the point of maximum synovial thickening, 2=Moderate/severe; > 2 mm thickness at the point of maximum synovial thickening
Joint enhancement ^a	Sagittal/ oblique T1-fat saturated images post iv contrast and sagittal/oblique T2 fat-saturated images	0=Normal; high signal intensity confined to signal perimeter of normal amount of fluid on corresponding fluid-sensitive image 1=Mild; high signal intensity focally exceeding signal perimeter of physiologic amount of joint fluid on corresponding fluid-sensitive image 2=Moderate/severe; high signal intensity diffusely involving 1 or both joint compartments

(continued)

APPENDIX C. (Continued)

Imaging Feature	Definition/Image Plane	Grading
Subjective impression of synovial thickening	Sagittal/oblique T2 fat-saturated images	0=No thickening 1=Mild thickening 2=Moderate/severe thickening
Bone marrow oedema	Coronal T1 images and sagittal/oblique T2 fat-saturated images	0=Absent 1=Present
Bone marrow enhancement	Sagittal/ oblique T1-fat saturated images before and post iv contrast	0=No enhancement 1=Subtle enhancement, considered normal 2=Increased, pathological enhancement

^a Adapted from reference 23.

APPENDIX D. Progressive Scoring System for Assessing Inflammation and Osseous Deformity of Temporomandibular Joint by Magnetic Resonance Imaging^a

Inflammation		Osseous Deformity	
Grade 0	No inflammation: No or small amounts of fluid in any recess with ≤ 1 mm width. No enhancement or enhancement confined to physiological joint fluid.	Grade 0	Normal shape of temporal bone and mandibular condyle according to age: S-shaped articular eminence/glenoid fossa. Round condyle (young patient) Less rounded, more angular appearing condyle (older patient) Smooth subchondral bone contour
Grade 1	Mild inflammation: Extension of joint enhancement exceeds that of physiological joint fluid but does not involve entire joint compartment and/or presence of bone marrow oedema.	Grade 1	Mild flattening of the mandibular condyle and/or temporal bone.
Grade 2	Moderate inflammation: Joint enhancement involves entire joint compartment or there is an enhancing joint effusion	Grade 2	Moderate flattening of the mandibular condyle and/or temporal bone
Grade 3	Severe inflammation: Detectable synovial thickening in addition to increased joint enhancement or effusion.	Grade 3	Severe flattening of the mandibular condyle with loss of height, and/or completely flat temporal bone, and/or presence of small erosions/irregularities
Grade 4	Joint space filled with and enlarged by pannus	Grade 4	"Destruction" of temporomandibular joint by large erosions, fragmentation of the mandibular condyle, intra-articular ossification or bone apposition on mandibular condyle or temporal bone.

^a Adapted from reference 14.

APPENDIX E. Grading of Position of the Mandibular Condyle and Disc Displacement

	Position of the Condyle in the Glenoid Fossa		Disc Displacement
Grade 0	Neutral	Grade 0	None
Grade 1	Anterior	Grade 1	Anterior
Grade 2	Posterior	Grade 2	Posterior
Grade 3	Medial	Grade 3	Lateral
Grade 4	Lateral	Grade 4	Medial
Grade 5	Superior	Grade 5	Disc cannot be defined
Grade 6	Inferior		

(RHA) and the Norwegian University of Science and Technology (NTNU) and “Norsk Revmatikerforbund.” The study has also been supported by the Northern Norway Regional Health Authority and by the Tromsø Research Foundation (TFS).

REFERENCES

- Berntson L, Andersson Gare B, Fasth A, et al. Incidence of juvenile idiopathic arthritis in the Nordic countries. A population based study with special reference to the validity of the ILAR and EULAR criteria. *J Rheumatol* 2003; 30(10):2275–2282.
- Cannizzaro E, Schroeder S, Muller LM, et al. Temporomandibular joint involvement in children with juvenile idiopathic arthritis. *J Rheumatol* 2011; 38(3):510–515.
- Billiau AD, Hu Y, Verdonck A, et al. Temporomandibular joint arthritis in juvenile idiopathic arthritis: prevalence, clinical and radiological signs, and relation to dentofacial morphology. *J Rheumatol* 2007; 34(9):1925–1933.
- Glerup M, Stoustrup P, Hauge L, et al. Long-term outcomes of temporomandibular joints in juvenile idiopathic arthritis. *J Rheumatol* 2019; 47(5):730–738.
- Ringold S, Cron RQ. The temporomandibular joint in juvenile idiopathic arthritis: frequently used and frequently arthritic. *Pediatr Rheumatol Online J* 2009; 7:11.
- Stoll ML, Sharpe T, Beukelman T, et al. Risk factors for temporomandibular joint arthritis in children with juvenile idiopathic arthritis. *J Rheumatol* 2012; 39(9):1880–1887.
- Isola G, Perillo L, Migliorati M, et al. The impact of temporomandibular joint arthritis on functional disability and global health in patients with juvenile idiopathic arthritis. *Eur J Orthod* 2019; 41(2):117–124.
- Rahimi H, Twilt M, Herlin T, et al. Orofacial symptoms and oral health-related quality of life in juvenile idiopathic arthritis: a two-year prospective observational study. *Pediatr Rheumatol Online J* 2018; 16(1):47.
- Frid P, Nordal E, Bovis F, et al. Temporomandibular joint involvement in association with quality of life, disability, and high disease activity in juvenile idiopathic arthritis. *Arthritis Care Res* 2017; 69(5):677–686.
- Fischer J, Skeie MS, Rosendahl K, et al. Prevalence of temporomandibular disorder in children and adolescents with juvenile idiopathic arthritis - a Norwegian cross-sectional multicentre study. *BMC Oral Health* 2020; 20(1):282.
- Navallas M, Inarejos EJ, Iglesias E, et al. MR imaging of the temporomandibular joint in juvenile idiopathic arthritis: technique and findings. *Radiographics* 2017; 37(2):595–612.
- Stoll ML, Kau CH, Waite PD, et al. Temporomandibular joint arthritis in juvenile idiopathic arthritis, now what? *Pediatr Rheumatol Online J* 2018; 16(1):32.
- Kellenberger CJ, Arvidsson LZ, Larheim TA. In: Ogaard B, editor. *Seminars in orthodontics*. 212015. p. 111-120.
- Kellenberger CJ, Junhasavasdikul T, Tolend M, et al. Temporomandibular joint atlas for detection and grading of juvenile idiopathic arthritis involvement by magnetic resonance imaging. *Pediatr Radiol* 2018; 48(3):411–426.
- Stoustrup P, Twilt M, Spiegel L, et al. Clinical orofacial examination in juvenile idiopathic arthritis: international consensus-based recommendations for monitoring patients in clinical practice and research studies. *J Rheumatol* 2017; 44(3):326–333.
- Taylor J, Giannini EH, Lovell DJ, et al. Lack of Concordance in interrater scoring of the provider's global assessment of children with juvenile idiopathic arthritis with low disease activity. *Arthritis Care Res* 2018; 70(1):162–166.
- Muller L, Kellenberger CJ, Cannizzaro E, et al. Early diagnosis of temporomandibular joint involvement in juvenile idiopathic arthritis: a pilot study comparing clinical examination and ultrasound to magnetic resonance imaging. *Rheumatology* 2009; 48(6):680–685. (Oxford, England).
- von Kalle T, Stuber T, Winkler P, et al. Early detection of temporomandibular joint arthritis in children with juvenile idiopathic arthritis - the role of contrast-enhanced MRI. *Pediatr Radiol* 2015; 45(3):402–410.
- Angenete OW, Augdal TA, Jellestad S, et al. Normal magnetic resonance appearances of the temporomandibular joints in children and young adults aged 2-18 years. *Pediatr Radiol* 2019; 48(3):341–349.
- Stoll ML, Guleria S, Mannion ML, et al. Defining the normal appearance of the temporomandibular joints by magnetic resonance imaging with contrast: a comparative study of children with and without juvenile idiopathic arthritis. *Pediatr Rheumatol Online J* 2018; 16(1):8.
- Koos B, Tzaribachev N, Bott S, et al. Classification of temporomandibular joint erosion, arthritis, and inflammation in patients with juvenile idiopathic arthritis. *J Orofac Orthop* 2013; 74(6):506–519.
- Vaid YN, Dunnivant FD, Royal SA, et al. Imaging of the temporomandibular joint in juvenile idiopathic arthritis. *Arthritis Care Res* 2014; 66(1):47–54.
- Tolend MA, Twilt M, Cron RQ, et al. Toward establishing a standardized magnetic resonance imaging scoring system for temporomandibular joints in juvenile idiopathic arthritis. *Arthritis Care Res* 2018; 70(5):758–767.
- Ranganathan P, Pramesh CS, Aggarwal R. Common pitfalls in statistical analysis: measures of agreement. *Perspect Clin Res* 2017; 8(4):187–191.
- Petty RE, Southwood TR, Manners P, et al. International League of Associations for Rheumatology classification of juvenile idiopathic arthritis: second revision, Edmonton, 2001. *J Rheumatol* 2004; 31(2):390–392.
- Miller E, Inarejos Clemente EJ, Tzaribachev N, et al. Imaging of temporomandibular joint abnormalities in juvenile idiopathic arthritis with a focus on developing a magnetic resonance imaging protocol. *Pediatr Radiol* 2018; 48(6):792–800.
- Kellenberger CJ, Abramowicz S, Arvidsson LZ, et al. Recommendations for a standard magnetic resonance imaging protocol of temporomandibular joints in juvenile idiopathic arthritis. *J Oral Maxillofac Surg* 2018; 76(12):2463–2465.
- Karlo CA, Stolzmann P, Habernig S, et al. Size, shape and age-related changes of the mandibular condyle during childhood. *Eur Radiol* 2010; 20(10):2512–2517.
- Abramowicz S, Cheon JE, Kim S, et al. Magnetic resonance imaging of temporomandibular joints in children with arthritis. *J Oral Maxillofac Surg* 2011; 69(9):2321–2328.
- Taylor DB, Babyn P, Blaser S, et al. MR evaluation of the temporomandibular joint in juvenile rheumatoid arthritis. *J Comput Assist Tomogr* 1993; 17(3):449–454.
- Kirkhus E, Arvidsson LZ, Smith HJ, et al. Disk abnormality coexists with any degree of synovial and osseous abnormality in the temporomandibular joints of children with juvenile idiopathic arthritis. *Pediatr Radiol* 2016; 46(3):331–341.
- Kellenberger CJ, Bucheli J, Schroeder-Kohler S, et al. Temporomandibular joint magnetic resonance imaging findings in adolescents with anterior disk displacement compared to those with juvenile idiopathic arthritis. *J Oral Rehabil* 2019; 46(1):14–22.
- Shelmerdine SC, Di Paolo PL, Rieter J, et al. A novel radiographic scoring system for growth abnormalities and structural change in children with juvenile idiopathic arthritis of the hip. *Pediatr Radiol* 2018; 48(8):1086–1095.
- Engesaeter IO, Laborie LB, Lehmann TG, et al. Radiological findings for hip dysplasia at skeletal maturity. Validation of digital and manual measurement techniques. *Skeletal Radiol* 2012; 41(7):775–785.
- Krabbe S, Eshed I, Pedersen SJ, et al. Bone marrow oedema assessment by magnetic resonance imaging in rheumatoid arthritis wrist and metacarpophalangeal joints: the importance of field strength, coil type and image resolution. *Rheumatology* 2014; 53(8):1446–1451. (Oxford, England).
- Olech E, Crues JV, 3rd Yocum DE, et al. Bone marrow edema is the most specific finding for rheumatoid arthritis (RA) on noncontrast magnetic resonance imaging of the hands and wrists: a comparison of patients with RA and healthy controls. *J Rheumatol* 2010; 37(2):265–274.
- Haavardsholm EA, Ostergaard M, Ejbjerg BJ, et al. Reliability and sensitivity to change of the OMERACT rheumatoid arthritis magnetic resonance imaging score in a multireader, longitudinal setting. *Arthritis Rheum* 2005; 52(12):3860–3867.
- Feinstein AR, Cicchetti DV. High agreement but low kappa: I. The problems of two paradoxes. *J Clin Epidemiol* 1990; 43(6):543–549.
- Fagerland MLS, Laake P. *Statistical analysis of contingency tables*. Boca Raton, FL: CRC Press, 2017:548–556.

Paper III

This paper is awaiting publication and is not included in NTNU Open

ISBN 978-82-326-6430-6 (printed ver.)
ISBN 978-82-326-6820-5 (electronic ver.)
ISSN 1503-8181 (printed ver.)
ISSN 2703-8084 (online ver.)



Norwegian University of
Science and Technology